

MISSILE INTERNAL POWER

by

ROBERT WELLESLEY MANN

S. B., Massachusetts Institute of Technology
(1950)

S. M., Massachusetts Institute of Technology
(1951)

SUBMITTED IN PARTIAL FULFILLMENT OF THE REQUIREMENTS
FOR THE DEGREE OF DOCTOR OF SCIENCE
AT THE
MASSACHUSETTS INSTITUTE OF TECHNOLOGY

June, 1957

Signature of Author _____
Department of Mechanical Engineering, May 20, 1957

Certified by _____
Thesis Supervisor

Accepted by _____
Chairman, Departmental Committee on Graduate Students

✓

MISSILE INTERNAL POWER

by

ROBERT WELLESLEY MANN

Submitted to the Department of Mechanical Engineering on May 20, 1957 in partial fulfillment of the requirements for the degree of Doctor of Science.

ABSTRACT

The Missile Internal Power (MIP) project has studied the problem of developing integrated power supplies of minimum weight capable of providing regulated electrical power in an isolated environment subject to severe climatic and force conditions. An initial study of alternative energy sources and components revealed the most promising system. Basic investigations of the properties and characteristics of solid fuels and of design criteria for partial admission turbines and electrical machinery were conducted, as was the study of several competitive regulation schemes. Based on the results of the basic investigations, and adhering faithfully to the requirements imposed by the environment and the specifications of the missile system, two electrical power units (EPU's) were developed and tested at the Dynamic Analysis and Control Laboratory (D. A. C. L.). Both units were subsequently exhaustively and successfully tested in the respective missiles and both units have proven successful in missile test flight. Extending the foregoing program, a study of optimum electrical voltage and frequency standards for missile systems has been made and recommendations which could materially reduce system weight have been advanced.

Thesis Supervisor: Prof. John A. Hrones
 Title: Professor, Mechanical Engineering

2561
 Feb 14, 1958
 For

ACKNOWLEDGEMENT

Professor J. A. Hrones, as Director of the Dynamic Analysis and Control Laboratory, provided the environment which made possible the prosecution of the missile internal power study; he assigned the author to the task and sympathetically supported all aspects of the endeavor; as Chairman of the author's Doctoral Committee he has been the source of never-failing counsel and encouragement.

The Doctoral Committee members, Professors E. S. Taylor, A. H. Shapiro and A. H. Stenning provided valuable counsel and timely understanding.

Professor D. C. White of the Electrical Engineering Department, as an associate in the initial stage of the project and as faculty adviser on certain of the theses subsequently, buttressed the electrical aspects of the project.

The staff of the project, by their collective ability and ingenuity, made possible the success of the effort through enthusiastic and conscientious endeavor. The contributions and loyalty of R. B. Downey, S. K. Grinnell and R. E. Turkington in particular are gratefully acknowledged.

Essential support was provided by a number of students, both within and without D. A. C. L., whose theses are recorded in the bibliography and whose contributions are acknowledge here.

Miss Grace Lynch's dedicated efforts made possible the preparation of this document.

The work on which this thesis is based was supported in part by the United States Navy, Bureau of Ordnance, under Contract NOrd 9661 and United States Navy, Bureau of Aeronautics, under Contract NOas 54-583-c sponsored by the DSR of the Massachusetts Institute of Technology.

TABLE OF CONTENTS

	<u>Page</u>
ABSTRACT	i
ACKNOWLEDGEMENT	ii
TABLE OF CONTENTS	iii
LIST OF FIGURES	vii
1. INTRODUCTION	1
1.1. The Nature of this Paper	1
1.2. The Nature of the Problem	1
1.3. Historical Perspective	3
2. AIR-TO-AIR MISSILE POWER SYSTEM	5
2.1. Requirements and Specifications	5
2.11. Electrical Power Requirements	5
2.12. Environmental Requirements	6
2.13. Mechanical Requirements	7
2.2. Alternative Energy Sources and Systems	7
2.21. Generalized Energy Comparison	8
2.22. Chemical Energy	16
2.221. Thermodynamic Considerations	17
2.222. Design Considerations	18
2.223. Logistic and Tactical Considerations	21
2.3. "Optimum" Energy Source	22
3. SOLID FUEL SYSTEMS	25
3.1. Solid Fuel Combustion Characteristics	25
3.2. Fuel Grain Dimensions	28
3.3. Solid Fuel Ignition	32
3.4. Characteristics of the Combustion Gases	34
3.5. Regulation Problems	36

TABLE OF CONTENTS (Cont.)

	<u>Page</u>
3. 6. Influence on the Prime Mover.	38
3. 61. Positive Displacement Prime Movers.	38
3. 62. Dynamic Fluid Prime Movers.	39
3. 63. Heat Transfer Considerations.	43
4. PARTIAL-ADMISSION TURBINES.	54
4. 1. Choice of Turbine Type.	54
4. 2. General Description of Losses.	55
4. 3. Analyses of Losses and Experimental Results.	57
4. 31. Partial Admission.	57
4. 32. Rotor Pumping.	60
4. 33. Supersonic Fluid Velocities.	60
4. 34. Aspect Ratio.	60
4. 35. Influence of Reynolds Number.	61
4. 36. Nozzle Efficiencies.	62
4. 37. Axial Clearance.	62
4. 38. Optimum Nozzle-Area Distribution.	63
4. 4. Test Facility and Instrumentation.	63
4. 5. Summary and Future Work.	65
5. MECHANO-ELECTRICAL CONVERSION.	79
5. 1. Air-To-Air Missile EPU Considerations.	80
5. 11. Pre-Launch Power Requirements.	80
5. 12. Post-Launch Requirements.	80
5. 13. Frequency.	82
5. 14. Voltages.	82

TABLE OF CONTENTS (Cont.)

	<u>Page</u>
5.15. A-C Power Versus D-C Generation.	82
5.16. Environmental Conditions.	83
5.17. Weight Minimization.	84
5.2. EPU Alternatives.	85
5.21. D-C Generators.	85
5.22. Wound Field Synchronous Alternator.	86
5.23. Permanent-Magnet Field Synchronous Alternator	87
5.24. Inductor (Variable Reluctance) Alternator	89
5.25. Inductor (Flux-Commutating) Alternator.	90
5.26. The Induction Asynchronous Alternator.	91
5.27. "Optimum" Electrical Machine	92
5.3. Isolated Induction Motor-Alternator.	93
5.31. Principle of Operation.	93
5.32. Operating Characteristics.	95
5.4. The Generalized Problem and Future Work.	97
6. REGULATION TECHNIQUES.	105
6.1. Input Power Regulators.	105
6.11. Static Pressure Control.	107
6.12. Dynamic Pressure Control.	112
6.13. Turbine Efficiency Control.	114
6.2. Load Regulators.	115
6.21. Torque Control.	116
6.211. Eddy Current Brake	117
6.212. Torque Control System.	119

TABLE OF CONTENTS (Cont.)

	<u>Page</u>
6.22. Electrical Power Control	124
6.3. Comparison of Regulation Techniques	127
7. PROTOTYPE DEVELOPMENT	147
7.1. Design Philosophy	147
7.11. Breadboard Hardware	147
7.12. Basic Unit.	148
7.13. Test Facilities	150
7.2. Prototype EPU's	151
8. MISSILE ELECTRICAL SYSTEM STUDY.	155
8.1. Power Utilization Equipment.	156
8.2. Power Transmission.	157
8.3. Power Generation and Conversion.	158
8.4. Prime Energy Source and Prime Mover.	161
8.5. Design Example	163
8.6. Conclusions	164
9. CONCLUSIONS AND FUTURE WORK.	170
9.1. Educational Contributions	170
9.2. National Significance.	171
9.3. Future Work.	171
APPENDIX A. ENERGY SOURCE CALCULATIONS	173
APPENDIX B. WEIGHT COMPARISON OF SOLID-FUEL AND LIQUID-FUEL GAS-GENERATION SYSTEMS	176
APPENDIX C. BIBLIOGRAPHY.	184

LIST OF FIGURES

Fig. No.		Page
1.	Alternative internal power systems for air-to-air missile.	23
2.	Gas generator weight and fuel weight vs. isentropic power for several durations for a solid fuel of $I_{sp} = 175$ sec.	24
3.	Gas-generator weight and fuel weight vs. isentropic power for several durations for a liquid monofuel of $I_{sp} = 175$ sec.	24
4.	Generalized missile internal power system.	47
5.	Solid fuel burning rate characteristics.	47
6.	Ignitor and solid fuels.	47
7.	Ignition recordings.	48
8.	Details of integrated ignitor.	49
9.	Recordings of ignition-pressure transients.	49
	a. Combustion of ignitor.	
	b. Combustion of ignitor and fuel.	
	c. Combustion of ignitor and fuel with pressure-relief valve attached.	
10.	Effects of solid fuel gases on pressure regulator seat.	50
11.	Effects of solid fuel gases on aluminum turbine.	51
12.	Plot of isentropic $hp/in.^2$ of nozzle throat area vs. total supply pressure for several supply-gas temperatures.	52
13.	Center and rim temperature of partial admission turbine vs. time for two admission percentages and for two materials.	53
14.	Efficiency vs. velocity ratio for several turbine types with nozzle angle of 20° and friction losses.	69
15.	Plot of turbine Mach numbers vs. velocity ratio for several ratios of wheel speed to supply-gas Mach number when $k = 1.4$ and $\alpha = 20^\circ$	69
16.	Geometry of partial-admission-turbine operation.	70
17.	Typical nozzle and rotor blading.	70

LIST OF FIGURES (contd.)

Fig. No.	Page	
18.	Plot of predicted analytical curve in relation to experimental points of efficiency ratio vs. ratio of nozzle arc width to rotor-blade spacing; $l_s = 0.2$ inch and $U/V_{a1} = 0.325$	70
19.	Plot of design-point turbine efficiency vs. velocity ratio for several ratios of nozzle arc width to rotor-blade spacing showing effect of partial admission.	71
20.	Plot of predicted analytical curve in relation to experimental points of partial-admission turbine efficiency vs. pressure ratio showing off-design-point performance.	71
21.	Plot of drag torque coefficient vs. Reynolds number for several bladed disks and disks with no blades	72
22.	Plot of turbine efficiency vs. area ratio for supersonic nozzles with $U/V_e = 0.325$	72
23.	Plot of turbine efficiency vs. aspect ratio for convergent nozzles; $C_s = 0.407$ inch, $C_r = 0.285$ inch, $U/V_e = 0.325$, and $P_2/P_{oo} = 0.45$	72
24.	Plot of nozzle efficiency vs. aspect ratio for convergent nozzles; $C_s = 0.407$ inch, $U/V_e = 0.325$, and $P_2/P_{oo} = 0.45$	73
25.	Plot of turbine efficiency ratio vs. pressure ratio showing effect of Reynolds number for convergent nozzles with several stator blade lengths; $U/c_o = 0.35$ and $P_2/P_{oo} = 0.45$	73
26.	Plot of turbine efficiency ratio vs. pressure ratio showing effect of Reynolds number for supersonic nozzles; $A/A^* = 1.295$, $l_s = 0.10$ inch, $U/c_o = 0.45$ and $P_2/P_{oo} = 0.10$	73
27.	Plot of flow ratio vs. pressure ratio showing effect of Reynolds number for convergent nozzles with several stator blade lengths.	74

LIST OF FIGURES (contd)

Fig. No.	Page	
28.	Plot of flow ratio vs. pressure ratio showing effect of Reynolds number for supersonic nozzles with stator blade length of 0.10 inch.	74
29.	Plot of nozzle efficiency vs. pressure ratio for convergent nozzles with several stator blade lengths.	74
30.	Plot of nozzle efficiency vs. pressure ratio for supersonic nozzles with several area ratios and stator blade length of 0.10 inch.	75
31.	Plots of efficiency and stator blade length vs. nozzle outlet area in the plane of the wheel for partial-admission turbines; $C_r = 0.285$ inch, $U/V_e = 0.325$, and $\alpha_1 = 20^\circ$	75
32.	Turbine air test facility.	76
33.	The D. A. C. L. air-absorption dynamometer	76
34.	Air absorption dynamometer characteristics	77
35.	Templates and finished nozzle block.	78
36.	Turbine wheels.	78
37.	Equivalent circuits for induction machine	100
	a. Standard representation for motor.	
	b. Modified form for induction alternator.	
	c. Simplified form for induction alternator.	
38.	Determination of machine operating point by intersection of curves of inductive and capacitive reactance.	100
39.	Electrical dynamometer.	101
40.	Induction-alternator voltage as a function of shaft speed, excitation capacity, and load resistance.	101
41.	Torque-slip characteristic of induction machine.	101
42.	Efficiency of induction machine both as an alternator and as a motor.	102
43.	Results of input-power changes.	102
44.	Results of load-resistance changes--Group I.	103
45.	Results of load-resistances changes--Group II.	103

LIST OF FIGURES (contd)

Fig. No.	Page
46. Results of capacitance changes--Group II.	104
47. Results of capacitance changes--Group II.	104
48. Pressure regulator.	129
49. Regulation characteristics of Model I regulator.	129
50. Recording with pressure regulator.	129
51. Schematic diagram of basic system and regulator.	130
52. Signal flow diagram of basic system and regulator.	131
53. Scale drawing of centrifugal pump.	132
54. Speed characteristics of centrifugal pump (Impeller diameter = 0.814 in.)	133
55. Flow characteristics of centrifugal pump (Impeller diameter = 0.814 in.)	134
56. Temperature characteristics of centrifugal pump (Impeller diameter = 0.814 in.)	135
57. Scale drawing of controller and dump valve.	136
58. Solid fuel ignition transient using entire regulator system.	137
59. Experimental transient response of control shaft.	138
60. Geometry of eddy-current-brake field structure.	139
61. Weight of field structure as a function of air-gap and iron flux density for a conventional wire coil.	139
63. Eddy-current brake and control amplifier.	140
63. Characteristic of eddy-current brake for fixed field current.	140
64. Eddy-current-brake torque and absorbed power as a function of brake function for fixed shaft speed.	141
65. Mathematical model of EPU system.	142
66. Mathematical model of proportional controller.	142
67a. Computed performance of EPU system model with off-on control.	143
67b. Recorded performance of simulation unit with off-on control.	143

LIST OF FIGURES (contd)

Fig. No		Page
68.	Recording of EPU operation in self powered mode at 165°F	144
69.	Recording of EPU operation in self-powered mode at -65°F.	144
70.	Operating characteristics of EPU in self-powered mode.	145
71.	Recording of EPU operation at high ambient temperature (+135°F).	145
72.	Recording of EPU operation at minimum ambient temperature (-70°F).	146
73.	Test setup of "breadboard" hardware.	153
74.	Basic unit.	153
75.	Energy source and prime mover.	154
76.	Assembly of EPU rotating parts.	154
77.	Relative characteristics of magnetic amplifiers (figure of merit M , power gain K_p , time constant τ , and weight W) vs. supply frequency.	166
78.	Relative weight of signal transformers as a function of frequency. Solid curve is for input impedance greater than or equal to a given value; dashed curve is for phase shift less than or equal to a given value.	166
79.	Transmission-line impedance per unit length per conductor vs. frequency for different wire sizes. Solid curves are for zero space between conductors, and dashed curves for 1-in. spacing between centers of conductors.	167
80.	Relative weight of alternators as a function of frequency.	167
81.	Relative weight of alterators as a function of number of poles.	168
82.	Relative weight of power transformers as a function of frequency.	168
83.	Weight comparison of a 400-cps 450-watt and a 3200-cps 450-watt power supply.	169

LIST OF FIGURES (contd)

Fig. No.	Page
B. 1. Geometry of solid fuel gas generation system.	183
B. 2. Geometry of liquid fuel gas generation system.	183

1. INTRODUCTION

1.1. The Nature of This Paper.

This paper is a discussion of an engineering project whose purpose it was to develop internal power supplies for several missile systems. It is intended to outline the basis on which the decisions which molded the direction of the project were made, to identify and review the basic investigations carried on by the project in order to determine the design criteria essential to the design of the components, to document some of the unique features of the power units developed, to outline the design philosophy which guided the project, and to touch on the specific design accomplishments of the project.

The project was the joint venture of a number of people of whom the author had the privilege to be supervisor. It was staffed entirely by research assistants and recent graduates supplemented by graduate and undergraduate thesis students. None of the individuals associated with the project had had any previous professional engineering experience. The results are offered as testimony of the remarkable capacity of well-trained, imaginative, ambitious young people.

Much of the material in this paper has been published as technical reports and theses as recorded in the bibliography.

1.2. The Nature of the Problem.

All flight vehicles have internal power needs such as electric, hydraulic or pneumatic control power, fuel and/or oxidizer pressurization etc., which must be provided by an internal power system.

On flight vehicles with propulsion systems which include a rotating shaft, the internal power generators are gear driven directly from the primary propulsion system.

Since most missile propulsive systems do not include a rotating shaft, and, since they usually are powered for only part of their total flight duration, missile internal power requirements must be provided by power systems which are completely independent of the prime propulsion system. Furthermore, the logistic and tactical applications of guided missiles are such that all their components including that of the internal power source must be capable of long-time storage under difficult logistic conditions and then very rapid and reliable activation under tactical conditions of extreme temperature, vibration, acceleration, etc.

In the comparison of alternative missile internal power (MIP) systems to satisfy a specific requirement, assuming comparable performance and reliability, the primary criterion is minimum weight. The significance of weight on flight vehicle performance is characterized by "growth" or "penalty" factors which are a relative measure of the incremental weight increase of the over-all vehicle required to maintain performance (in terms of range, speed, altitude, etc.) per unit weight of added sub-system or component. Typical penalty factors range from 1.5 to 2 for air-to-air missiles to 30 - 70 for long-range ballistic missiles and up to 200 when a weapon system including a launching aircraft is considered.

The problem, then, is to develop internal power components of minimum weight which meet all other requirements.

In the consideration of any system, it should be recognized that the optimization of the system with respect to a desired variable, i. e., weight, is not necessarily achieved by independently optimizing the several components of the system with respect to the same variable since the refinement of a particular component may deleteriously affect the optimization of an associated component. However, in the major part

of this dissertation, the concern will be with the weight optimization of the internal power generating system. In Sec. 8, the optimization of the over-all electrical system is discussed.

1.3. Historical Perspective.

In light of the rapid evolution of missile research and development, it is appropriate to comment briefly on the status of MIP.

Glamour and expediency have conspired, in almost all cases, to reduce missile power system considerations to lowest priority. In comparison with the challenge and essentiality of guidance, propulsion, supersonic aerodynamics, and control, power has been considered mundane. What is worse, it has often been considered that the miniaturized short-life components necessary for missile power systems could be designed by scaling-down larger more thoroughly understood components such as the turbines, generators and control systems found in commercial power applications.

These attitudes have greatly prejudiced the development of good components and have militated against support of much of the basic work which must be done before really optimal components and systems can be evolved.¹⁺

This unwholesome approach results largely from the availability of batteries, vibrators, commercial accumulators, etc., suitable for providing internal missile power for experimental and system feasibility studies. Although the logistic and tactical feasibility and reliability of these temporary supplies are suspect their existence has distracted major attention from the MIP problem.

⁺ Superscript numerals designate the references in the Bibliography, Appendix C.

A strong case can be made that MIP had been one of the last considerations in the "fixing" of missile systems to make them logistically and tactically feasible and sufficiently reliable. * In fact the major hardware developments of the Massachusetts Institute of Technology (M. I. T.) Dynamic Analysis and Control Laboratory (D. A. C. L.) program have had as their goal the satisfaction of the already established requirements of several missile systems. The most significant detriment of this policy of temporary expedient and "fix" components is that the missile internal power system is very rarely considered as a system in the early stages of a new missile design. The existence of MIP components which demonstrate adequate performance and reliability and power system studies which indicate the substantial advantages of new missile power standards will most certainly result in the recognition of and application of the system concept to MIP.

* "The auxiliary power plant has been the unloved step-child of both the electrical and power plant groups. The auxiliary power plant has not progressed in reliability, efficiency, weight and adaptability to the degree the main propulsion systems have because no sustained development program has been followed. -----It is recommended that provision be made for a sustained program of aircraft auxiliary power plant research and development of a minimum size to insure orderly and continuous improvement." Report of the advisory staff for aircraft electrical systems, Report No. AD-78412, March 14-25, 1955.

2. AIR-TO-AIR MISSILE POWER SYSTEM

The work discussed in this paper relates primarily to power units for air-to-air missiles, although the interests of the program and the applications of many of the conclusions are much broader in scope. In Sec. 8 the electrical systems of all missile categories are discussed and in Sec. 9 missile component and system research and development needs are discussed generally.

MIP requirements include both electrical and pressurized fluid power, usually hydraulic. For the reasons given in Sec. 2.21 the M.I.T. -D.A.C.L. projects' major emphasis has been on electrical power unit (EPU) development.

2.1. Requirements and Specifications

In order to quantitatively characterize the problem and in order to establish standards by which the applicability and appropriateness of certain design techniques and decisions may be made, it is important that the general requirements imposed on an EPU of an air-to-air missile be outlined. Both in the interests of military security and in the interests of generality, no attempt is made to describe the specific requirements of any particular missile system; rather, the intent is to express a quantitative appraisal of the typical specifications imposed on this kind of system.

2.11. Electrical Power Requirements

Practically all air-to-air missile systems require internal electrical power prior to their launching from the parent aircraft in order to be in a state of readiness for very rapid commitment. Guidance systems which are passive pre-launch require only that electron-tube filaments be heated, gyros be at desired speed, etc. Active pre-launch guidance systems have

similar power requirements pre-and post-launch. Very rapid commitment (a fraction of a second) is essential to achieve successful interception by the missile since the attacking aircraft and target may both be traveling at supersonic speeds with a very high closing velocity. As a general rule, the missile electrical loads require voltage and frequency regulation between 2 and 5 per cent both pre-and post-launch. During the commitment interval when the transfer of power from external to internal means is achieved some loosening of the frequency and voltage tolerance is usually permitted although severe transients are prohibited.

In the case of air-to-air missiles, the missile electrical system load is predominantly electron-tube heaters and plate voltages and is therefore, relatively time invariant. The major load variations are due to statistical manufacturing variations in the resistances of the numerous system components and the change of electrical resistance with ambient temperature.

A variety of a-c and d-c voltages at different levels and at one or more a-c frequency is required. Specific requirements as to harmonic distortion, phase angle, etc., are prescribed.

2.12. Environmental Requirements

At the present time, missile components are required to endure nonoperating temperature storage over a temperature range from -85°F to $+185^{\circ}\text{F}$ for periods exceeding a year.

The present operating temperature range is between -65°F and $+165^{\circ}\text{F}$. This upper limit is actually too low considering the ram air recovery temperatures of new supersonic aircraft. Relative humidity from 0 to 100 per cent is prescribed as is an altitude range from sea level to upwards of 100,000 feet.

The shock, acceleration, and vibration requirements are particularly severe. Typically, accelerations up to 50 times gravity for periods of several seconds are not unusual. Vibration requirements necessitate sweeps between 3 and 500 cycles per second at amplitudes up to eight times gravity, and shocks applied at the rate of 100 g per millisecond are typical.

2.13. Mechanical Requirements

As suggested in the introduction, the emphasis is on minimum weight and minimum volume. Absolute restrictions occur when an internal power unit is to be developed to fit a specific missile application. In such a case, the electrical requirements are usually fixed as is the space and volume available, since the EPU is a substitute for a previous experimental component such as a battery box.

In the case where the over-all missile power system is considered at the inception of the missile study the emphasis is on over-all system minimum weight and volume. Here interplay and compromise between the statement of the electrical requirements and the feasibility of providing same could contribute greatly toward the over-all optimization of the missile electrical system by the simultaneous study of power generation, transmission, and utilization problems. This ideal has not as yet been achieved.

2.2. Alternative Energy Sources and Systems

The problem of optimizing a complicated real system with regard to one or more variables is a formidable if not literally impossible task. To begin with, to optimize with regard to a particular variable, for example, weight, one assumes maintaining constant all the other significant variable attributes of the system. In the MIP case, significant variables might be tactical and logistic compatibility, reliability, and performance. In a practical engineering sense, compliance with

these three system attributes can only be confidently measured by the actual design and test of the alternative solutions to the problem.

The optimization decision is greatly compounded in systems composed of a variety of components by the relative state of ignorance of the various components. For example, the maximum attainable power-per-weight-ratios of the divers sorts of energy conversion equipment pertinent to MIP are rarely known with any precision until detailed investigations, including experimental studies, of the particular component are made.

Beyond these difficulties of the assurance of comparable compatibility, performance, and reliability, and relative ignorance as to the power-weight ratio of components, is the fact that any final system is a conglomeration of components plus other hardware such as frames, plumbing, wiring, connections, etc., the details of which cannot be known prior to the actual design of the system comprising the particular components. Thus, the optimization problem is a multi-dimensional problem with a great margin of unreliability attached to the input information. Of course, it is in no way an unusual problem to the engineer whose aim (and charge) it is to make decisions in the absence of the concrete and specific information he would like to have.

2.21. Generalized Energy Comparison.

Very early in the MIP investigation, comparisons of prime energy sources and estimates of energy conversion devices on a volume and weight basis were made recognizing all of the above limitations. In order to establish a basis of comparison at that time, a total energy requirement was assumed and the volume and weight of the prime

energy source necessary to provide this requirement was evaluated. In this particular case, the required energy was assumed to be 3.5 kw for 45 seconds or 11.6×10^4 foot-pounds.

Objective comparison is difficult since the energy from various sources is obtained in different forms and the complications in applying these various forms to the ultimate power need varies greatly. To minimize these disparities and to provide a measure of relative energy capacity, the energy is measured in the form it appears immediately external to the source and the weight and volume of the energy source necessary to provide the assumed requirement excluding all containers, supports, etc., is indicated in Table I. A figure of merit, in foot-pounds per pound and foot pounds per inch³ is given for each different source at this total energy level. For each source the comments column in the tabulation indicates the prime assumptions inherent in the energy calculations. Greater detail on each calculation is indicated in Appendix A.

Not even considering the very trying problems of initial energy input and mechanical support, the purely mechanical sources, the flywheel and the spring are not competitive. Batteries likewise bulk large comparatively although their output energy is in the form almost directly useable for a part of the missile load. *

* Battery research and development for EPU applications has been and continues to be sustained at a high level of support. Integrated battery units capable of remote activation, i. e., automatic insertion of electrolyte and concomitant long storage life, are just becoming available but are not yet adequately evaluated. They are presently limited to low-voltage high-drain types suitable for electron-tube filament loads. The high-voltage plate and grid load requirements which constitute about one-half of the average missile electrical load have to be provided by means of conversion by mechanical vibrators or conventional inverters or dynamotors. Either of these solutions is quite unsatisfactory. The possibility of static transistorized inverters is quite attractive weight, volume and reliability-wise but awaits transistors with suitable temperature characteristics. Many-celled high-voltage rapid-activate batteries are under development but their feasibility has not yet been demonstrated.

Energy Source	Wt. (lbs)	Vol. (in. ³)	Specific Weight $\left(\frac{\text{Ft-lbs}}{\text{lb}} \times 10^{-4}\right)$	Specific Vol. $\left(\frac{\text{Ft-lbs}}{\text{in.}^3} \times 10^{-3}\right)$	Comments
Solid Fuel Fast Burning	0.216	3.93	54.	29	Jet energy from empirical specific thrust. Grain: 0.54 in. dia. -17.1 in. long
	0.631	12.4	18.	9.4	
Hydrogen Peroxide 90 per cent	0.344	6.82	34.	17.	Jet energy from theoretical specific thrust Actual peroxide turbine performance from Bendix Data
	3.31	65.7	3.5	1.7	
Flywheel	6.65	23.8	1.7	4.9	Extracting all the kinetic energy of the disc; losses assumed to be zero.
Batteries	2.92	43.8	4.0	2.6	Electrical energy--45 sec discharge to 90 per cent of initial terminal voltage.
Compressed Air $\frac{P_2}{P_1} = \frac{1}{5}$	4.62	302.	2.5	0.38	Work for adiabatic reversible expansion $P_1 = 5000$ psia
	1.39	91.1	10.0	1.3	
Spring	773	6150	0.015	0.019	Helical power spring-extracting all the potential energy

Table 1. Weight and volume estimate of prime energy sources.

In comparison with high temperature gaseous working fluids, compressed gas weight and volume is seen to be inordinately high and the figures do not include the very high weight of high-pressure storage containers.

The use of air pressurized by ram impact of the rapidly moving missile is impractical for air-to-air missiles because of the usual need for internal power during the launching transient, the wide variations in missile velocity and air density, and the effects of angle of attack on performance of the diffuser which usually cannot be mounted in the nose where it would interfere with the guidance system. The incorporation of a ram air system in any missile, since it affects the missile in a major way, presumes more and earlier missile internal power system consideration than has been the usual practice.

Section 2.22 develops in some detail the relative merits of liquid versus solid fuels.

In order to estimate the relative weights of systems based on the more attractive of the prime energy sources, an estimate was made of the weight and volume of the components necessary and intermediate between the prime energy source and final desired energy form. Estimated specific volume and weight with regard to power and efficiency of these devices is given in Table II. This data was derived by interpolation, extrapolation and intuition from existing commercial components as of January, 1952. With the estimates of Table I and Table II, the weight and volume of comparative power systems can be estimated.

Figure 1 and Table III compare on a weight and volume basis alternative schemes of furnishing the electrical and hydraulic require-

Components	v	w	n	V	W
High Speed d-c Motors	34	420	0.7		
Hydraulic pumps	80	400	0.65		
Alternators	12	175	0.8		
Turbines plus gearing	30	300	0.3		
Accumulators precharged (commercial)				$\frac{2\omega}{\frac{P_1}{P_3} - \frac{P_1}{P_2}}$	$1.4\sqrt{V}$
propellant pressurized				1.2ω	$1.4\sqrt{V}$
Inverters	4	120	0.5		
Electrical Filtering Components	?	?			

Stacking Factors:

Batteries	0.7
Rotary Systems	
German V-2	0.4
Bendix	0.5

Nomenclature:

v = watts/in.³

w = watts/lb.

n = efficiency

ω = working volume of hydraulic
fluid

V = packaged Volume (in.³)

W = packaged Weight (lb.)

P_1 = precharged pressure psi

P_2 = maximum working pressure

P_3 = minimum working pressure

Table II. Weight, Volume and Efficiency estimate
of MIP components as of January, 1952.

ments of a missile using either batteries or chemical fuels as the primary energy source. For reasons which are discussed in the Sec. 2.22 only solid fuels are considered. The output power requirement is assumed to consist of 1 kw of electrical power equally divided between low-voltage filament and high-voltage plate requirements, and a hydraulic fluid requirement of 0.7 gallons per minute at 3000 lbs. per square inch or 1.23 horsepower, all for 45 seconds.

On a comparative basis it is seen that battery systems are by and large heavier than solid fuel systems. The weight of pre-charged accumulators for hydraulic power is compared to the estimated weight of accumulators using the solid fuel gases directly. The alternative of generating hydraulic power mechanically by a turbine-driven pump versus a solid-fuel accumulator is considered. The regulation problem of the combined turbine-driven alternator and pump system would be much more severe than the case of separated electrical and hydraulic power systems since the electrical load of the missile is essentially constant, whereas the hydraulic power requirements fluctuate widely.

Of the systems shown in Fig. 1 and Table III, initial energy storage in batteries was not feasible at the time of the initiation of this project due to the complicated and time consuming task of inserting the electrolyte into the battery and the very short storage life of the batteries when so activated. A solid fuel system was clearly indicated. It was further decided to separate the electrical and hydraulic requirements of the missile on the basis of the regulation problem and due to the desirability of locating the electrical and hydraulic

Table III

COMPARISON OF SYSTEMS TO SATISFY THE INTERNAL POWER REQUIREMENTS OF A TYPICAL AIR-TO-AIR MISSILE

Electrical Requirements

1. 0.5 kw low voltage d-c or a-c power.
2. 0.5 kw various high voltage d-c power.

Hydraulic Requirement

1. 58 in.³ between 3400 and 1700 psi.
- and 2. 30 in.³ between 3400 and 800 psi.
- or 3. 162 in.³/min. at 3000 psi - pumped with small storage for peak demands.

System(1)		1 (2)	2	3	4	5	6	7
Battery	Weight (lbs.)	25. (3)	7.5 (7)	7.5 (7)				
	Volume	375.	150.	350.				
Converter(5)	Weight							
	Volume							
Transformer Rectifier and Filter(6)	Weight							
	Volume							
Motor	Weight			3.4				
	Volume			41.				
Pump	Weight			3.5	3.5			
	Volume			18.	18.			
Solid Fuel (Turbine)(8)	Weight				2.	2.	1.5	1.5
	Volume				20.	20.	15.	15.
Solid Fuel (Hot Gas Accum.)(8)	Weight							2.
	Volume							20.
Turbine(9)	Weight				10	5.5	5.5	5.5
	Volume				100.	55.	55.	55.
Alternator	Weight				9.5	9.5	9.5	9.5
	Volume				136.	136.	136.	136.

System (Cont.)		1	2	3	4	5	6	7
Pre-Pressurized(4) Accum. (57 in. ³)	Weight	22.	22.					
	Volume	236.	236.					
P. P. Accum. (4) (30 in. ³)	Weight	13.	13.				13.	
	Volume	80.	80.				80.	
P. P. Accum. (4) (5 in. ³)	Weight			7.	7.			
	Volume			25.	25.			
Hot Gas Accum. (87 in. ³)	Weight					10		
	Volume					104		
Hot Gas. Accum. (57 in. ³)	Weight							7.
	Volume							68.
Hot Gas Accum. (30 in. ³)	Weight							5.
	Volume							36.
System	Weight	60.	42.5	31.4	32.	27.	51.5	30.5
System	Volume	691.	466.	434.	299.	315.	522.	330.

NOTE: 1. Component weight, volume, and efficiency indicated in Table II based on conservative projection of components available in January 1952.

2. System 1 was realizable at the time and was used for feasibility and experimental study of the missile system. It provides a basis of comparison for projected systems 2 to 7.

3. Derived directly from existing experimental low and high-voltage battery pack, unsuited for logistical storage and handling and tactical applications.

4. Derived from commercial components with assumed 15 per cent possible reduction in weight and volume.

5. Dearth of data on minimum weight and volume a-c to d-c converters precluded useful estimate.

6. Extent of transforming, rectification and filtering equipment necessary precluded useful estimate. Furthermore, this equipment essential to any tactical power supply.

7. Projection of characteristics of hypothetical low-voltage remote-activate battery suited to logistic and tactical situation.

8. Estimate of fuel and ignitor system only.

9. Turbine changed with majority of structural elements (frame, combustion chamber, supports, etc.).

power generators immediately adjacent to the respective utilization equipment in the missile.

The volume figures given in Table III for the several systems is the total of the estimated volumes of respective components and does not include the fact that the elements cannot be closely packed together. Table II gives some very approximate stacking factors based on several systems existing at that time. A firm estimate of the necessary volume for any of the given systems would have to include a consideration of the stacking factor.

2.22. Chemical Energy

Based on the study of Sec. 2.21 five years ago and subsequently confirmed by experience, for the great majority of applications, chemical fuels, either liquid or solid are the preferred prime energy source for minimum-weight systems considering volume factors, logistical considerations, tactical and environmental conditions, producibility and reliability.

Almost exclusively the design of MIP systems have had to draw on chemical fuel research that has been directed toward the propulsion problem rather than the internal power problem. This is a natural consequence of the more urgent and prior need for rocket fuels and the difficulty of justifying the expense involved in the development of specialized MIP fuels in small quantities. The redirection of some of the effort involved in rocket development, reoriented with regard to the particular requirements of MIP, would be a long step toward improved fuels.

The requirements of a fuel satisfactory for propulsion can be quite different from those for an internal power application. For MIP

requirements, high specific thrust, which is of paramount importance in the propulsion case, has to be weighed against such considerations as fluid temperature and nonerosive qualities and stable burning or decomposition at very low flow-rates. The desirable characteristics of a solid or liquid fuel for MIP application also include ease, convenience, and safety of handling, stable storage under long duration and widely varying temperature conditions, short activation time, and combustion or decomposition products which are suitable for utilization in the prime mover.

For purposes of comparison of the various chemical fuels, it is convenient to study thermodynamic, design, and logistic and tactical considerations.²

2.221. Thermodynamic Considerations

The maximum energy per pound of fuel which can be extracted in an expansion process between initial temperature T_{oo} and pressure P_{oo} and ambient pressure P_2 is given by the isentropic enthalpy change ΔH_s .

$$\Delta H_s = c_p T_{oo} \left[1 - \left(\frac{P_2}{P_{oo}} \right)^{\frac{k-1}{k}} \right] \quad (1)$$

where

c_p is the specific heat at constant pressure

k is the ratio of specific heats at constant pressure and constant volume.

System and design considerations establish practical values for initial temperature and pressure ratio. The maximum limit on T_{oo} is related to prime-mover heat-transfer and material strength considerations

whereas the ratio P_2/P_{00} is determined by ambient pressure, stability of combustion of the fuel, and strength and weight considerations for the combustion chamber and, in some cases, the fuel storage containers.

The specific energy for several fuel systems is indicated in Table IV to provide a comparison between both presently used solid and liquid fuels and conceivable combinations of available chemicals. In all cases T_{00} is taken as 2000°F and P_2/P_{00} as 0.02. The fluid properties are evaluated at 1500°F and assumed constant.

2.222. Design Considerations

Weight optimization of a MIP system requires that the fuel storage and combustion be achieved with minimum-weight components. To provide a comparison between the weight of gas-generation systems using solid fuels versus those using liquid fuels, fuel weight and gas-generator weight (comprised of factors such as fuel, storage containers, pressurization equipment, combustion chamber, associated valving and piping) are plotted versus isentropic gas power and duration of operation in Figs. 2 and 3. As indicated in Appendix B, the curves are predicated on fuels with a specific impulse I_{sp} of 175 seconds ($I_{sp}^2 = 2\Delta H_s/g$) and densities of 0.055 pounds per inch³ for solid fuels and 0.036 pounds per inch³ for liquid fuels. Component geometries and strength of materials given in Appendix B are characteristic of the design practice applied to the components described in this paper. For solid fuels Fig. 2 takes into account the dependence of burning rate on temperature, in this case a 30 per cent increase in burning rate at $+165^{\circ}\text{F}$ over that of -65°F (see Sec. 3.1).

Table IV

SPECIFIC ENERGY OF FUEL SYSTEMS

Fuel System			Isentropic Enthalpy Change ΔH_s (BTU/lb)
Fuel	Oxidizer	Coolant	
Hydrogen	Oxygen	Hydrogen	1820
Hydrogen	Oxygen	Water	825
Methane	Oxygen	Methane	792
Normal Propyl Nitrate ($T_{oo} = 1920^{\circ}F$)			688
Ethylene Oxide ($T_{oo} = 1800^{\circ}F$)			670
Kerosene	Oxygen	Kerosene	622
Double-Base Solid Fuel (AOK)		Water	612

The liquid fuel system assumes compressed gas pressurization of the fuel storage container for fuel weight under 20 pounds and pump pressurization with small gas bottle for initiation for fuel weight above 20 pounds.

Figures 2 and 3 demonstrate that the simplicity of storage and combustion of solid fuels favors them over liquid fuels for low-power, short-duration systems. This condition results from the low weight of the hardware associated with the solid fuel system contrasted with the hardware for a comparable monopropellant liquid system. As power demand and the duration increase, the facility of control of the liquid fuel system overcomes its initial hardware weight disadvantage and the liquid system becomes clearly preferable. Bipropellant liquid systems carry somewhat higher hardware weight penalty.

Thus, energy flux regulation is a major consideration in the choice of a fuel system. As will be developed later, the mass-flow or burning-rate of a solid fuel is a function only of its geometry and of its storage temperature. On the other hand, flow of liquid fuel to the combustion chamber can be controlled by means of a metering valve. Therefore in cases where the load demand varies greatly and in cases where it is desirable or necessary to shut down the system and then to reinitiate it without intervening maintenance, a liquid fuel system is indicated. In the case of air-to-air missile systems electrical load variations are small and the reinitiation problem does not arise, since there appears little likelihood that multiple passes by the attack plane on the target before final missile launching will be necessary or possible due to the high closing rates and the marginal speed advantage of the attacking plane.

By and large, the adiabatic flame temperatures of the products-of-combustion of solid fuels are higher than monopropellant combustion or decomposition gases. High gas temperatures are particularly associated with those solid fuel-oxidizer combinations which exhibit easy ignition and relatively clean and non-erosive products of combustion. High temperature gases, when cooling techniques such as dilution, are not convenient or appropriate, impose stringent heat transfer problems on the prime mover. Operation is limited to durations compatible with the thermal-transient, a technique which has been exploited in the air-to-air missile EPU's described in this paper. The lower gas temperatures of certain of the monopropellants make them a more satisfactory choice for long duration and high power systems which require steady-state thermal operation.

The erosion, clogging and corrosion of the internal passages of the MIP gas generator or prime mover by the products of combustion must be considered. Section 3.4 discusses this problem for solid fuels; certain liquid fuels exhibit similar tendencies.

Other design considerations essential to reliable MIP performance are rapid and reliable ignition, discussed for solid fuels in Sec. 3.3, and uniform burning when subjected to all missile operational and environmental conditions. For reasons which are as yet not understood high accelerations can seriously affect the burning characteristics of solid fuels.

2.223. Logistic and Tactical Considerations

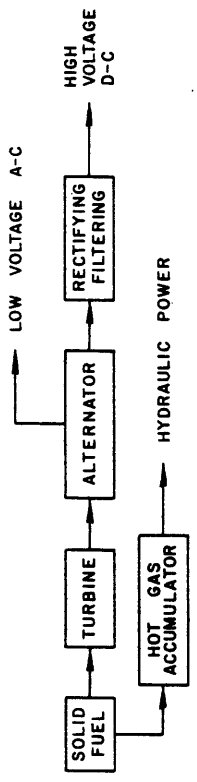
Fuels must withstand storage with no deterioration for extended periods of time under severe environmental conditions both in the MIP supply and in bulk storage. They should be amenable to indifferent

handling and should not constitute an undue personnel hazard. The personnel hazard of completely fueled units installed in missiles during storage and preflight handling must be established³ because design, reliability, and tactical considerations strongly indicate the desirability of an absolute minimum of access to the system prior to commitment.

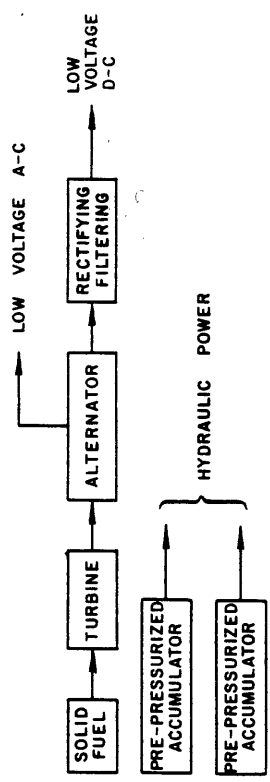
2.3. "Optimum" Energy Source

Based on the foregoing considerations the choice of energy source for the D. A. C. L. EPU's was made. For the requirements of an air-to-air missile EPU a solid fuel offered the most attractive choice for the following specific reasons:

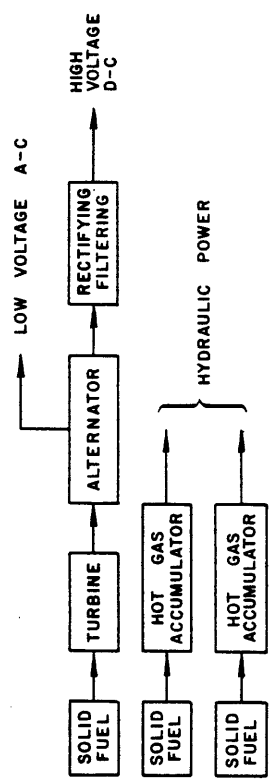
1. Lightest on a fuel energy per pound basis. Gas temperature appeared compatible with duration and temperature transient considerations.
2. Associated hardware, combustion chamber, storage chamber, and regulation devices considered to be lightest of all alternative energy sources.
3. Capable of long duration storage with no maintenance or deterioration.
4. Properties apparently compatible with environmental conditions.
5. Capable of very rapid and hopefully reliable ignition.
6. Products of combustion considered compatible with gas generator and prime mover passageways.
7. Safety hazard low.



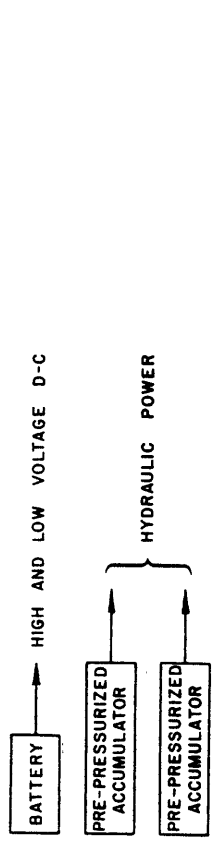
SYSTEM 5.



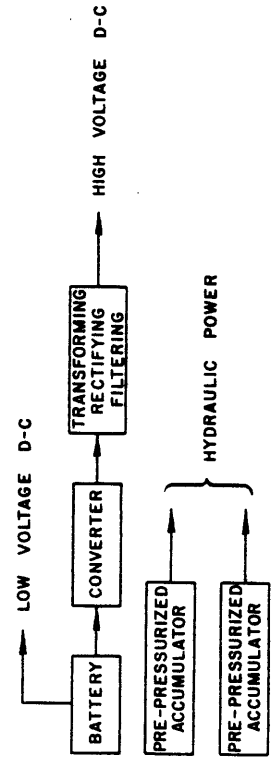
SYSTEM 6.



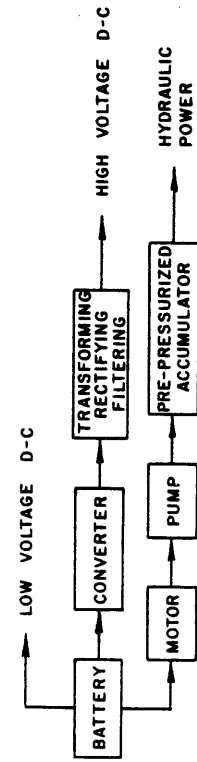
SYSTEM 7.



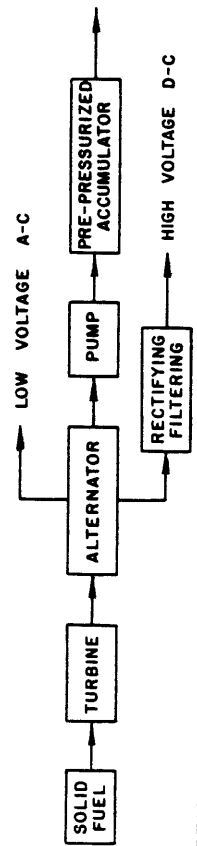
SYSTEM 1.



SYSTEM 2.



SYSTEM 3.



SYSTEM 4.

Fig. 1. Alternative internal power systems for air-to-air missile.

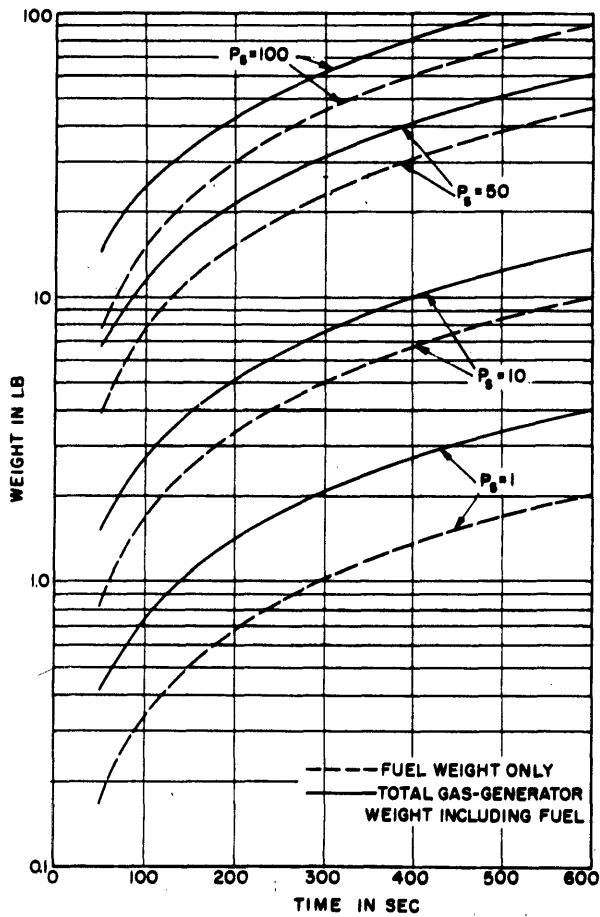


Fig. 2. Gas-generator weight and fuel weight vs. isentropic power for several durations for a solid fuel of $I_{sp} = 175$ sec.

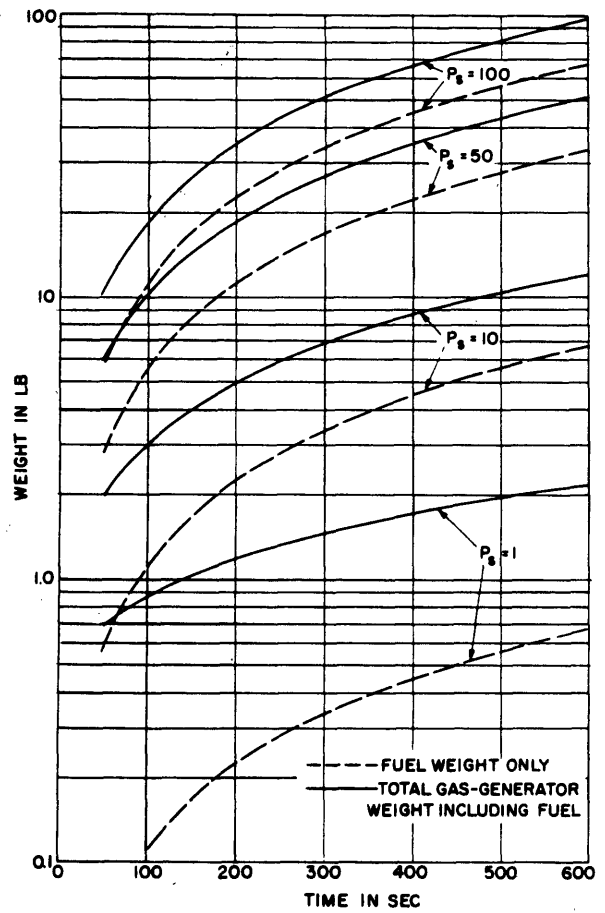


Fig. 3. Gas-generator weight and fuel weight vs. isentropic power for several durations for a liquid monofuel of $I_{sp} = 175$ sec.

3. SOLID FUEL SYSTEMS

The generalized power supply system is shown in Fig. 4 which indicates the typical elements and the energy flow between elements. A combustion chamber, which includes the solid fuel, delivers to a prime mover a mass-flow rate G of combustion gases at a pressure P which is determined by the fuel-burning characteristics and the system components as described later. This hot-gas flow may be controlled between combustion chamber and prime mover by a pressure controller as suggested in the block diagram. Regulated parameters are indicated by the subscript R . The prime mover in turn delivers shaft power to (torque \mathcal{T} and speed ω) an electrical generator, which in turn delivers electrical power, (voltage V and current I), to the load. The possible insertion of torque control between the turbine and electrical machine is indicated as is the possibility of power control between the generator and load. The general nature of these several controllers will be suggested by an understanding of the burning characteristics of the fuel.

3.1. Solid Fuel Combustion Characteristics

For most applications the solid fuel takes the form of a right-circular cylinder inhibited at one end and on its cylindrical surface by a noncombustible material which restricts the burning of the fuel to the uninhibited surface. The flame front progresses everywhere at the same rate down the length of the cylinder, remaining plane and perpendicular to the axis of the cylinder. This configuration is known as "cigarette" burning. Assuming a burning-rate constant with time this configuration provides a constant mass flow rate of products of combustion and is known as a neutral configuration. For rocket motor applications configurations which provide a much larger burning surface

area to mass ratio are provided. These take the form of multiple holes through a cylindrical grain or star-shaped perforations through a grain. In most cases these configurations are either regressive or progressive in the sense that mass-flow rate changes with time. In most rocket propulsion applications the thrust (which is proportional to the mass rate of flow) need not be constant with time as it must be for most internal power devices.

The burning characteristics of a typical solid fuel are indicated in Fig. 5. The mass flow rate G is determined by the burning rate, r , multiplied by the area of combustion A multiplied by the density of the solid fuel ρ .

$$G = r A_f \rho .$$

The burning rate is a function of the pressure at the combustion flame-front P_{oo} and the equilibrium temperature T_e at which the solid fuel was soaked prior to ignition.

$$r = f (P_{oo}, T_e)$$

The shape of the burning rate versus pressure curve for a given equilibrium temperature can vary between two extremes depending on the chemistry of the fuel. One limit is a rate proportional to pressure to a power; the other limit is represented by the so-called plateau-burning compositions which have burning rate independent of pressure over a limited pressure range. All solid fuels fall somewhere between these two extremes depending upon the formulation of the fuel, the geometry of the fuel grain, and the heat transfer conditions under which they are burned.

The effect of storage equilibrium temperature on burning rate can be very considerable, up to a 50 per cent change in burning rate based on the mean burning rate over the temperature range -65°F to $+165^{\circ}\text{F}$.

It is important to point out that burning rate versus pressure curves available from fuel manufacturers are usually determined by "strand" tests in which known lengths of fuel are burned under constant ambient pressures after controlled soaking at prescribed temperatures over the operating range. These data cannot be reliably applied to "vented-vessel" burning wherein the fuel is ignited in a vessel having a nozzle. Furthermore, the experimental burning-rate curve of the same fuel in different applications will vary somewhat depending upon the geometry of the grain configuration and the design of the vented vessel since heat transfer effects in the fuel are influenced by its burning geometry and the heat transfer capacity of the combustion chamber. Figure 5 illustrates the difference between the fuel manufacturers' strand tests and D. A. C. L. vented-vessel tests.

The wide burning rate variation with temperature poses a serious regulation problem. It has been proposed that this temperature dependence of the fuel be minimized or eliminated by externally heating the fuel prior to use to keep it at its maximum anticipated operational temperature. In most applications this external heating proves to be impractical due to the relatively high power demand on the launching system (for air-to-air missiles, the parent aircraft) and the time involved in bringing the grain to a standardized equilibrium temperature, from what might be a very low storage temperature.

The thermal conductivity of typical double base (nitroglycerine-nitrocellulose) fuel is 0.12 BTU/ft. hr. °F which is about the same as asbestos. The specific heat of the solid is 0.35 BTU/lb. °F and the mass density 0.055 lb/in.³. If the surface heat transfer coefficient, which will depend upon the design of the storage can, is known, the elapsed time to reach a new equilibrium temperature can be readily estimated by the use of the Gurney-Lurie charts⁴ which are the graphical presentation of the solution of the partial differential equation of unsteady heat-conduction in a cylindrical solid. In a typical application the time to reach equilibrium can be on the order of an hour.

The temperature dependence of the burning rate is directly related to the low thermal conductivity. The grain "remembers" its storage temperature even though the flame front advancing towards the yet uncombusted and cold fuel is at a temperature on the order of 2000 - 3000°F.

Since the EPU must perform satisfactorily over a broad operational temperature range, the design must accommodate to the concomitant wide range of burning rates.

3.2. Fuel Grain Dimensions

The dimensions of the fuel grain to achieve a certain desired output power may be determined with satisfactory accuracy as a first approximation by application of the specific thrust data of the fuel.⁵ These data are usually available since specific thrust is one of the primary characteristics of solid fuels used in propulsive rockets and is therefore analytically and experimentally determined and cataloged by solid fuel manufacturers.

Power in the jet P_j from a nozzle in terms of the kinetic energy of the gases is

$$P_j = \frac{G V_e^2}{2}$$

The effective exit velocity V_e and the specific impulse are related by the equation

$$V_e = g I_{sp}$$

where g is the gravitational constant.

Specific impulse is determined both theoretically from chemical reaction equations and empirically from static test firings. Experience on the project in comparing fuel power and output power has indicated that the effective I_{sp} in MIP applications is less than the experimental values reported by fuel manufacturers. This is not surprising since heat transfer effects are much more significant in MIP than in rocketry. The ratio of heat transfer surface and system heat capacity to gas mass flow rate is very much higher in MIP applications. Reduction in the reported experimental I_{sp} of from 15 to 20 per cent seems to be necessary. A concurrent S. B. thesis⁶ in which the actual gas temperature is being measured by burying several platinum-rhodium thermocouples in the fuel and dynamically recording the temperature as the flame front approaches and engulfs the couples has indicated gas temperatures which confirm this 15 - 20 per cent reduction.

The prime mover and power conversion machine efficiencies η_t , η_e are estimated in order to determine the mass flow required to provide the desired output power P , then

$$P = \eta_t \eta_e G \frac{(g_{sp}^I)^2}{2} ,$$

Thus the mass-rate of flow may be expressed as

$$G = \frac{2P}{(g_{sp}^I)^2} \cdot \frac{1}{\eta_t \eta_e} .$$

This value is the minimum flow of gas required from the combustion of the solid-fuel grain under all operating conditions. For a "cigarette" burning grain configuration,

$$G = rA_f \rho .$$

where the burning rate is determined from the solid fuel characteristics and the combustion chamber pressure which is determined by combustion stability, plateau burning characteristic, or design considerations. The lowest anticipated burning rate r_{min} will be determined by the minimum environmental temperature. Therefore, the minimum fuel area to provide the required flow is

$$A_f = \frac{G}{r_{min} \rho} .$$

The minimum charge length L must be adequate to provide the desired duration of burning t at the maximum burning rate r_{max} corresponding to the maximum environmental temperature.

$$L = r_{max} t$$

For space-restricted applications a technique was developed of folding the over-long grain into several shorter grains.⁷ The grains are

located in separate combustion chambers connected by a tube. A small hole through the inhibitor sheet on the bottom of the first grain permits hot gases to initiate the burning process in the second grain. This self-ignition technique can be extended to as many parallel grains as are necessary to achieve the desired duration. Depending on the diameter and depth of the hole in the prior grain the pressure-time relationship at "cross-over" for a given soaking temperature can exhibit over-pressure, under-pressure, or essentially constant pressure.

Since the over-all ratio between the combustion chamber pressure (250 - 1000 psi) and ambient pressure is always greater than the critical pressure ratio the flow from the combustion chamber is choked and is given by

$$G = \frac{A^* P_{oo}^*}{\sqrt{T_{oo}}} \sqrt{\frac{k}{gR} \left(\frac{2}{k+1}\right)^{\frac{k+1}{k-1}}} = \frac{A^* P_{oo}^*}{\sqrt{T_{oo}}} C_1 \quad (1)$$

where C_1 is a constant depending only on the gas constants R and the ratio of specific heats k . Stagnation temperature T_{oo} depends upon the solid fuel chemistry, the combustion process, and heat transfer from the combustion chamber.

Combining the nozzle flow rate with the solid fuel burning rate and solving for combustion-chamber pressure gives

$$P_{oo} = \frac{r\rho\sqrt{T_{oo}}}{C_1} \cdot \frac{A_f}{A^*}$$

The expression $r\rho\sqrt{T_{oo}}/C_1$ is determined for a particular choice of solid fuel, and combustion chamber design, ρ and C_1 are properties

of the fuel, r depends upon operating point pressure and soaking temperature, while T_{oo} is determined by the fuel and heat transfer. Thus, to maintain a particular pressure there is a particular ratio A_f/A^* . This ratio is usually designated as K_f and its experimental value is reported by fuel manufacturers for various pressures and fuel soaking temperatures. Frequently an existing EPU must be tailored to a different power output. Because of the choked flow through the nozzle, power will be related linearly to combustion-chamber pressure. If two values of power versus pressure are known experimentally, the K_f ratio together with the nozzle throat area will give the fuel area necessary to provide any desired pressure or power.

3.3. Solid Fuel Ignition

Systems to provide rapid and reliable ignition of solid fuels in small-free-volume restricted-exit chambers are determined by experimental evaluation of various ignition trains.^{5,7} Basically an ignition train consists of an electrical squib to initiate the burning process, black powder and intermediate fuels of higher burning-rate than the main solid fuel grain. Figure 6 illustrates these components as used in a typical power unit. The squib consists of an electrical resistance element encased in a molded pellet of match-head material initiated by 28V d-c at approximately 1 ampere. The delay time in the match is negligibly small. To prevent water absorption and consequent deterioration of the highly hygroscopic black powder the squib together with the black powder can be heat-sealed into a piece of plastic tubing as illustrated. Here the intermediate fuel is mortar

sheet cut into strips and inserted and cemented into saw slots in the uninhibited end of the solid fuel.

Upon ignition the squib ignites the black powder which burns very rapidly pressurizing the free volume of the combustion chamber, and providing hot particles of powder which ignite the mortar sheet. The mortar sheet which has a burning rate approximately four times greater than that of the main fuel grain maintains a high pressure in the combustion chamber which increases the burning-rate and therefore the ignitability of the main fuel grain. Ignition of the main grain results primarily from the impingement of hot particles on its surface.

The importance of the mortar sheet is shown in Fig. 7, where elements in the ignition train are sequentially studied. Figure 7a is a pressure recording of the black powder ignition alone. Figure 7b shows the high sustained pressure due to the presence of the mortar sheet. The ignitor peak pressure is a function of the quantity of black powder and mortar sheet and the combustion chamber free volume as well as the storage temperature prior to ignition. Thus a quantity of black powder which is adequate for proper ignition at plus 68°F is inadequate at -65°F. To compensate for the temperature range the quantity of black powder in the ignitor must be increased considerably to achieve proper -65°F operation. The pressure peak of the ignitor system and fuel at +70°F for an ignitor suitable for low temperature is indicated in Fig. 7c. A pressure regulator, discussed in detail in Sec. 6.11, can serve an incidental but very valuable purpose in eliminating this ignition peak as indicated in Fig. 7d. This relief action is particularly important after high temperature (+165°F) storage for which case the peak would be very high indeed.

An integrated ignitor train⁸ is shown in Fig. 8. This self-contained ignitor screws into the head of the combustion chamber and includes the electric squib, a mixture of sodium peroxide-magnesium powder and black powder and some AOK solid fuel substituting for the mortar sheet. The unit is sealed by a rupturable mylar diaphragm on the combustion chamber side and by rubber gasket on the wiring side. The performance of this ignitor with and without fuel and with a very simple pressure relief valve is shown in Fig. 9. In this case, the very high pressure peak results from the trebling of the quantity of magnesium and sodium peroxide powder used at room temperature to insure reliable operation at -65°F .

Although the estimating of the kinds and quantities of the several constituents in an ignitor is enhanced by studying the pressure-ignition transients, the detailed design of an ignitor for a given combustion chamber to provide reliable operation over the entire environmental range is largely cut-and-try experimental process. Not enough is presently known about the criteria for solid fuel ignition or the transient combustion characteristics of the several constituent components to make detailed analysis of the process useful. Extensive study is necessary and justified since the reliability of a solid fuel device depends entirely upon proper ignition.

3.4. Characteristics of the Combustion Gases

The products of combustion of solid fuses are predominately gaseous, the constituents depending upon the chemistry of the particular fuel-oxidizer combination. However, all solid-fuel combustion-products, in varying degrees, contain small percentages of solid particles, in the form of uncombusted fuel or oxidizer or ash. Since these solid particles do not seriously affect rocket motors the fuel industry has displayed little

interest in studying them. For any given fuel it is not possible at the present time to get quantitative information on the solid content of the combustion products nor any details on their erosive or corrosive or agglomerative nature. A real need exists to develop techniques for measuring and establishing standards on dirt content and its effects.

As an indication of the influence of dirt on EPU performance,⁹ Figs. 10 and 11, respectively show a pressure regulator seat and turbine wheel after a single 30-second operation using two different fuels. While the products of combustion of double-base fuel (nitroglycerine-nitrocellulose) contain solid particles (predominately finely divided carbon) the particles have no tendency to agglomerate and little tendency to erode or corrode the various passageways as indicated by the center photo, Fig. 10 and top photo Fig. 11. On the contrary the lower photo of Fig. 10 and center photo of Fig. 11 show the effects of a polyvinyl base ammonium perchloride fuel of similar ballistic properties. Turbine performance was so reduced due to clogging of the rotor channels that the wheel stalled. The post operative corrosion caused by the polyvinyl fuel is indicated in the lower photo of Fig. 11. A completely erratic pressure versus time record indicated the total inacceptability of this second fuel for MIP applications, whereas its use in rocket devices has proven completely acceptable. The presence of solid particles can be particularly objectionable for systems with very small passageways as in servovalves or in pressurized gas bearings.

Some beginning efforts have been made on the project to determine the percentage and nature of the solid particles in double-base fuels and the effectiveness of sintered stainless steel filters. The pressure drop across a 5 micron 1-1/4 inch diameter filter seems to level off at

50 psi for 30 second runs at 500 psi stagnation and 0.001 lb/sec. flow. The percentage-by-weight of the solid particles determined by weighing the filter before and after testing is approximately 2.5 per cent. At the present time the only measure of the cleanliness of the filtered gas is the visual examination of a white card upon which the exhaust gas impinged. Much needs to be done in this area to develop techniques and establish standards.

3.5. Regulation Problems

As indicated in Sec. 2.11 power systems specifications require regulation of one or more of the output parameters with the load demand which is either constant or which varies with time. Missile electrical system loads which are predominately electronic or magnetic-amplifier very closely approximate a constant demand. When electromagnetic devices, motors, etc., are included load variations can increase. For very simple systems hydraulic power demands are often constant since dump valves are used to regulate pressure by by-passing unnecessary flow. More sophisticated systems use unloading valves which impose upon the power system load fluctuations which can become quite large.

A study of the parameters which affect the rate of energy generation by the solid fuel suggests means by which control may be accomplished and indicates those unpredictable parameters which will influence performance. Once ignited the energy flux from the fuel is a function of its chemistry, the storage equilibrium temperature, the chamber pressure and burning area. Control of the energy flux to the prime mover may be effected by one of these variables. As indicated in Fig. 5 storage temperature plays an important role in the power generation of the fuel. In most applications little can be done about this variation. (see Sec. 3.1).

The burning rate can be a strong function of the combustion chamber pressure, therefore control of combustion chamber pressure can determine mass flow rate. Manufacturing variations in the fuel batches result in small variations in the burning-rate pressure curve.

The burning area of the fuel could be used as a control variable if the time variation of the mean desired output power were known in advance. However, in light of the other variables which influence burning rate this approach is probably fraught with difficulty.

Since for any given system there is a specified mean output power independent of environmental conditions the reduction in burning rate at low temperatures requires that the mass flow rate and therefore the area of combustion be adequate to maintain the maximum power output demand at the low temperature. To accommodate load demand variations the instantaneous output energy flux of the fuel will have to be always adequate to the maximum possible output demand. At any temperature above the minimum a higher than desired energy flux results from the increased burning rate.

The intractability of the chemical activity of the fuel to external control suggests that the control system, rather than being a prime-energy modulation system, must be a prime-energy dissipation system controlling the rate of dissipation or dumping of energy in such a way as to achieve the desired regulation of the output. Generally speaking, dissipative systems are uneconomical of volume and weight. However, for many applications the very high energy-density of the solid fuel in comparison with the energy-conversion density of the over-all power supply makes the fuel weight a relatively small part of the over-all system weight. In fact in the EPU's^{5, 8} described briefly in Sec. 8 the total fuel weight was but 5 per cent of the over-all weight.

3.6. Influence on the Prime Mover

The weight optimization of a solid fuel MIP is influenced by the efficiency of the prime mover in converting the fluid energy into mechanical shaft power for subsequent conversion to the final form desired. The characteristics of the working fluid and the operational specifications of MIP influence the choice of prime mover.²

3.61. Positive Displacement Prime Movers

Fluid properties, minimum weight requirements, and design considerations militate against positive displacement prime movers. The relative complexity of positive displacement equipment, particularly reciprocating engines, compared with dynamic fluid machinery is a serious disadvantage since, by and large, complexity and reliability are inversely related.

Since for a solid fuel system the gas generation must be external to the prime mover, expansion engines would be necessary. At the very high average gas temperature and with the solid content of the combustion gases the relative motion sealing and wear problems and the resulting friction losses would be very severe.

Furthermore, the displacement necessary to provide adequate gas expansion considering the available pressure ratio and the consequent size and weight of the expansion engines would be very high compared to dynamic fluid machinery. Piston velocity limitations due to dynamic forces and wear would reduce shaft speed well below that desirable for direct drive of low-weight electrical generators. As shown in Sec. 8, the trend is towards higher and higher shaft speeds and frequencies for electrical machinery. Vane motors using the compressible fluid would be of very low efficiency and would similarly exhibit relative

motion and friction difficulties at the high gas temperatures in the presence of solid particles.

3.62. Dynamic Fluid Prime Movers

The fluid properties (that is high temperature, pressure, and the presence of solid particles) the minimization of friction, wear and sealing problems, and relative simplicity favor the use of dynamic fluid machines as prime movers.

The specific energy of the working fluid and the desired output power strongly influenced turbine design. One convenient way to illustrate this is to calculate isentropic power per unit area for choked flow as a function of stagnation pressure and temperature. As indicated previously the mass flow through the choked nozzle is given by

$$\frac{G}{A^*} = \frac{P_{oo}}{\sqrt{T_{oo}}} \sqrt{\frac{k}{gR} \left(\frac{2}{k+1}\right)^{\frac{k+1}{k-1}}} = \frac{P_{oo}}{\sqrt{T_{oo}}} C_1$$

The isentropic available work is given by

$$\Delta H_s = c_p (T_{oo} - T_2)$$

Considering isentropic expansion of the gas

$$\frac{P}{\rho^k} = \text{constant}$$

and since isentropic power is given by

$$P_s = G\Delta H_s$$

combination of the above equations gives

$$\frac{P_s}{A} = C_1 c_p \sqrt{T_{oo}} P_{oo} \left[1 - \left(\frac{P_2}{P_{oo}} \right)^{\frac{k-1}{k}} \right],$$

the isentropic power per square inch of nozzle throat area as a function of gas properties and stagnation temperature and pressure and exhaust pressure. In Fig. 12 this relationship is plotted for a typical high energy fuel with a specific heat ratio of 0.5 BTU/lb-mass per degree, specific heat ratio of 1.25 and a back pressure of 15 lbs. per square inch. Typical properties of the products of combustion of high energy fuels is given in Table V.

A representative point at $T_{oo} = 2500^{\circ}\text{R}$, $P_{oo} = 300$ psi gives an isentropic power of 2000 hp/in.² illustrating the diminutive dimensions of the fluid flow passages of MIP prime movers, the power requirements of which may be as low as 1 horsepower or less.

Figure 12 indicates that in the majority of applications, the nozzle outlet area in the plane of the turbine rotor is very small compared to the peripheral inlet area of the rotor. The admission, defined as nozzle outlet area divided by total rotor inlet area, may be as low as two to three per cent. The resultant turbine is referred to as a partial admission turbine and will be discussed in Sec. 4.

The large enthalpy change available in the working fluid results in a very high fluid velocity in an expansion process

Table V

TYPICAL PROPERTIES OF PRODUCTS OF COMBUSTION OF HIGH ENERGY FUELS

	Liquid Monopropellant Fuel	Solid Fuel
c_p BTU/lb ^o F	0.514 - 0.533	0.45
k	1.28	1.25
T_{oo} (°F)	1800 - 2500	2500 - 3000
P_{oo} (psi)	300 - 500	350 - 3000
$C_1 = \sqrt{\frac{k}{Rg} \left(\frac{2}{k+1}\right)^{\frac{k+1}{k-1}}}$	0.398	0.428 - 0.450

$$V_e = \sqrt{2g\Delta H_s} = gI_{sp}$$

which for the fuel systems listed in Table 4 range between 5500 and 9500 feet per second. Since mechanical limitations restrict rotor blade velocity to the range of 1200 to 1500 feet per second the velocity ratio U/V_e can be as low as 0.12 for a single stage turbine, placing an upper limit on the turbine performance as shown in Fig. 14 in Sec. 4. Other restrictions such as the power frequency of direct driven electrical generators can result in even lower velocity ratios.

An unconventional type of turbine that has been proposed as competitive to a single-stage impulse turbine for very low velocity ratios is the drag turbine¹⁰ in which the pressurized gas is directed around the periphery of a radially bladed rotor. Leakage between inlet and outlet ports is minimized by a block seal. The basic fluid phenomena of this device have been attributed to the drag on the bladed rotor of the through-flow around the peripheral channel. The geometry of this turbine is identical to that of the regenerative pump, the basic principle of which has been suggested to be the superposition of a circulatory flow pattern due to centrifugal pumping of the radial blades on the peripheral through-flow.¹¹ The possible use of this drag turbine for low-power, very low velocity ratio applications suggests the need for further investigations, directed particularly toward a better understanding of the controlling physical phenomenon. Specific applications of the drag turbine have not been encouraging so far.

The pure-reaction or Heron turbine has received some attention due to its apparent simplicity, although the upper limit on its efficiency is half of that of bladed turbines. The need for a rotating seal for the hot

pressurized gases is a serious drawback. Attempts to eliminate the seal by rotating a solid-fuel grain have been limited to low-power short-duration systems and have been thwarted by the low mechanical strength of solid fuels.

3.63. Heat Transfer Considerations

The very high temperature of the products of combustion of certain solid fuels (in the case of double-base fuels as high as 3000^oF) raises the question of suitable turbine materials. The high temperature is compounded by the fact that for high efficiency, high rotor blade velocities corresponding to stress limited conditions are necessary.

As suggested earlier, in the case of air-to-air MIP units of low-power demand and short duration, it is often possible to work within the thermal transient so as not to exceed the hot strength of the rotor material. The heat transfer from the nozzle jet to the turbine wheel is considerably reduced for a partial admission turbine since any particular turbine blade is only subjected to the hot, high-velocity gases for a very small percentage of its total travel per shaft revolution. The peripheral temperature distribution due to this localized heating is very small.¹²

The radial temperature distribution has been investigated by first determining a heat transfer film coefficient based on flow about a streamlined body and the gas properties. The resulting film coefficient is of the order of 700 BTU/ft.²-hr. Due to the pulsing nature of the hot gas flow as seen from the rotor, the effective heat transfer coefficient is much less than this steady-state value. The steady-state coefficient multiplied by the ratio of the total area of the rotor blades (fin area) to the peripheral

area of the rotor disk and multiplied by the fractional arc of admission of the turbine nozzle provides an estimate of the effective coefficient. For a typical 4 inch diameter turbine rotor with an admission of 2.5 per cent the effective heat transfer coefficient is about $40 \text{ BTU/ft.}^2\text{-hr.}$ By applying this effective film coefficient in the unsteady-heat conduction analysis of a circular cylinder heated on its periphery and insulated on its sides, the temperature rise of the turbine rotor may be determined as a function of time. Figure 13 gives the center and rim temperature of a 4 inch diameter rotor for 2.5 and 5 per cent admission, for steel and aluminum rotors for a gas with an adiabatic recovery temperature of 2500°F.

Table VI which gives the pertinent physical properties of the several metals helps to explain the very different results between aluminum and steel. In the case of an aluminum rotor, high thermal conductivity results in a small radial temperature gradient but operation over a minute for 2.5 per cent admission results in disk temperatures above which the strength of aluminum is materially reduced. In the case of steel rotors the radial temperature gradient is large and for the case of 5 per cent admission the absolute temperature is high but the temperature corresponding to materially reduced strength of steel is much higher than for aluminum. Table VI also gives the physical properties of titanium which is particularly interesting due to its very high hot strength. Titanium's low specific gravity makes it particularly useful for applications where rapid acceleration of the turbine rotor inertia is essential. Figure 13 applied to the EPU problem indicates that for applications under a minute with low percentage admission (which corresponds to low power) aluminum rotors may be

Table VI

PHYSICAL PROPERTIES OF TURBINE ROTOR MATERIALS

	Aluminum 75ST	Stainless Steel A151 302	Titanium 3A1-5Cr
Melting point ($^{\circ}\text{F}$)	1220	2600	3135
Specific Heat BTU/lb $^{\circ}\text{F}$)	0.226	0.118	0.129
Thermal Conductivity BTU/ft 2 /hr/ $^{\circ}\text{F}$ /in.	845	113	105
Specific Gravity	2.7	7.85	4.5
Ultimate Strength psi x 10 3	82	89.4	150
Linear Coefficient of expansion in/in. $^{\circ}\text{F}$ x 10 $^{-6}$	12.9	7.8	5.0

Ref: Titanium in Industry, S. Abkowitz, J. J. Burke, and R. H. Hietz, Jr.,
New York, N. Y., D. Van Nostrand Company, Inc., 1955.

used greatly facilitating manufacture. The results of Fig. 13 have been supported by hot-gas tests up to and exceeding 100 seconds on aluminum and stainless steel rotors. Successful operation up to about one minute with aluminum rotors at 2.5 per cent admission has been demonstrated whereas extending operation to 110 to 120 seconds results in major structural failure. For steel rotors satisfactory operation up to two minutes has been achieved with 5 per cent admission. Attempts to measure temperatures directly using temperature-sensitive paints have been unsuccessful due to centrifugal effects and dirt in the combustion gases.

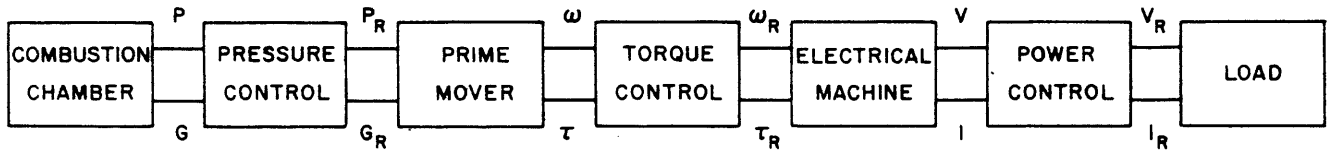


Fig. 4. Generalized missile internal power system

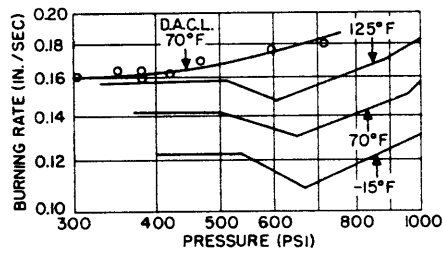


Fig. 5. Solid fuel burning rate characteristics.

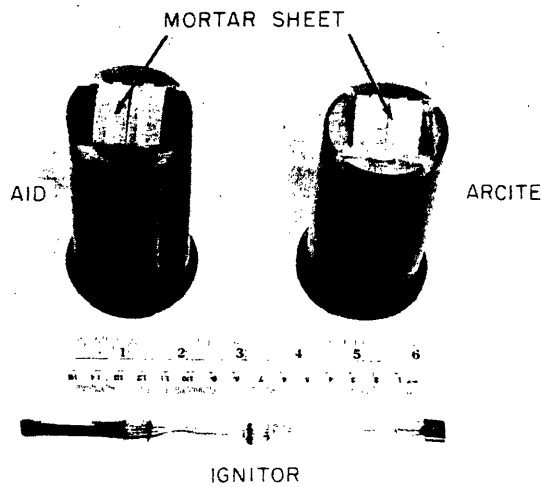
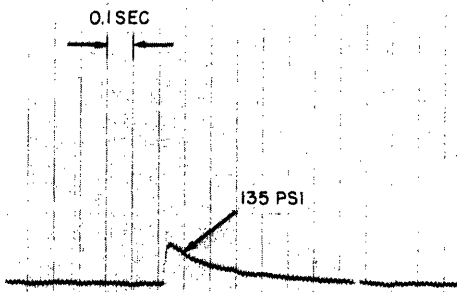
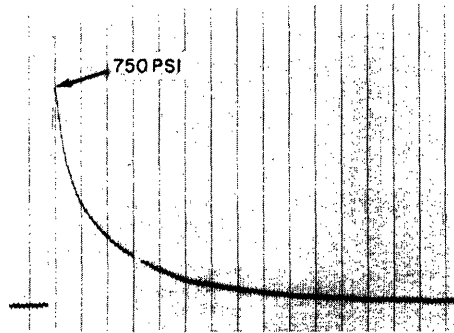


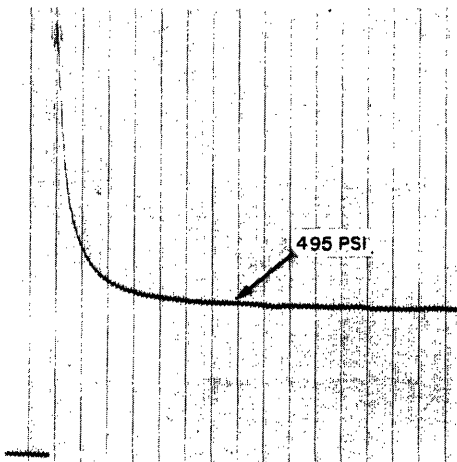
Fig. 6. Ignitor and solid fuels.



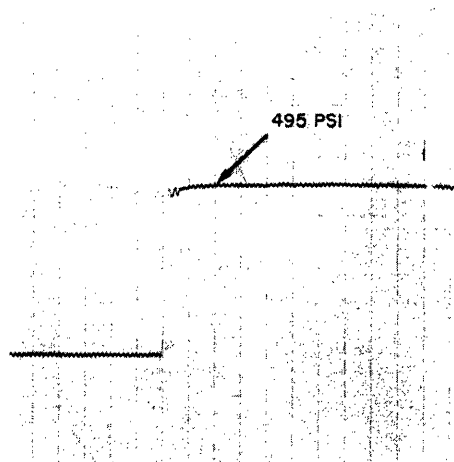
a. Black powder.



b. Black powder plus mortar sheet.



c. Black powder, mortar sheet, and propellant with nozzle.



d. Black powder, mortar sheet, and propellant with pressure regulator.

Fig. 7. Ignition recordings.

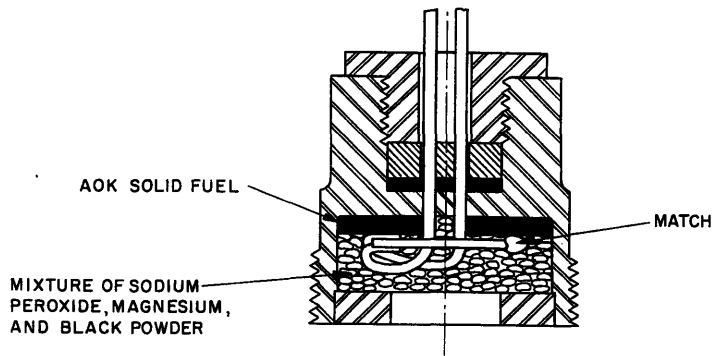


Fig. 8. Details of integrated ignitor.

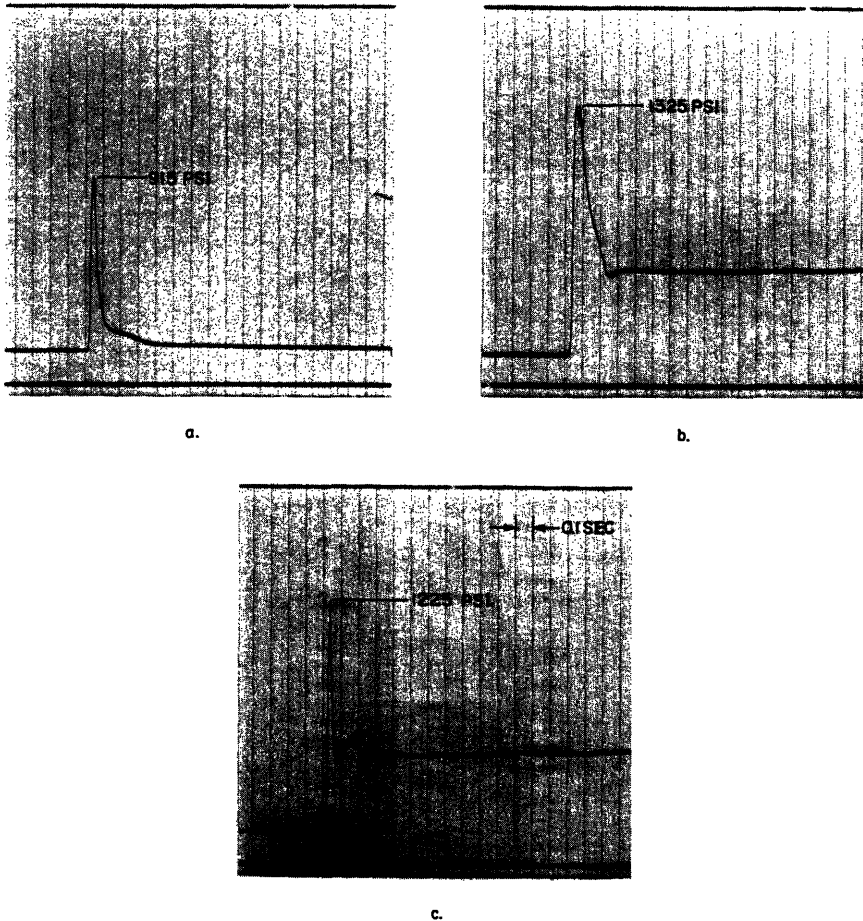


Fig. 9. Recordings of ignition-pressure transients.

- a. Combustion of ignitor.
- b. Combustion of ignitor and fuel.
- c. Combustion of ignitor and fuel with pressure-relief valve attached.

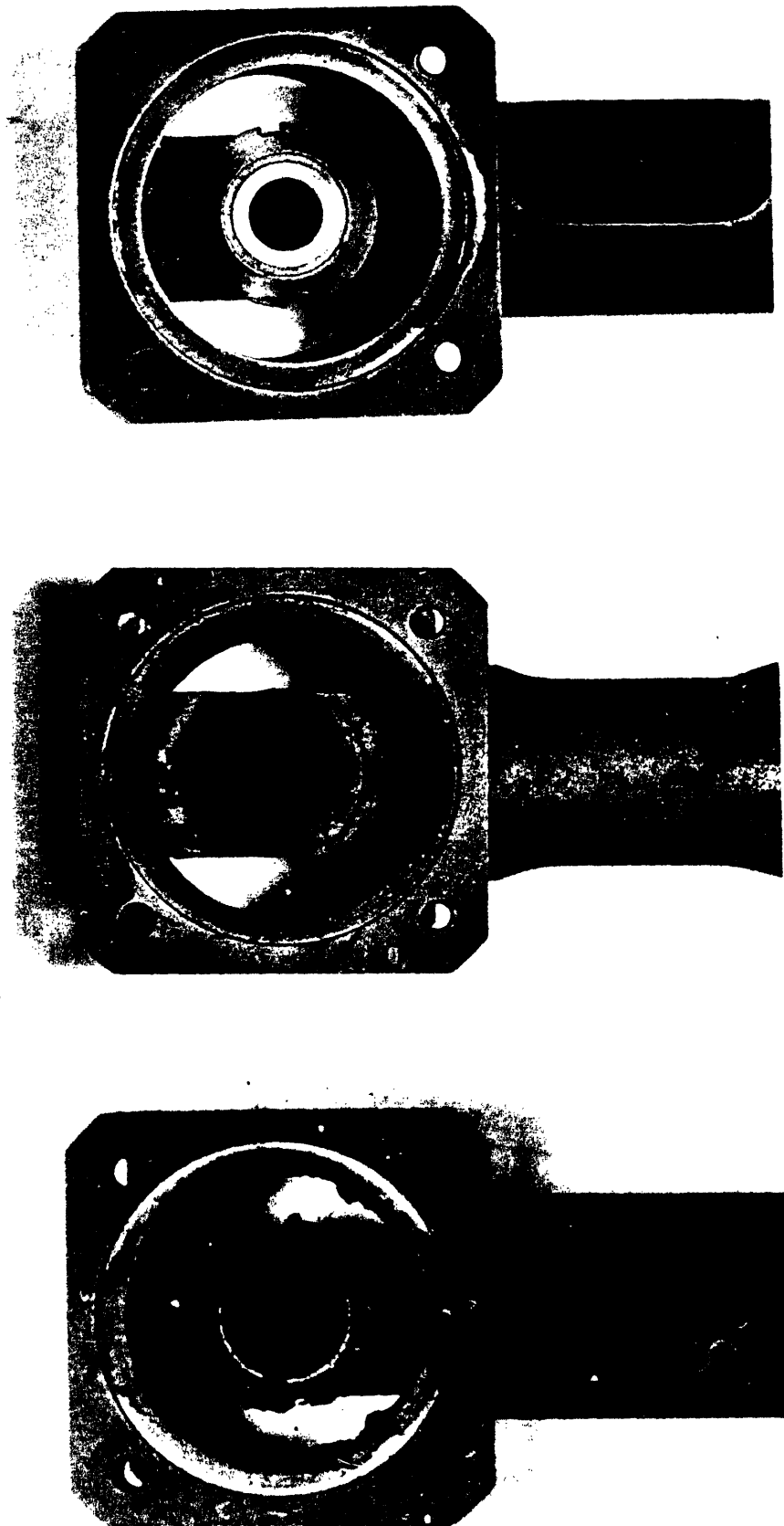


Fig. 10. Effects of solid fuel gases on pressure regulator seat.
Top: Clean
Center: After 45 seconds with double-base fuel
Bottom: After 45 seconds with composite fuel.

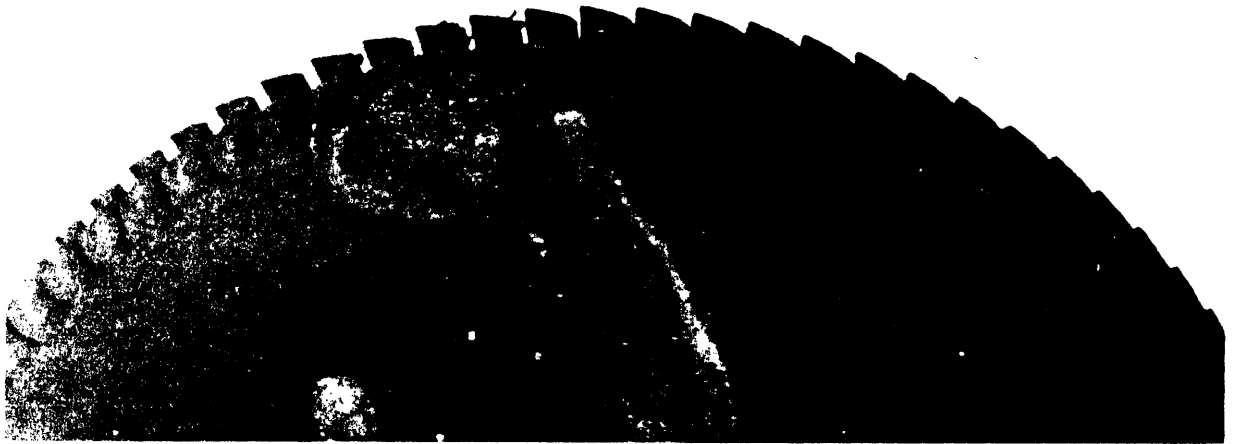


Fig. 11. Effects of solid fuel gases on aluminum turbine.
Top: After 45 seconds with double-base fuel.
Center: After 45 seconds with composite fuel.
Turbine stalled after 30 seconds.
Bottom: Corrosion due to composite fuel
12 hours after operation.

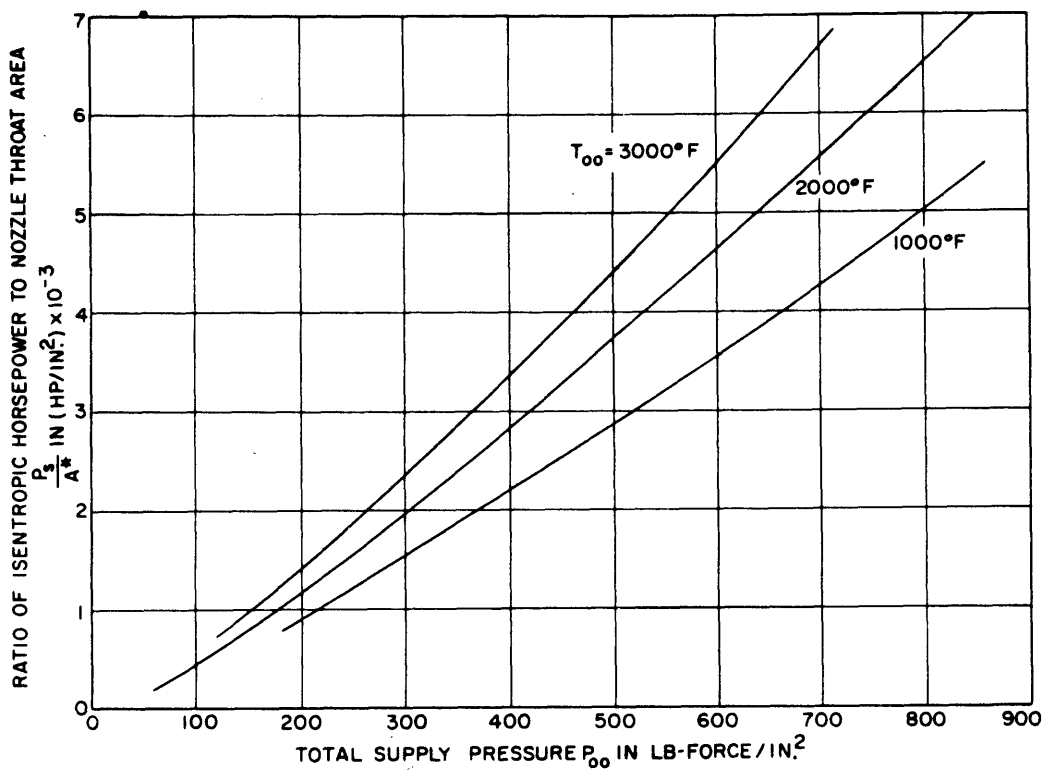


Fig. 12. Plot of isentropic hp/in.² of nozzle throat area vs. total supply pressure for several supply-gas temperatures.

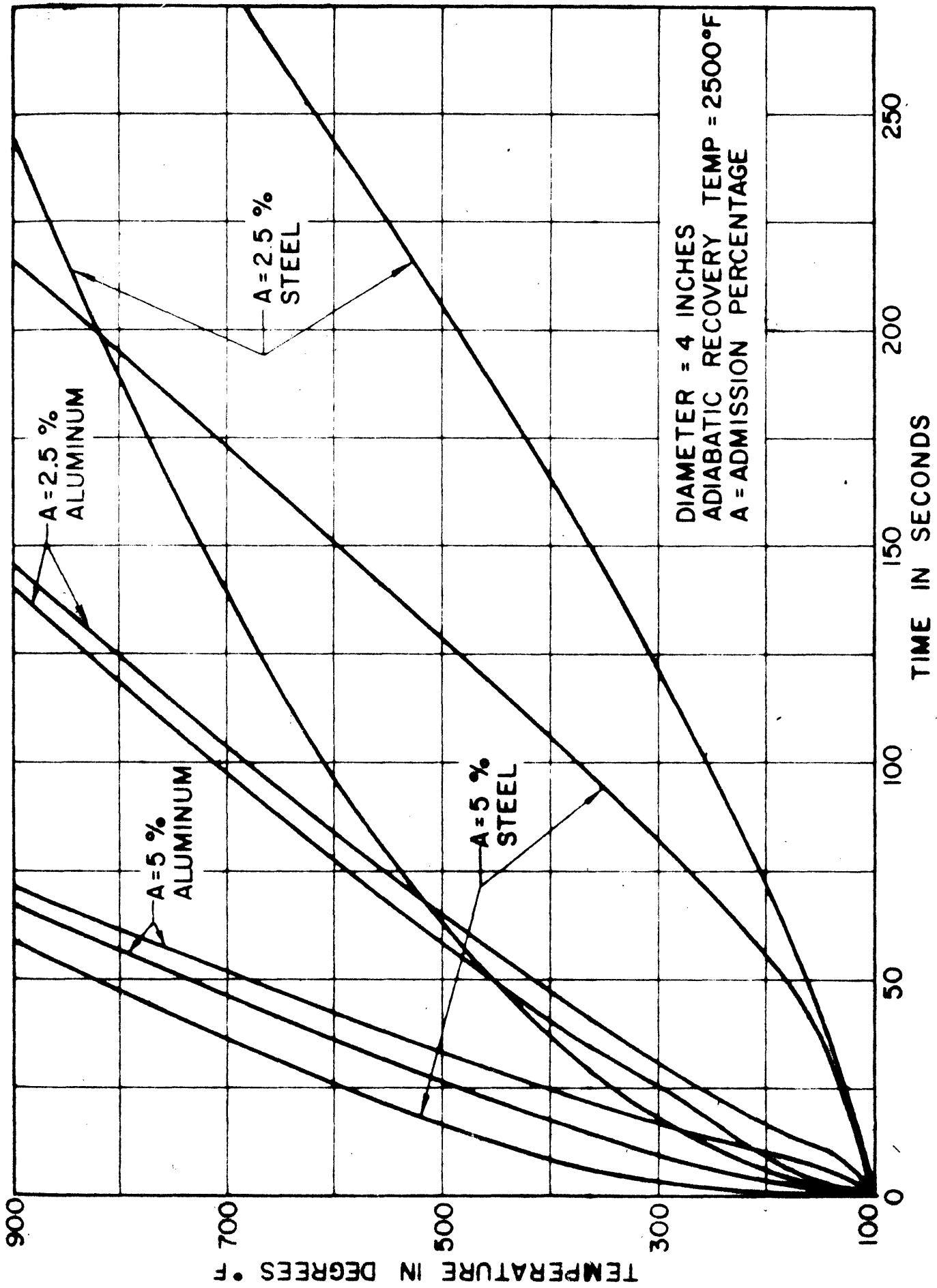


Fig. 13. Center and rim temperature of partial admission turbine vs. time for two admission percentages and for two materials.

4. PARTIAL-ADMISSION TURBINES

The partial-admission turbine is used almost exclusively as the prime mover in MIP. Because the turbine efficiency directly influences the weight optimization of the MIP system, the choice of turbine type and the physical phenomena affecting efficiency are considered in detail in this section in an attempt to develop design criteria for partial-admission turbines.

4.1. Choice of Turbine Type

The choice of turbine for MIP applications can be determined from the study of the full-admission performance of various types of turbine. Figure 14 indicates high efficiencies at low velocity ratios for the impulse two-stage and impulse single-stage turbines and a somewhat lower efficiency for the radial inflow.

Two-stage turbines for MIP usually have proved less efficient than single-stage turbines operating under the same conditions. A better understanding and ordering of the flow pattern in the first stage may improve the design of velocity-compounded turbines. Recent English attempts at velocity compounding look promising.¹⁴

Radial-inflow turbines have been applied profitably whenever full or nearly full admission could be used, but radial machines with a large radius ratio, owing to the small number of blades, are unsuited to partial admission except when the ratio of outer to inner radius is so near unity that a machine may be analyzed in the same manner as an axial machine.

Turbines with reaction, such as the symmetrical-stage turbine, are impractical for low admission because a pressure difference cannot be maintained across the wheel unless very small axial clearances between

wheels and nozzles can be ensured. In practice, these clearances are not realizable. The reaction turbine also poses the problem of compensating for end-thrust loads due to the pressure drop across the turbine. Additional complications of a thrust-balancing device are often undesirable in comparison with the almost zero end-load of an impulse turbine.

The temperature of the gas leaving the nozzles of an impulse turbine is lower than that of an equivalent reaction turbine because almost the total pressure drop available occurs across the impulse turbine nozzles.¹³ This reduces the recovery temperature of the blades in the turbine and permits the use of somewhat higher gas-supply temperatures for the same over-all pressure ratio.

According to the foregoing process of elimination, the single-stage impulse turbine is the most likely candidate for the partial-admission application in the velocity-ratio range under consideration. Accordingly, the remainder of this discussion is limited to small single-stage impulse turbines. Efficiency is defined for the isentropic enthalpy drop between upstream stagnation pressure and downstream static pressure because, in most applications, the kinetic energy in the exhaust gas stream cannot be recovered.

4.2. General Description of Losses

For convenience, the several distinct losses incurred in a partial-admission turbine are considered separately. In addition to the usual disk-friction loss, two factors that are not present in axisymmetric (100 per cent admission) turbines must be taken into account for partial-admission turbines.

A major loss arises from the fact that the flow through the rotor blading, with coordinates considered fixed at the rotor, is unsteady.

As a rotor channel filled with relatively stagnant fluid enters the nozzle flow, the jet must accelerate the stagnant fluid until the channel is completely filled by active flow from the nozzle. For a short time interval, the fluid flow may be identical to that in the rotor channel in an axisymmetric turbine. As the rotor channel leaves the active jet, a deceleration of flow occurs. During the period of acceleration and deceleration, one boundary of the flow from the nozzle into the rotor channel is undefined, and mixing occurs. Furthermore, because the jet is not bounded by a uniform axisymmetric pressure distribution, some spillage occurs when the jet is exposed to the flow resistance of the rotor blading. A substantial part of the difference between full-admission and partial-admission performance is attributable to this momentum-exchange phenomenon.

The other loss in partial-admission turbines is due to pumping by a major percentage of the rotor blades as they circulate the relatively stagnant fluid in the turbine shroud.

The preceding losses are present in all partial-admission turbines; for MIP applications, where the fluid temperatures and stagnation pressures are high and power requirements are low, two additional problems arise. First, owing to the low velocity ratios, supersonic fluid velocities often occur in blading. Figure 15 gives the Mach number for the fluid leaving the nozzle and the Mach number relative to the wheel versus velocity ratio for several ratios of wheel velocity to sonic velocity in the supply gas. Secondly, as indicated previously, the small nozzle area and flow area in the plane of the wheel require that the blade heights of the rotor and the aspect ratio be much smaller than is usual.

4.3. Analyses of Losses and Experimental Results

In order to provide the essential design criteria for partial-admission turbines used in the M. I. T. -D. A. C. L. MIP program, an analytical and experimental program investigating partial-admission turbines was inaugurated.

As described in Sec. 4.4 the great majority of the experimental work was performed on a test facility which used air with an inlet stagnation-temperature corresponding approximately to room temperature. Compared with testing with the products of combustion of solid fuels, which are too hot and erosive for long duration testing, the use of air is a great convenience which permits steady-state operation and the use of rather simple instrumentation.

Mach number and Reynolds number similitude is maintained to insure model correspondence between the cold-gas test turbines and their hot-gas counterparts. This section describes the important results^{2, 12, 13, 15} of the program to date.

4.31. Partial Admission

The analysis of losses due to partial admission is based on a model that postulates as the significant variable the ratio of nozzle-outlet peripheral length in the plane of the wheel, a , to the blade spacing s , as shown in Fig. 16. The time interval is assumed to start when the active nozzle jet is aligned with an integral number of blade passages and ends when the rotor has advanced through a distance equivalent to one blade spacing. During this interval, the jets in the partly filled buckets are assumed to expand and to fill the end channels and, as a result, are slowed down by the ratio of the jet width entering the rotor (x , $s-x$) to the jet width leaving the rotor (s). Density changes are

neglected, and a constant-area passage and constant direction and magnitude for the entering velocity are assumed. Integration of the momentum change over this interval gives the mean momentum \bar{m} leaving the blades:

$$\bar{m}_t = \frac{GV_{r1}}{g} \left(1 - \frac{s}{3a}\right)$$

where G is the mass flow, and V_{r1} is the relative velocity entering the rotor blades. Mixing losses in the active blading are evaluated by considering the ratio of the mass of stagnant fluid brought into the jet per second to the mass rate of flow of active fluid from the turbine nozzle and by assuming that each mass of fluid pumped out of the passage by the incoming jet represents a loss equal to $f(U^2/2g)$:

$$\frac{UC}{V_{a1} a \sin \alpha} = f \frac{U^2}{2g}$$

where C is the rotor disk width, V_{a1} is the absolute velocity at the nozzle exit, α is the nozzle angle, and the mixing-loss coefficient f is assumed constant.

Combination of these two losses with the loss incurred as a result of tip clearance and comparison of this work output with that obtainable from a full-admission turbine gives as the predicted efficiency

$$\eta_{tp} = \frac{1 + K \left(1 - \frac{s}{3a}\right)}{1 + K} \eta_t - \frac{f_p \eta_n}{\sin \alpha} \left(\frac{U}{V_{a1}}\right)^3 \left(\frac{C}{s}\right)\left(\frac{s}{a}\right). \quad (2)$$

The value of f is taken as approximately 1.4; K is the rotor velocity ratio (V_{r2}/V_{r1}), η_t is the full-admission turbine efficiency, p is the ratio of blade area over the total area including leakage space, and η_n is the nozzle efficiency.

Experimental points for different nozzle geometries, as shown in Fig. 17, for stator blade lengths of 0.2 inch, for velocity ratios of 0.325, and with pressure ratios resulting in best turbine efficiency are plotted in Fig. 18. A comparison of the analysis of Eq. (2) with the experimental data indicates that the momentum losses are greater than predicted. Therefore, the partial-admission efficiency relation must be adjusted:

$$\eta_{tp} = \frac{1 + K \left(1 - \frac{s}{a}\right)}{1 + K} \eta_t - \frac{f_p \eta_n}{\sin \alpha} \left(\frac{U}{V_{al}}\right)^3 \left(\frac{C}{s}\right)\left(\frac{s}{a}\right) \quad (3)$$

which is represented by the curve in Fig. 17.

In Fig. 19, Eq. (3) is applied to predict the design-point partial-admission efficiency for turbines with $C/s = 2$, $\alpha = 20^\circ$, $\eta_n = 0.85$, and $K = 0.85$.

Because MIP turbines must operate over a wide range of atmospheric pressures, the off-design performance for varying pressure ratio is of interest. For a full-admission impulse turbine, the efficiency drops off on both sides of the design point owing to increased blading loss coefficients resulting from a change in the pressure across the wheel. In a partial-admission turbine, the absence of a uniform axisymmetric pressure distribution in the axial clearance space between nozzle and wheel permits spillage around the rotor blades, thus main-

taining the pressures on either side of the rotor equal for all operating conditions. Therefore, the partial-admission turbine can be analyzed as an impulse turbine for all pressure ratios. In Fig. 20, the curve of partial-admission turbine efficiency versus pressure ratio is based on an analysis that assumes that the fluid enters the blading at a relative angle that is a function of velocity ratio U/V_{a1} and leaves at the blade angle β_2 . The turbine is designed with $a/s = 2$, and $\alpha = 20^\circ$. The test points for a similar turbine tested under similar test conditions also are plotted in Fig. 20.

4.32. Rotor Pumping

The drag torque coefficient C_m of a rotating disk has been shown to be a function of shroud geometry and Reynolds number.¹⁶ The additional drag due to the idle rotor blades of a partial-admission turbine is likewise a function of shroud geometry, Reynolds number, and blade length, or aspect ratio. Experimental values¹⁷ for disk torque coefficient, as well as a few points for bladed wheels, are compared with disk theory in Fig. 21.

4.33. Supersonic Fluid Velocities.

Figure 22 indicates that high nozzle-area ratios resulting in supersonic nozzle-outlet velocities and supersonic rotor-inlet relative velocities do not affect appreciably the performance of well-designed turbines.

4.34. Aspect Ratio

The efficiency of geometrically similar cascades of different aspect ratios has been shown¹⁸ to be

$$\eta = \eta_\infty - \frac{\text{constant}}{\text{aspect ratio}}$$

where η_{∞} is the efficiency of an infinitely long blade. Although the aspect ratios of MIP turbines are usually much lower than those of conventional turbines (aspect ratios between 1 and 3), test results of experiments on a group of geometrically similar turbines with very low aspect ratios correlate well, as indicated. For the turbine stage, the efficiency versus aspect ratio is given by Fig. 23, and the aspect-ratio correction is

$$\eta = 0.69 - \frac{0.023}{\frac{l_s}{C_r}}$$

where l_s is the length of the stator blade and C_r is the width of the rotor disk. The experimental stator efficiencies given in Fig. 24 can be expressed by the same form of equation:

$$\eta_n = 0.92 - \frac{0.014}{\frac{l_s}{C_s}}$$

where C_s is the chord of the stator.

4.35. Influence of Reynolds Number

For passages as small as those in MIP turbines, frictional effects may be important.

An equation that relates¹⁹ turbomachinery efficiency and Reynolds number is

$$\frac{1 - \eta_1}{1 - \eta_2} = \left(\frac{R_{e2}}{R_{e1}} \right)^Y$$

where the value of the exponent γ is in the range of 0.035 to 0.15 for several impulse turbines.

The effect of Reynolds number on the efficiency and mass flow of geometrically similar turbines (except for blade height) is given in Figs. 25, 26, 27 and 28. For these tests, the design point was maintained constant, and the Reynolds number was changed by varying the upstream stagnation pressure. The surface roughness of the blade passages was estimated to be between 60 and 120 microinches rms. For these test data, which are based on a turbine efficiency of 0.60 at a pressure ratio of 3.5, the experimental exponent for blade lengths of 0.04, 0.1 and 0.2 inch is approximately 0.043 (near the lower limit of the referenced exponents), and the losses associated with Reynolds number effect are small. For the 0.02-inch blades, the losses are large, and the exponent is 0.26.

4.36. Nozzle Efficiencies

Experimental convergent and supersonic nozzle efficiencies versus nozzle pressure ratio are given in Figs. 29 and 30.

4.37. Axial Clearance

Experiments were performed to evaluate the effect of axial clearance between the stator and rotor. Tests were run for axial clearances of approximately 0, 0.04, and 0.42 inch.

For full-admission operation, the effect on stage performance was very small except for a slight trend towards lower efficiency at the greatest spacing for the smallest blade height, as might be expected.

For partial-admission operation, the effects were more pronounced. As suggested in Sec. 4.2, as the spacing is increased, the restraints on the flow are removed. In the absence of a uniform axisymmetric pressure distribution, the nozzle jet diffuses in the clearance space and tends to spill when exposed to the resistance in the

rotor blading. As the clearance space is reduced to a minimum, there appears to be an increase in disk friction resulting in a lowered efficiency. In all cases, the optimum spacing was 0.04 inch.

A concurrent thesis²⁰ is analytically investigating leakage flow.

4.38. Optimum Nozzle-Area Distribution

For low partial admission, the small available nozzle area can be distributed either radially, which increases the aspect ratio, or peripherally, which increases the arc of admission. Therefore, the question of optimum distribution of the nozzle area in the plane of the wheel arises.

Combination of the plots indicating the effects of the two variables is given in Fig. 31. The blade heights that will maximize efficiency and the resulting efficiency are given for a known nozzle-outlet area.

4.4. Test Facility and Instrumentation

Most of the experimental data recorded in Sec. 4 were obtained on the small-turbine test facility of Fig. 32 designed and constructed for and by the M. I. T. -D. A. C. L. MIP project and located in and using the air system of the Gas Turbine Laboratory of M. I. T. The air is supplied at room temperature by a 100 psi 400-cfm compressor. Upstream pressure can be as high as 7 atmospheres. Exhaust from the facility is ducted to a steam ejector which permits turbine downstream pressures as low as 2 psia, depending upon mass flow. Valves upstream and downstream of the turbine permit variation of turbine pressure ratio and mass flow. A 3000-psi "blowdown" stored-air system capable of delivering much drier air than the 100-psia system has been used to a limited extent to study the effects of condensation shock on performance.

The turbine test housing is essentially a support for a high-speed shaft with provisions to accommodate a variety of nozzle and wheel configurations with outside diameters up to 4 inches. Thermodynamic instrumentation of the turbine housing consists of three static-pressure taps in the stagnation volume upstream of the nozzle block, three static pressure taps downstream of the wheel, and several taps between the wheel and nozzle arranged to read blading hub and tip pressures. These pressure taps are connected to mercury-filled "U-tube" manometers, the upstream manometers consisting of two "U-tube" in series with compressed air in between in order to achieve the required 17.5 foot column of mercury. Stagnation temperatures before and after the turbine are determined by three iron-constantan half-cylindrical probe couples located upstream and three downstream. Mass flow rate is determined from the pressure drop across a standard ASME orifice meter.

Mechanical turbine power output is measured by means of the air-absorption dynamometer shown in Fig. 33. This unique dynamometer, designed and built at D. A. C. L., and subsequently patented, is intended to cover the range of speeds (up to 75,000 rpm) and powers (up to 25 hp) anticipated in the turbine program. The dynamometer consists of a small centrifugal compressor circulating air in a closed cycle through an integral air-to-water heat exchanger. By varying system pressure between 100-psia supply and vacuum, the air density, and therefore work-absorbing capacity of the dynamometer, can be varied over a wide margin. The housing, including the exchanger, was formerly swung on ball bearings. This suspension has been replaced with a static pressurized air bearing. Torque is measured by determining housing rotation against restraining springs which include the inlet water pipe and pressurizing tube. Shaft speed is determined by means

of a reluctance pickup and suitable instrumentation. The torque and power characteristics for each of two interchangeable rotors of the dynamometers are given in Fig. 34.

Turbine wheels and nozzle blocks for the investigation are produced on a two-dimensional profile miller. Hand-filed master profiles which are ten or more times actual size are reduced to size in two stages of reproduction and end milled directly into duraluminum disks. Figure 35 illustrates the two template stages and a finished nozzle block, Figure 36 illustrates a radial flow impulse wheel, scaled for use on the air test facility, and the hot gas version of the same turbine which was used in a solid fueled EPU.^{5, 8}

4. 5. Summary and Future Work

The M. I. T. -D. A. C. L. MIP program, described in the foregoing sections, has provided design criteria that have found wide acceptance and application by manufacturers of missile power systems and turbo-pumps. However, to date, the actual fluid dynamics in the partial-admission stage have been treated in a very simplified manner. Experiments have correlated well with the form of the equation based on the simple models postulated, but the losses have been found higher than anticipated.

A more detailed understanding of the development of active flow in the rotor blading, the nature of the flow leaving the rotor, and the influence of factors such as blading design, velocity ratio, Mach number relative to rotor blading, nozzle outlet width to blade spacing on these flows should suggest means by which performance can be improved. These improvements, which are directly applicable to single-stage turbines, would

be even more important to successful multiple-stage turbines. Single-stage turbine performance is always severely limited by low velocity ratios (see Fig. 14), which would be even lower for the higher energy fuels listed in Table IV. In fact, at present, increases in fuel energy are just about counterbalanced by decreases in single-stage turbine performance due to decrease in the velocity ratio.

For both velocity staging (where the over-all pressure ratio is assumed to be almost wholly in the nozzles) and pressure staging (where the over-all pressure ratio is distributed between several nozzle and rotor stages, thus increasing the velocity ratio), improvement of single-stage performance and ordering of the rotor outlet flow would be beneficial.

Present plans are to study visually the flow patterns by means of high-speed Schlieren and interferometric photography. A large-scale model of a partial-admission single-stage turbine that maintains dynamic similitude with fluid properties and mass flows typical of MIP and turbopump components is being designed. To facilitate the photography, the equipment probably will incorporate a stationary rotor arranged for radial outward flow with a radius ratio close to unity and a rotating nozzle block. An identical rotating rotor stage will be tested to determine the velocity profile leaving the stage. In both models, provision will be made for changing blading as well as varying other important parameters in the ranges pertinent to current usage. The validity of existing theoretical models of the flow will be tested against the actual flow character, and present design criteria will be expanded and amended appropriately.

NOMENCLATURE (Cont.)

(For Sections 1, 2, 3, and 4)

Symbol	Definition	Unit
R_e	Reynolds number or gas constant	
r	Radius	in.
r_f	Burning rate of solid fuel	in./sec
s	Rotor or nozzle blade spacing	in.
t	Time	sec
T_e	Fuel storage equilibrium temp.	deg F
T_{oo}	Supply temperature	deg F
U	Turbine blade velocity	ft/sec
V	Voltage	Volts
V_{al}	Absolute velocity nozzle exit	ft/sec
V_{r1}	Relative velocity entering rotor blades	ft/sec
V_{r2}	Relative velocity leaving rotor blades	ft/sec
V_e	Velocity equivalent of isentropic enthalpy change	ft/sec
α	Nozzle angle	deg
β_1	Angle of flow (relative to wheel) entering blades	deg
β_2	Angle of flow (relative to wheel) leaving blades	deg
η	Efficiency	
η_e	Electrical machine efficiency	
η_n	Nozzle efficiency	
η_t	Full-admission turbine efficiency	
η_{tp}	Partial-admission turbine efficiency	
μ	Coefficient of viscosity	lb-force sec/ft ²
$\pi = P/14.70$	Pressure ratio	
ρ	Fluid density	lb-mass/ft ³
ρ_f	Fuel density	lb-mass/ft ³
τ	Torque	lb-force ft
ω	Speed	Rad/sec

NOMENCLATURE

(For Sections 1, 2, 3 and 4)

Symbol	Definition	Unit
A	Nozzle outlet area	in. ²
A*	Nozzle throat area	in. ²
A _a	Nozzle outlet area in the plane of the wheel	in. ²
A _f	Fuel combustion area	in. ²
a	Nozzle arc width	in.
C	Rotor or stator disk width	in.
C _m	Drag torque coefficient	
c _o	Speed of sound in supply gas	ft/sec
c _p	Specific heat at constant pressure	BTU/lb-mass °F
D _f	Diameter of fuel grain	in.
f	Mixing loss coefficient	
G	Mass flow rate	lb-mass/sec
g	Gravitational constant	lb-mass/ft
ΔH _s	Isentropic enthalpy change	BTU/lb-mass
I	Current amperes	
I _{sp}	Specific impulse	lb-force sec/lb-mass
K	V_{r2}/V_{r1} for full admission	
K _f	A_f/A^*	
k	Ratio of specific heats	
L _f	Length of fuel grain	in.
l _r	Rotor blade length	in.
l _s	Stator blade length	in.
M	Mach number	
\bar{m}	Mean momentum	lb·force
P	Output power	ft lb-force/sec
P _i	Power in nozzle jet	ft lb-force/sec
P _s	Isentropic horsepower	ft lb-force/sec
P _{oo}	Total supply pressure	lb-force/ft ²
P ₁	Nozzle-exit-plane static pressure	lb-force/ft ²
P ₂	Exhaust static pressure	lb-force/ft ²
p	Leakage factor	

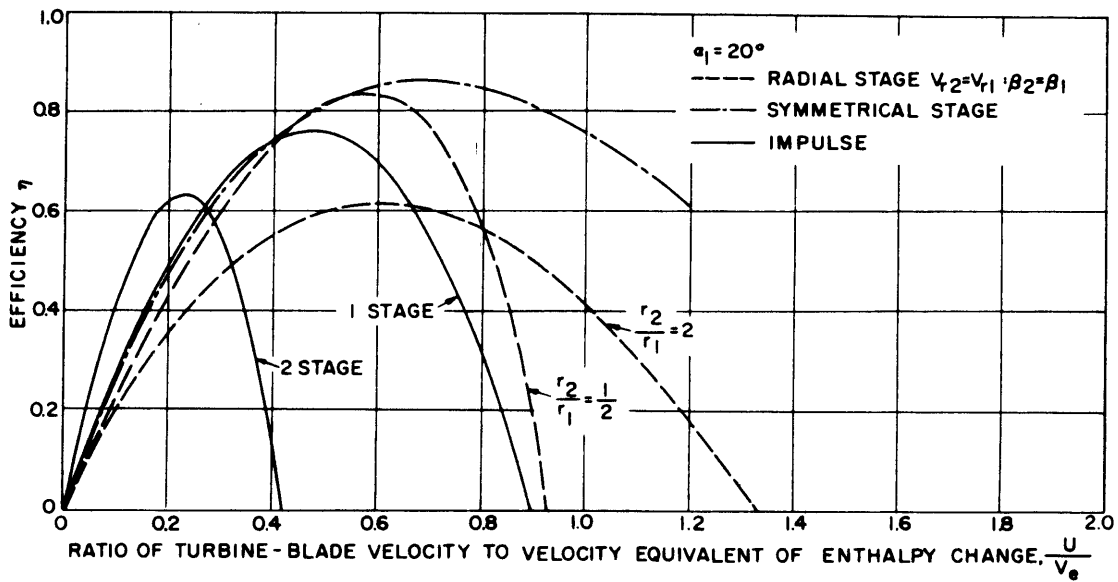


Fig.14. Efficiency vs. velocity ratio for several turbine types with nozzle angle of 20° and friction losses.

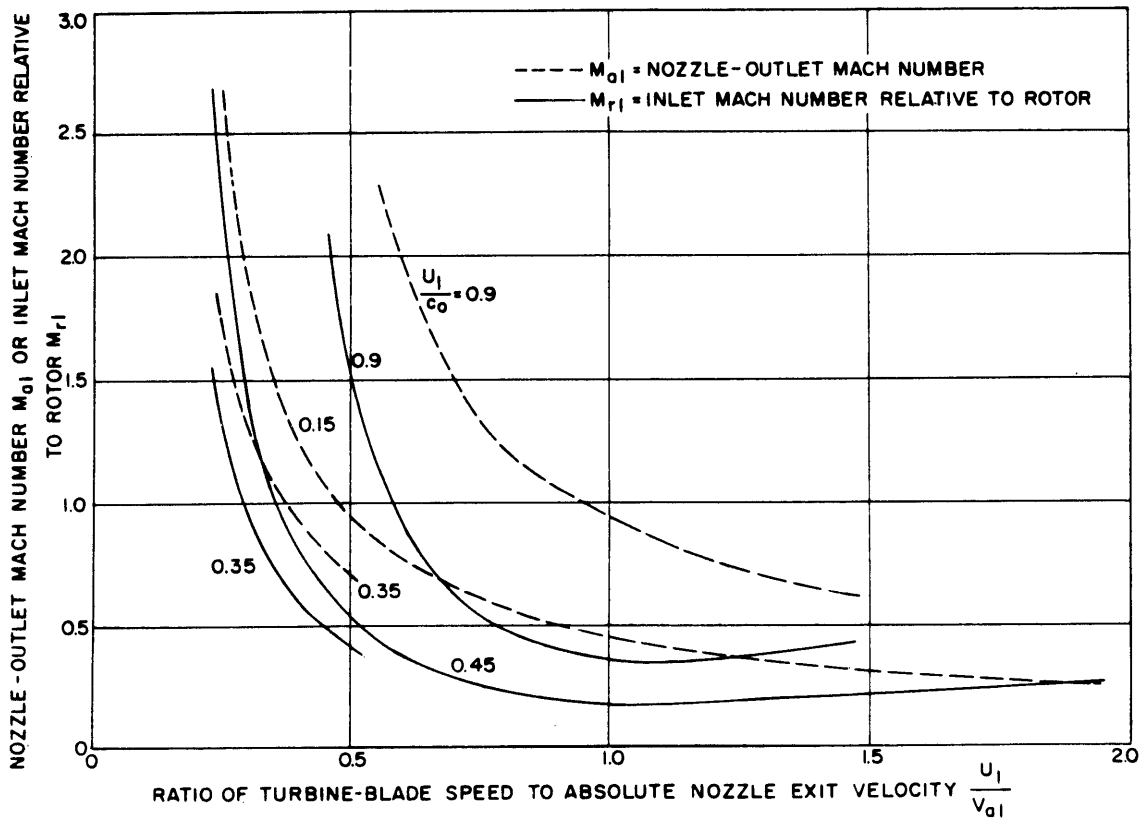


Fig. 4. Plot of turbine Mach numbers vs. velocity ratio for several ratios of wheel speed to supply-gas Mach number when $k = 1.4$ and $\alpha = 20^\circ$.

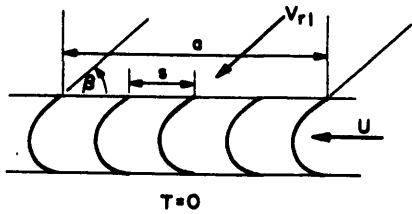


Fig.16. Geometry of partial-admission-turbine operation.

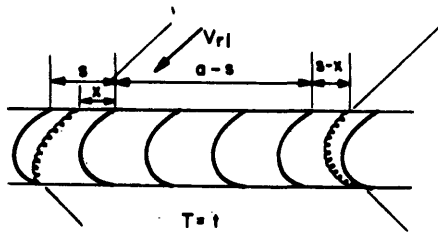


Fig.17. Typical nozzle and rotor blading: (a) convergent nozzle, (b) two-dimensional supersonic nozzle, (c) axisymmetric supersonic nozzle, and (d) rotor.

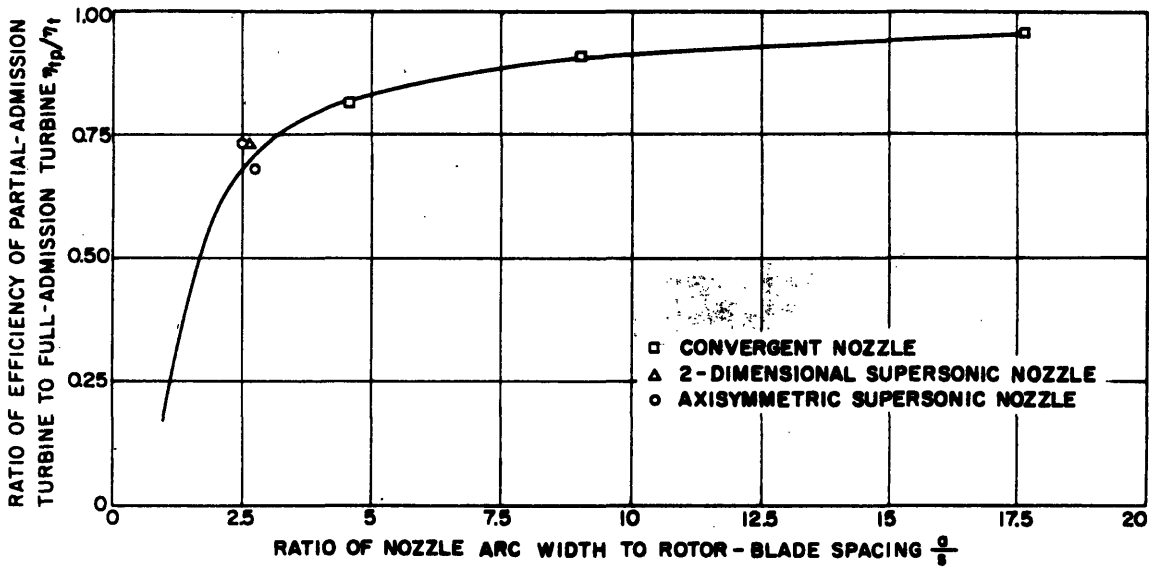
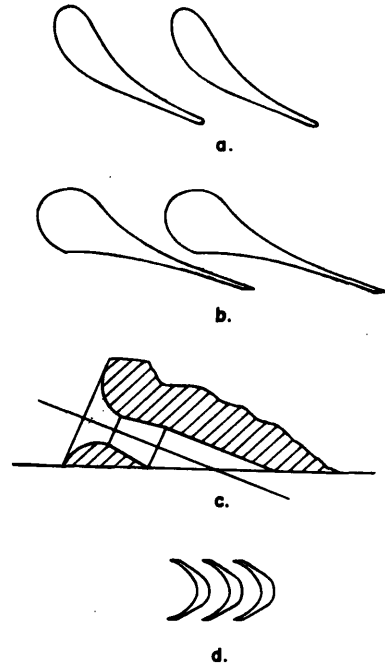


Fig.18. Plot of predicted analytical curve in relation to experimental points of efficiency ratio vs. ratio of nozzle arc width to rotor-blade spacing; $l_s = 0.2$ inch and $U/V_{a1} = 0.325$.

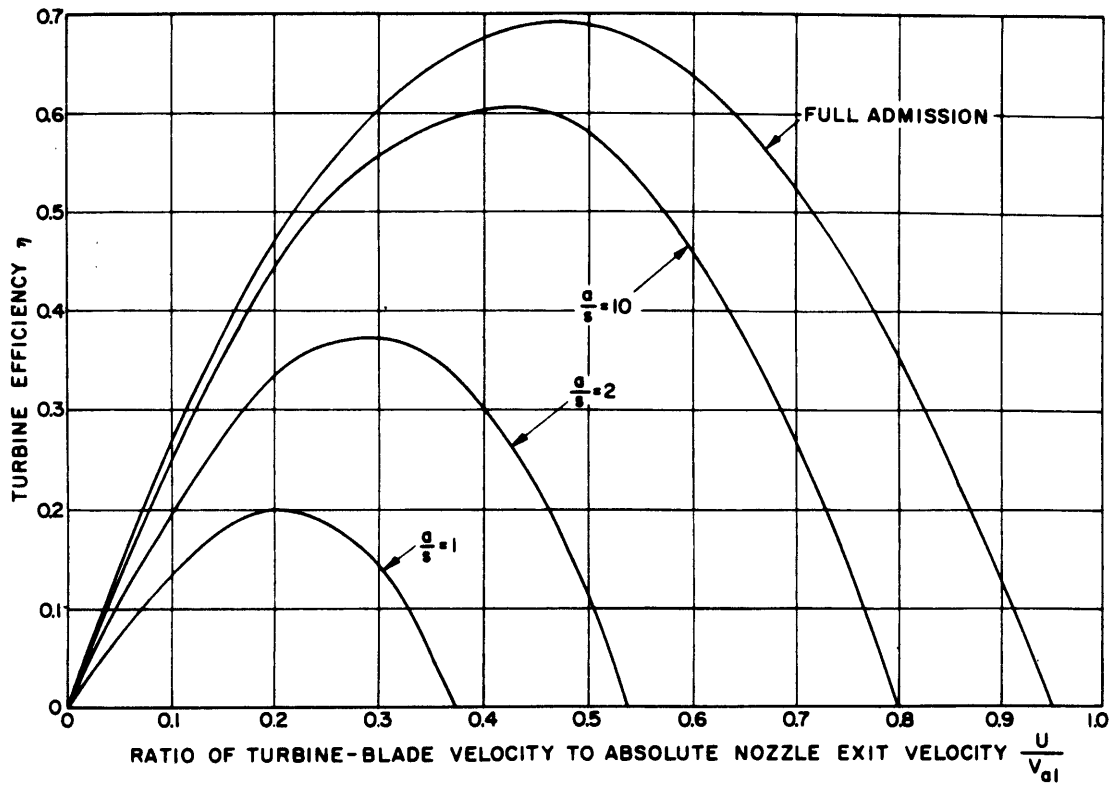


Fig. 19. Plot of design-point turbine efficiency vs. velocity ratio for several ratios of nozzle arc width to rotor-blade spacing showing effect of partial admission.

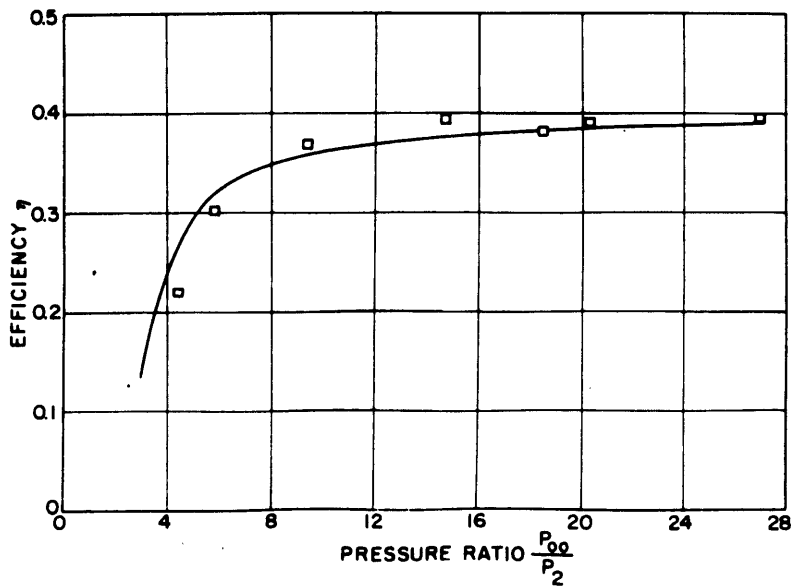


Fig. 20. Plot of predicted analytical curve in relation to experimental points of partial-admission turbine efficiency vs. pressure ratio showing off-design-point performance.

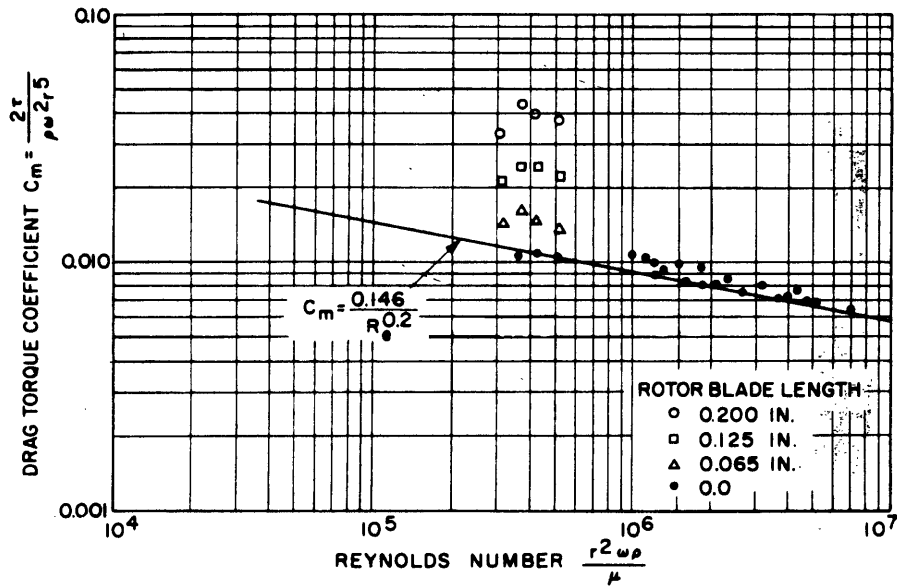


Fig. 21. Plot of drag torque coefficient vs. Reynolds number for several bladed disks and disks with no blades.

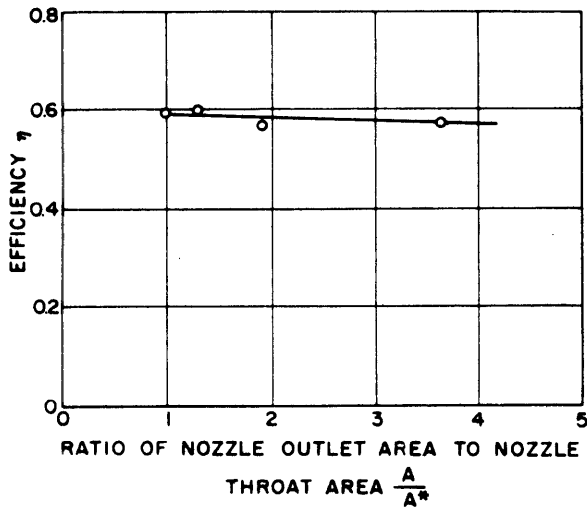


Fig. 22. Plot of turbine efficiency vs. area ratio for supersonic nozzles with $U/V_e = 0.325$.

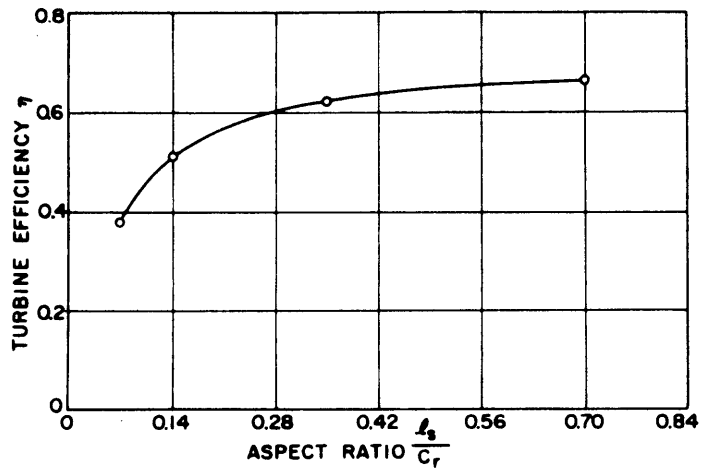


Fig. 23. Plot of turbine efficiency vs. aspect ratio for convergent nozzles; $C_s = 0.407$ inch, $C_r = 0.285$ inch, $U/V_e = 0.325$, and $P_2/P_{00} = 0.45$.

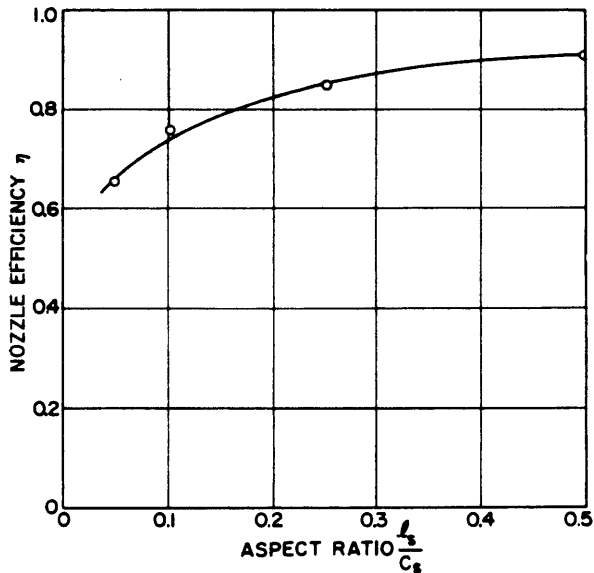


Fig. 24. Plot of nozzle efficiency vs. aspect ratio for convergent nozzles; $C_s = 0.407$ inch, $U/V_e = 0.325$, and $P_2/P_{00} = 0.45$.

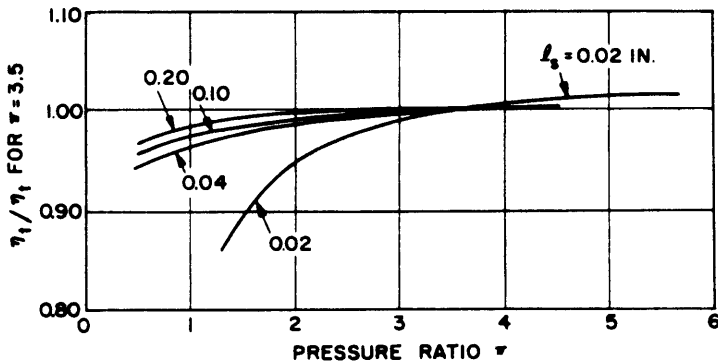


Fig. 25. Plot of turbine efficiency ratio vs. pressure ratio showing effect of Reynolds number for convergent nozzles with several stator blade lengths; $U/c_0 = 0.35$ and $P_2/P_{00} = 0.45$.

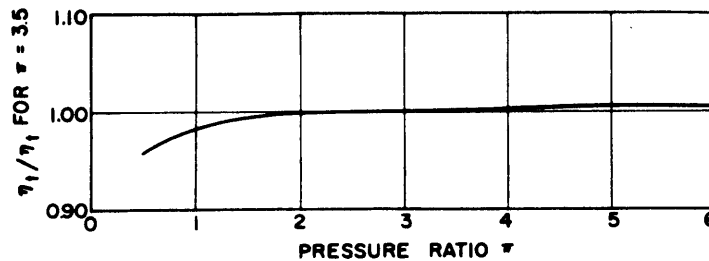


Fig. 26. Plot of turbine efficiency ratio vs. pressure ratio showing effect of Reynolds number for supersonic nozzles; $A/A^* = 1.295$, $l_s = 0.10$ inch, $U/c_0 = 0.45$, and $P_2/P_{00} = 0.10$.

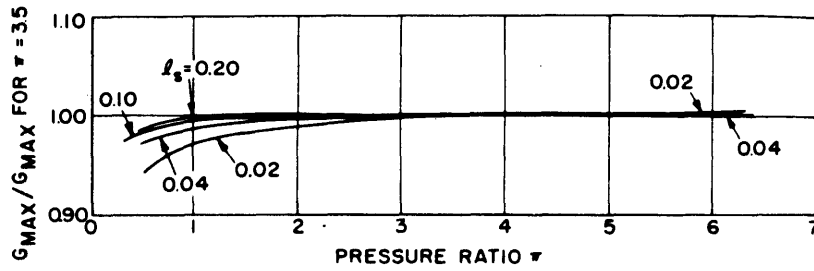


Fig. 27. Plot of flow ratio vs. pressure ratio showing effect of Reynolds number for convergent nozzles with several stator blade lengths.

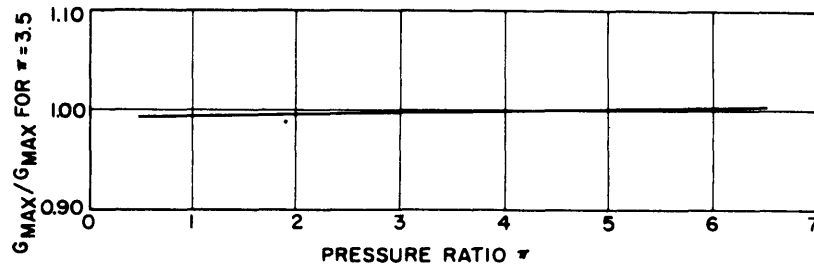


Fig. 28. Plot of flow ratio vs. pressure ratio showing effect of Reynolds number for supersonic nozzles with stator blade length of 0.10 inch.

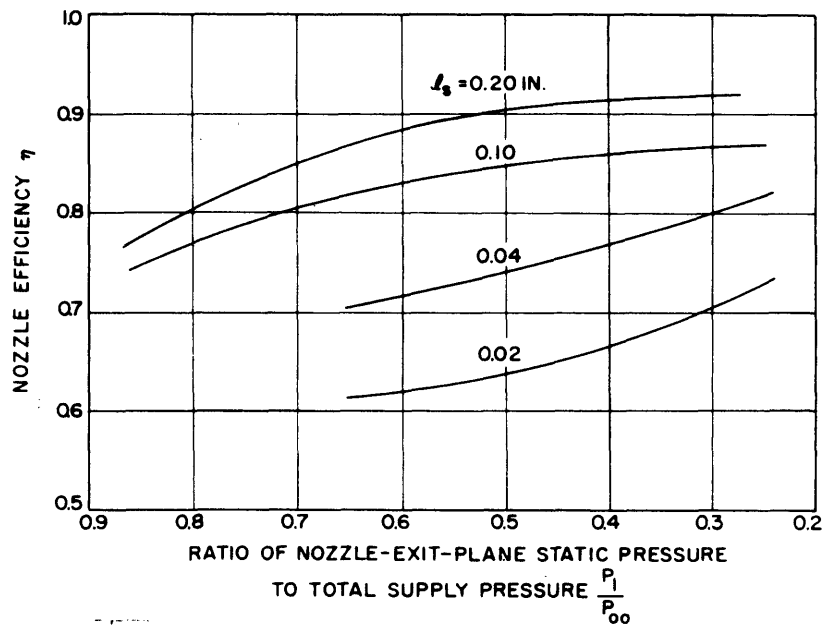


Fig. 29. Plot of nozzle efficiency vs. pressure ratio for convergent nozzles with several stator blade lengths.

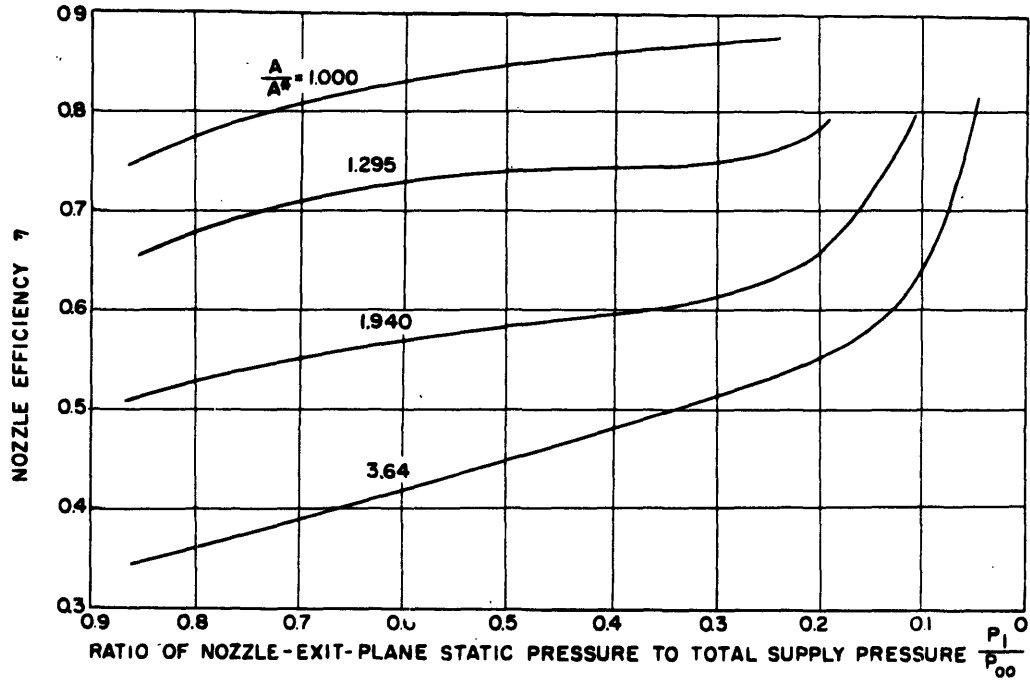


Fig. 30. Plot of nozzle efficiency vs. pressure ratio for supersonic nozzles with several area ratios and stator blade length of 0.10 inch.

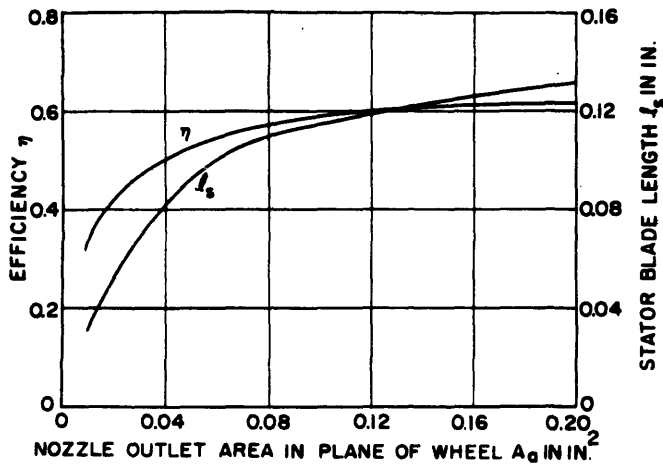


Fig. 31. Plots of efficiency and stator blade length vs. nozzle outlet area in the plane of the wheel for partial-admission turbines; $C_r = 0.285$ inch, $U/V_e = 0.325$, and $\alpha_1 = 20^\circ$.

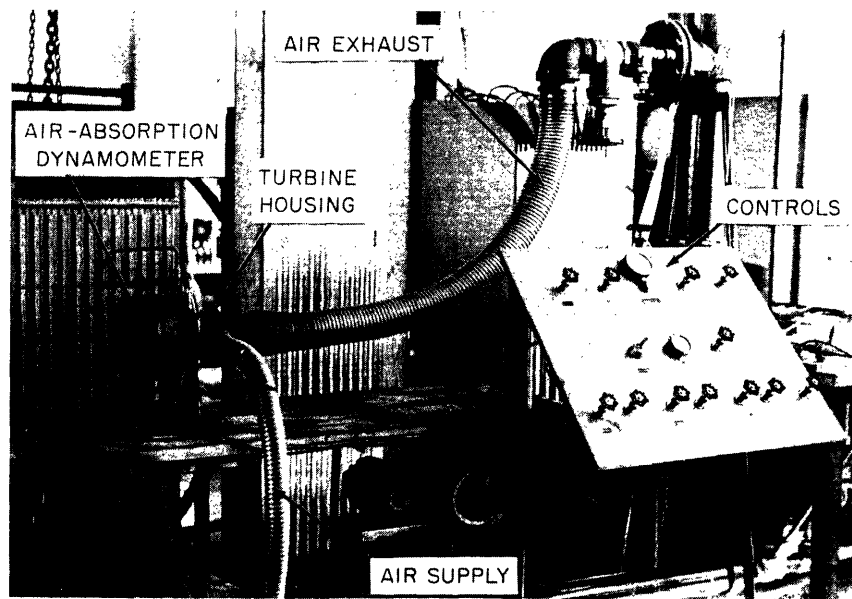


Fig. 32. Turbine air test facility.

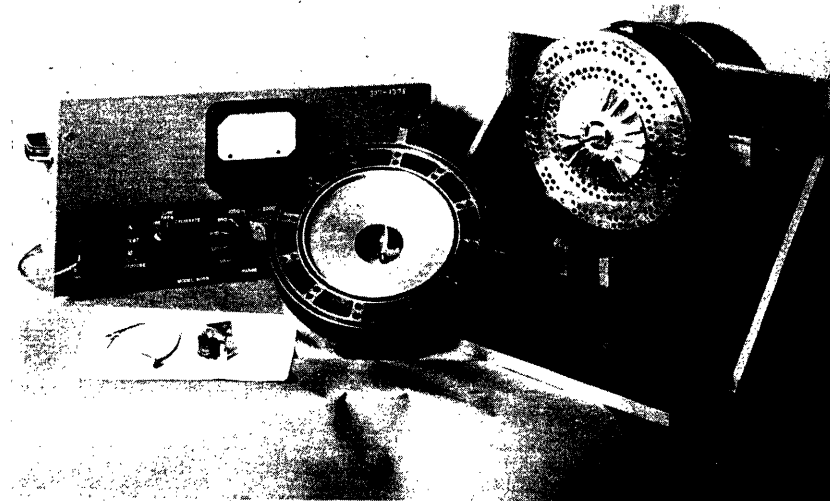


Fig. 33. The D. A. C. L. air-absorption dynamometer.

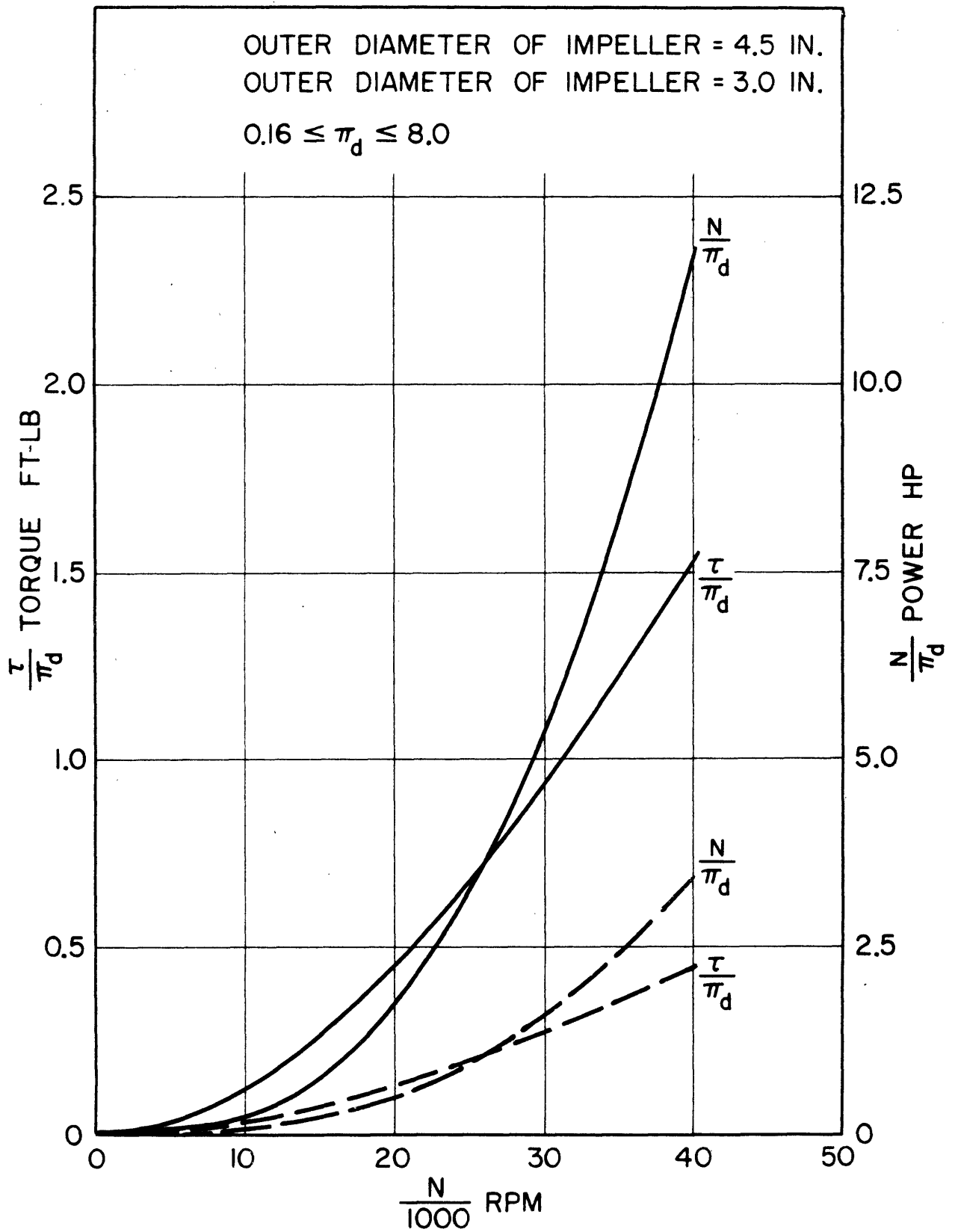


Fig. 34. Air absorption dynamometer characteristics.

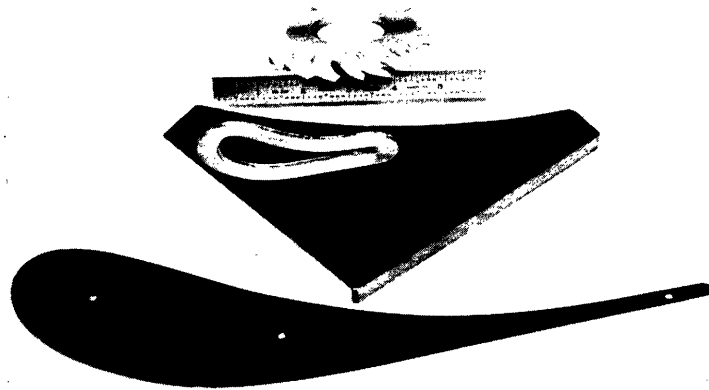


Fig. 35. Templates and finished nozzle block.

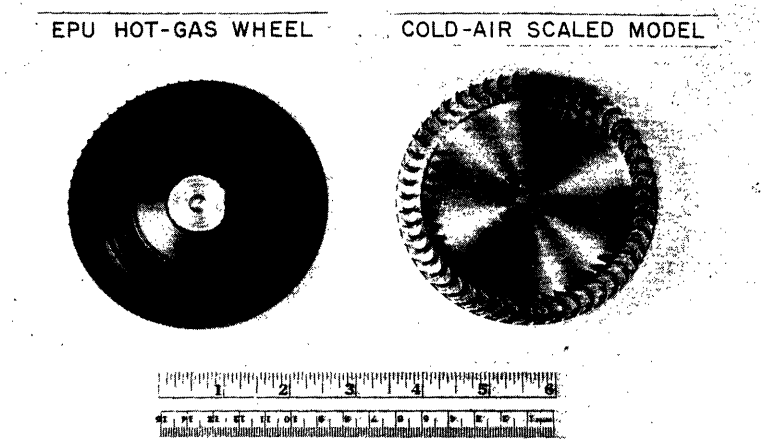


Fig. 36. Turbine wheels.

5. MECHANO-ELECTRICAL CONVERSION

The design of optimum mechanical-to-electrical energy conversion machinery for MIP systems is a more complex problem than either the choice of optimum prime energy source or prime mover. The problem is constrained by mechanical structural limitations and thermodynamic heat transfer considerations as well as electrical and electromagnetic considerations. The cross-influences of the several disciplines is intimately related, especially the interrelationship between internal electrical losses and heat transfer in apparatus designed for maximum output-power-to-weight-ratio and short-duration transient operation.

Even more than in other design areas, art and experience play dominant roles in the design of electrical machinery. For the most part industrial design groups concern themselves with particular types of machines in particular power ranges. Their present best designs are very slight extrapolations from previous design, test, and application experience. Almost without exception experience is limited to continuous-duty machinery designed for commercial applications where the environmental conditions, mechanical requirements and emphasis on output-power-per-weight are much less severe. The regulated voltage and frequency characteristics of machines are rarely considered from the systems (prime mover plus electrical machine) point of view. Rather, the regulation characteristics of the electrical machine are considered for constant-speed drive or for constant output load. The interactions of prime mover, electrical machine, and load are rarely considered together in the determination of the type of machine to be used

and in the development of the design of the machine and its internal or external control devices.

The choice of and design of electrical machinery for the MIP project was probably the most difficult aspect of the over-all program. Satisfactory machines were developed but as indicated in Sec. 5.4, this area is a very fruitful one for future generalized study directed toward understanding, characterization, and the development of design criteria.

5.1. Air-To-Air Missile EPU Considerations

The electrical, environmental, and mechanical requirements imposed on an air-to-air missile EPU are given in Sec. 2.1. The implications of these requirements as applied to the electrical machine are as follows:

5.11. Pre-Launch Power Requirements

Consideration of the total imposed burden (penalty factor) on the launching aircraft, comparing systems using aircraft-mounted conversion equipment to satisfy all the missile pre-launch requirements and systems which use the missile internal power system to satisfy some of the pre-launch power requirements, clearly indicates that it is desirable for the missile EPU to provide some of the transforming and rectification needs of the missile system. This is true both for guidance systems which are active prior to launch and guidance systems which need only be in a ready-to-commit condition prior to launch. Depending upon the guidance system an electrical machine to perform as an electrical generator prior to launch may or may not be required.

5.12. Post-Launch Requirements

Short commitment time, a fraction of a second, is enhanced if the rotating inertia of the power unit is near operating speed prior to commitment. This can be achieved with an electrical machine which serves as a

motor pre-launch overcoming the friction and windage of the rotating assembly.

Acceleration from rest in the short commitment time would require auxiliary turbine nozzles and fuel or a composite solid fuel with a fast-burning section for the acceleration period. Either of these techniques represents considerable complication with concomitant reduced reliability. The composite fuel technique is complicated by the temperature dependence of the burning rate since increased mass flow for acceleration purposes at the low temperature environment results in very high pressures in the combustion chamber under high temperature environmental conditions. Acceleration from rest also imposes severe heat transfer on the turbine rotor. The heat transfer coefficients in Sec. 3.63 are based on high-speed rotation of the turbine in the nozzle jet. In accelerating from rest, a few turbine buckets are exposed to the hot gases for a much longer uninterrupted time. The use of easily machinable materials such as aluminum under these conditions is questionable. Furthermore, nonuniform application of heat on the periphery of the wheel during acceleration may result in distortion and warpage of the turbine rotor and subsequent stalling of the rotor by the closely fitting turbine shroud.

In light of the above considerations, it was decided to maintain the rotating assembly near final operating speed during pre-launch. Thus, the most desirable electrical machine will provide the dual function of motor pre-launch and alternator post-launch although the possibility of using several machines to achieve the same result was not ignored.

5.13. Frequency

The power frequency of the EPU is either determined by the existing missile system or optimized as indicated in Sec. 8.

5.14. Voltages

The output voltages of the EPU are either determined by existing missile requirements or by combined consideration of the missile requirements and optimum voltages for the electrical generation and transmission system as in Sec. 8.

5.15. A-C Power Versus D-C Generation

Of the missile electrical loads, the high-voltage plate supply must be d-c power, the low voltage filament supply is preferably d-c, whereas a-c power loads are usually limited to gyros, synchros, transducer excitation, etc., which together constitute only a small part of the total requirement. This apparent advantage of d-c generation is offset by the mechanical and electrical limitations of high-speed, low-weight d-c machinery described in Sec. 5.21. In brief, these limitations are:

1. The impossibility of d-c voltage transforming which usually requires separate d-c machines for each principle voltage level of which there are several,
2. The resulting output voltage matching problem from several machines on a common shaft, a much more tedious and difficult task with machine windings than with transformer coils,
3. The low, but essential requirement of some a-c power which requires an additional machine or a static or dynamic inverter,
4. The restriction to a-c parent airplane power pre-launch which necessitates an inverter in the parent plane with concomitant penalty factor.

5. The complication of the control function, since voltage and frequency control of several machines on a common shaft is more difficult both post-launch and pre-launch when the parent aircraft voltage and frequency tolerances are multiplied by the d-c missile components, and
6. The pre-launch motoring problem, which requires a separate machine or other special arrangements.

Contrasted with the problems of d-c generation, a-c power generation, transforming and rectifying is, based on the experience of the project, much more advantageous. An a-c alternator can be made very rugged and troublefree; one single-winding machine can greatly simplify pre-launch motoring and post-launch control. The incorporation of a transformer provides great flexibility in output voltage matching and is used pre-launch to transform the parent airplane a-c power directly with no compounding of frequency and voltage tolerances. The availability of silicon power diodes and tantalitic capacitors makes possible the design of extremely compact rectifier-filter systems which are simple, rugged and easily modified or rearranged to compensate for changes in current, voltage and ripple requirements and which are capable of operating at ambient temperatures of 85°C.

5.16. Environmental Conditions

The electrical machine must operate satisfactorily under the temperature, humidity, altitude, shock, vibration and acceleration requirements given in Sec. 2.12. The temperature requirement influences heat transfer from the electrical machine. A combined

motor-alternator, for example, must have a steady-state rating adequate to provide windage and friction loads and any required power generation load pre-launch. This same machine must have a transient power rating perhaps ten times its steady-state rating for post-launch operation. Either of these requirements, the steady-state or the transient, may control the design; the best design is the best compromise of the two requirements. Environmental temperature also affects the resistance of the windings of the machine and therefore influences internal voltage regulation. Temperature, humidity and altitude requirements adversely affect brush, slip ring and commutator applications. The support of the machine rotor when subjected to the acceleration, vibration, and shock requirements poses a design problem.

5.17. Weight Minimization

The influence of shaft speed on turbine performance as given in Sec. 4 indicates the desirability of high shaft speeds for the turbine. The study discussed in Sec. 8 indicates that electrical machine output per weight is increased at higher frequencies corresponding to higher shaft speeds. Comparing the weight, complexity, and reduced reliability associated with a gear reduction between turbine and electrical machine, with the fuel weight-penalty for operation at less than mechanically limiting turbine speeds, indicated the desirability of direct drive of the generator by the turbine. With 400 cps systems this limits shaft speed to 24,000 rpm. New higher frequencies as suggested in Sec. 8 will permit higher shaft speeds and improved turbine performance, limited only by mechanical considerations in the bearings and rotating members.

Since several output voltages are always required, either a single-winding alternator with a separate transformer⁸ or a multiple-winding alternator⁵ may result in a lower weight, lower volume system. Analytical generalizations on this question are not possible due to limited understanding of the extent of possible electrical machine optimization; however, the experience of the project indicates that separation of the generating and transforming tasks is advantageous. The iron and copper in a transformer can be utilized much more efficiently than in an alternator, due to the more complicated geometry and the existence of air gaps in the rotating machine. A tangible advantage of a separate transformer is that its simple coil design greatly simplifies the problem of balancing the several output voltages at the desired power levels whereas adjusting the output of a multiple-winding alternator is an extremely tedious design and fabrication problem. For the same reasons, a separate transformer makes it relatively easy for the EPU design to accommodate to the seemingly inevitable changes in the missile power requirements.

5.2. EPU Alternatives

Based on the above requirements the known generator types were considered and their advantages and disadvantages were compared.

5.21. D-C Generators

D-C generators for EPU applications where the emphasis is on high-speed and low-weight can be as efficient weightwise as synchronous alternators but unfortunately they are plagued with a number of almost disqualifying mechanical and electrical problems. High rotational speeds disturb low strength rotor windings, result in rapid brush wear and cause concentrated heating of the commutators owing to brush friction. Brush

wear is greatly accelerated at high altitudes due to the low atmospheric water vapor content.²¹ A major portion of the power losses occurs in the rotor which is a difficult part to cool.

Electrically commutation is made difficult by the high speed. To maintain low ripple voltages in the output, special interpoles must be used to compensate for the reactance voltage during commutation. High and low voltage experimental 24000 rpm d-c machines were designed and evaluated during the course of the MIP program.⁸

5.22. Wound Field Synchronous Alternator

For moderate to high kilowatt ratings in the frequency range up to several thousand cps the wound field synchronous alternator is the most efficient generating device from the standpoints of material utilization and operating efficiency. For the EPU power range the weight advantage is not so marked. Between 1000cps and 10,000 cps other less conventional alternators become competitive.

The most serious disadvantage of the wound field alternator for MIP is the high rotary speed of the turbine drive, and the concomitant problem of keeping windings on the rotor, and maintaining operative the brushes and slip rings. These problems have limited industrial alternator design to a maximum of 24,000 rpm and this only after considerable development effort. For present-day aircraft 12,000 rpm is considered the highest practical speed for wound rotor alternators.

Based on the considerations of Sec. 5.2, the advantages and disadvantages of the wound field alternator are as follows:

Advantages:

1. Minimum volume per unit power output.
2. Good inherent voltage regulation.
3. Voltage control equipment simple and practical (by means of regulation of the rotating d-c field).
4. Will operate as a motor if damper windings are installed.

Disadvantages:

1. Rotor construction unsuited for high peripheral speeds.
2. Brushes required for exciting the field.
3. Source of d-c required to excite the field (rectifiers in the output can supply the field).
4. Frequency control determined exclusively by speed control.

5.23. Permanent-Magnet Field Synchronous Alternator

The permanent-magnet field (PM) alternator is similar to the wound field alternator except that its field excitation is provided by a permanent magnet instead of a separate d-c source. The field structure, air-gap density, and resulting over-all physical size is determined by the magnetic characteristics of the permanent magnet material. Commercially-available material such as the Alnicos can be used to produce maximum air-gap densities of the order of 30 to 40 thousand lines per square inch under stable operating conditions, approximately one-half of the flux density which can be realized with other types of alternators in the frequency range up to two thousand cps. (These flux-densities are not typical of commercial design practice, but have been successfully realized in EPU's in the M. I. T. program). The voltage output of a PM machine is linearly related to speed assuming a constant load resistance.

The armature reaction or demagnetizing effect of the load current in the armature conductors of a PM machine is much less than in the wound rotor machine because of the higher permeability of the rotor material, improving inherent voltage regulation but increasing susceptibility to short circuit demagnetization. Short circuit stabilization decreases the efficiency of utilization of the permanent magnet of the rotor which then must be made proportionately larger. In the case of large load changes voltage regulation can be improved by externally controlled saturation of the armature structure.²² Because of the reduced flux-densities, the electromagnetic portion of the PM alternator will be larger than that of the wound field alternator. However, since no field excitation source is required and since voltage control can be achieved by inherent regulation, the over-all size and weight of the PM alternator power supply ought not be appreciably larger than its competitors.

The PM rotor tensile strength limits rotor tip speed. Cast rotors, which may be ordered in any size or geometry, have a tensile strength of the order of 15,000 psi. Sintered materials have tensile strengths of the order of 60,000 psi but are available only in a very limited size range. Various design techniques of inserting the weaker magnetic material into a steel structure or of reinforcing a cast rotor with a nonmagnetic band shrunk over its periphery have been considered and applied.

A small 1200 cps PM generator was designed, evaluated and applied quite successfully in an EPU during the MIP program.⁸

The characteristics of the PM alternator are as follows:

Advantages:

1. No source of field excitation needed.
2. No brushes required.
3. Simple rotor construction that can be mechanically reinforced to operate at high speeds.
4. Good inherent voltage regulation especially for a constant load.
5. Indefinitely long storage capability.

Disadvantages:

1. No inherent motor action.
2. Frequency tolerance directly related to speed control.
3. Voltage regulation difficult if inherent regulation is not satisfactory.
4. Low air-gap flux density results in larger alternator for the same electrical output, particularly if short-circuit stabilization is necessary.

5.24. Inductor (Variable Reluctance) Alternator

The variable-reluctance inductor alternator produces a useful a-c flux by mechanical variation of the air-gap reluctance as the rotor revolves. The air-gap flux is unidirectional, produced by d-c field windings located on the stator of the machine. The maximum theoretical peak-to-peak flux variation is equal to the maximum a-c flux density, thus the maximum a-c flux variation is only 50 per cent the maximum d-c flux density. Practical design considerations limit the useful a-c flux variation to approximately 40 to 45 per cent of the d-c flux level. This limits the a-c flux density of the inductor alternator

to approximately one-half that of a conventional wound field machine, and results in an electromagnetic structure approximately twice as large as that of conventional wound field machines for the frequency range around 1,000 cps. In order to dynamically balance the rotor a symmetrical rotor design is essential. For an inductor alternator, the resulting structure has inherently twice as many poles as a conventional synchronous machine and therefore produces twice the frequency for the same shaft speed. The high leakage reactance results in poor inherent voltage regulation. However, the d-c field excitation is readily available for external voltage control. The inductor alternator has no intrinsic motoring action and auxiliary windings or an auxiliary machine must be provided.

The design of high-speed low-weight variable reluctance alternators was studied during the MIP program and an experimental unit was fabricated and evaluated.²³

The characteristics of the inductor alternator are as follows:

Advantages:

1. Rugged and simple rotor construction suitable for high speeds.
2. D-C excited stator means easy voltage control.

Disadvantages:

1. Larger than other alternators.
2. Minimum output frequency is twice that of a conventional synchronous machine for the same shaft speed.
3. Poor inherent voltage regulation.
4. Frequency regulation determined by speed control.

5.25. Inductor (Flux-Commutating) Alternator

The flux-commutating alternator is an inductor alternator in which, by means of a clever geometrical arrangement of the rotor and stator,

the flux variation is made to change between maximum positive and negative values rather than to vary around a positive steady-state value, as is the case in the variable reluctance machine. The rotor is a very simple magnetic structure. The stator excitation can be provided either by a d-c winding or by permanent magnets which since they are located in the stator structure are not subject to high centrifugal acceleration. The flux-commutating machine can be built in very compact form; however, it can generate only single-phase power. Three-phase power generation is considerably more economical of machine size and weight for a given power rating. Similar to the variable reluctance machine the flux-commutating alternator shaft speed for a given output frequency is half of the maximum shaft speed of an equivalent synchronous machine.

The flux-commutating machine exhibits no motoring action. Its advantages and disadvantages are very similar to the variable reluctance alternator, with the added advantage of a flux variation at least 50 per cent higher which decreases its weight, and the disadvantage that it can generate only single-phase power, increasing its weight relative to three-phase generators. The characteristics of the flux-commutating alternator were studied during the MIP program and a borrowed machine was evaluated.²⁴

5.26. The Induction Asynchronous Alternator

The induction asynchronous alternator is essentially an induction motor driven by an external source and excited by a leading power factor load or a static capacitor in parallel with the load. The machine will operate either as a generator or a motor depending upon whether it is driven mechanically or energized electrically. The squirrel-cage rotor

of an induction alternator is rugged and satisfactory for very high speed rotation. The physical size of the induction alternator closely approximates that of the wound field alternator although it will normally be slightly larger.

The frequency of the induction alternator is determined primarily by the speed of the driving source and by the slip of the torque-speed curve of the machine considered as a generator; the latter curve is the mirror image about synchronous speed of the machine's characteristic as an induction motor.

The inherent voltage regulation of an induction alternator is quite poor and voltage is related to the speed by a power function with an exponent between three and four. Excitation control is very difficult if not impossible. Thus the induction machine poses unusual regulation problems. The advantages and disadvantages of the induction alternator are as follows:

Advantages:

1. Rugged rotor construction satisfactory for high rotor speed.
2. No brushes.
3. Will operate as a motor.
4. No separate source of power needed to excite the alternator.
5. Indefinitely long storage capability.

Disadvantages:

1. Control is likely to be complicated.
2. The inherent voltage regulation is poor.
3. The frequency is related both to prime mover shaft speed and generator torque-speed characteristics.

5.27. "Optimum" Electrical Machine

On a basis of the requirements of the electrical machine for the EPU, Sec. 5.1, and considering the characteristics of the respective

machine types, it was decided to investigate more thoroughly the induction motor-alternator machine as the type best suited to the air-to-air missile power system requirements.^{25, 26} As is the case in the other areas common to the MIP project, the specific choice of this type of machine for this particular application has not precluded continued consideration of other machine types perhaps better suited to other than air-to-air, short duration, low power requirements. The thesis activity investigating alternative machine types and more general considerations has continued parallel to the hardware prototype development as indicated in the preceding section and as attested to in the Bibliography.

5.3. Isolated Induction Motor-Alternator

For electrical energy generation in a solid-fuel, turbine-alternator, missile power supply, the induction machine has a number of attractive features. Its rugged rotor construction and absence of brushes lends it to high-speed operation which enhances high-output-per-unit volume performance. Its motoring characteristic permits its use as an integral motor which, by bringing the system to near operating speed prior to launch, reduces electrical switching transients and minimizes heat transfer to the turbine buckets in the hot gas stream. In the course of the EPU project, several induction machines were developed and tested and a number of frequency and voltage regulating schemes were investigated.^{5, 8, 27} The purpose of this section is to discuss briefly the characteristics of representative induction machines.

5.31. Principle of Operation

Although induction alternators have been used in some commercial power applications, the isolated induction alternator has been principally of academic interest. An understanding of the parameter relationships

that determine machine operation can be obtained by reference to the equivalent circuit shown in Fig. 37 a for each phase of an induction machine. Whereas leakage reactances are a function of the flux that links either the stator winding or the rotor winding, the magnetizing reactance is a function of the flux that links both windings. The $\left[(1 - s)/s \right] r_2$ term accounts for shaft power output and friction and windage losses. This basic circuit can be modified to the form shown in Fig. 37b to represent the induction alternator. Because the alternator generates power, the slip is negative and the $\left[(1 - s)/s \right] r_2$ represents a power source consisting of shaft input power minus friction and windage losses. A capacitor C for excitation and a resistor R_ℓ for loads comprise the circuit external to the machine. The equivalent circuit of Fig. 37b can be simplified further to the form shown in Fig. 37c for evaluation of the performance governing parameters. In the circuit of Fig. 37c, stator resistance, linkage reactances, and core loss are neglected. The magnetizing inductance is defined as $L_m = x_m/2\pi f$. Also, because the power generated in the machine and the power dissipated in the load must be equal,

$$\frac{V^2}{\frac{r_2}{s}} = \frac{V^2}{R_\ell}, \text{ or } R_\ell = \frac{r_2}{s} \quad (4)$$

where V is the machine terminal voltage. Furthermore, the leading and lagging reactance components of power in the circuit also must be equal.

$$\frac{V^2}{2\pi f L_m} = \frac{V^2}{\frac{1}{2\pi f C}}, \text{ or } L_m = \frac{1}{(2\pi f)^2 C} \quad (5)$$

where f is frequency. Equation (5) determines the operating point in Fig. 38 which shows voltage versus reactive current for both the magnetizing reactance and the capacitive reactance. The capacitive reactance is constant (fixed slope) but the magnetizing reactance due to saturation in the machine is a function of voltage (decreasing slope). Assuming constant shaft speed and constant electrical load resistance, Eq. (4) determines a fixed slip. The combination of fixed shaft speed and fixed slip determines the generator frequency. Therefore, because the magnetizing inductance is a function of voltage only (if the frequency and capacitance are fixed) the voltage level that causes the magnetizing inductance to satisfy Eq. (5) must be achieved. This simplified explanation of the operation has been verified by the performance characteristics of actual machines.

5.32. Operating Characteristics

The experimentally determined characteristics of several induction motor-alternators were determined by tests with an electrical dynamometer Fig. 39, which either supplied or absorbed power. For one of the machines tested⁸ the alternator output voltage is a function of shaft speed, excitation capacitance, and load resistance as shown in Fig. 40. The isolated turbine alternator system operates at a speed dictated by the induction alternator because the alternator torque-speed characteristic, shown in Fig. 41, is very steep compared to that of the turbine. Typical machine efficiency as an alternator and as a motor are shown in Fig. 42.

Since the systems analyses of, and the performance of a regulated solid-fuel, turbine, induction alternator system will depend upon the influence of input power and load resistance changes on the performance

of the alternator, and since the capacitance of the excitation capacitors, whose value can only be predicted within a certain manufacturing tolerance, will also influence operation, experiments were conducted on another machine⁵ to investigate the effect of changing each of these three parameters during open-loop steady-state operation of an air-turbine driven test alternator. The tested machine was a 3-phase nominal 400 cps alternator with a high-voltage plate winding and low-voltage filament winding. Tests were conducted at two power levels, identified as Group I, 450 watts and Group II, 600 watts.

As an isolated power system, the voltage obeys the relationship $V^2/R_L = P$ where P is the system power. Figure 43 illustrates this. While load resistance and capacitance were constant, input power (air pressure) was changed and plate voltage and filament voltage recorded. Figures 44 and 45 illustrate the relationship $V^2/R_L = P$ when input power and capacitance are constant and load resistance is changed. For each group the load resistance was varied plus or minus 20 per cent about the nominal values. The total power remains essentially constant even though load resistance changes 40 per cent.

The effects of phase unbalance which usually occurs to some extent when the load is divided among the 3 phases are shown in Figs. 44 and 45. With no change in the nominal conditions, load resistance in Phase C was changed plus or minus 20 per cent and the other two phases were constant. Total power remains constant but it divides in each of the phases inversely as the phase load resistance. The voltage regulation phase-to-phase is very good, the changes being less than 2 per cent even when there is a 20 per cent phase unbalance. The slight voltage rise is due to the increase

in the total mean load resistance. Frequency is affected slightly, approximately 2 per cent for a total load change of 40 per cent.

As noted previously the primary frequency-determining elements in the induction alternator system are the excitation capacitance and the effective machine inductance. Since operating frequency is a resonance phenomenon, the relationship $f = 1/2\pi\sqrt{L_m C}$ should hold, that is to say, the total effective inductive reactance equals the capacitive reactance at only one frequency. This relationship does hold as can be seen in Figs. 46 and 47 where capacitance variation of plus or minus 20 per cent were made and the results recorded. Except that turbine efficiency changes slightly with speed, the power and voltage remain essentially constant. Two items should be noted in the capacitive unbalance graphs of Figs. 46 and 47. The maximum voltage difference phase-to-phase is 2 per cent although the unbalance in capacitance was 20 per cent, and the frequency changed the same as though all three capacitors were changed to an amount equal to the mean of the unbalanced capacitors. For the extreme 40 per cent change of one capacitor in the unbalanced condition, frequency shifts approximately 6 per cent. For the extreme 40 per cent change of all three capacitors, frequency shifts approximately 20 per cent.

A typical induction-alternator output-voltage waveform has a total harmonic content of 0.33 per cent distributed as follows: 0.18 per cent third harmonic, 0.27 per cent fifth harmonic and 0.7 per cent seventh harmonic. All other harmonics are less than 0.02 per cent.

5.4. The Generalized Problem and Future Work

Typically (as seems to be the case in all areas of design endeavor) commercial electrical machine design is essentially a cut-and-try

experimental process. Early in the EPU program efforts were initiated and have been continued to attempt to place the design process on a firmer basis of scientific knowledge, and to develop systematic design techniques and the basic information essential to the implementation of these techniques.

The common design procedure is to ignore certain of the significant relationships, for example, internal temperature rise, at the outset and then subsequently to check the resulting design for the omitted effect. This trial-and-error design technique may require many iterations before a near-optimum is achieved. The use of this approach to determine a true optimum design for a complex device may be impractical even if the facilities of a large-scale digital computer are available.²⁸

It is, of course, conceptually possible to write down all the equations which control the performance of the machine. These would include mechanical, electromechanical, electromagnetic, electrical, and heat transfer equations and would include among their variables the magnetic properties of the iron, electrical properties of copper, insulation factors, mechanical strength, heat transfer characteristics, etc. These equations could, at least theoretically, be explicitly solved. If a certain optimization, for example, minimum weight is desired, a solution giving the values of the parameters for the optimum minimum weight could be obtained. This process was carried out during the MIP project for a very simple machine configuration, the homopolar generator.

Attempts at closed analytical solutions, as in the case of the homopolar machine, and the iterative technique, have both dramatically

pointed out the dearth of useful heat transfer data on internal conductance and internal and external transfer of heat from an electrical machine. In order to provide better information for electrical machine design, a program was inaugurated to determine the heat transfer characteristics of the nonhomogeneous structures found in electrical machinery. A heat-conductivity measuring device was designed and built²⁹ in order to determine the characteristics of small samples of laminated iron structures, impregnated coils, encapsulating compounds with aluminum powder added to increase heat conductivity, etc.

Since the MIP work has indicated that, in minimum volume designs, the weight of iron and of copper are approximately equal, it is proposed to study the basic methods of designing and constructing minimum volume coils and windings for use in small airborne electromagnetic devices.

In summary, a systematic and multi-pronged attack on the optimization of, and the development of systematic design techniques for electrical machinery has not received the attention it deserves.

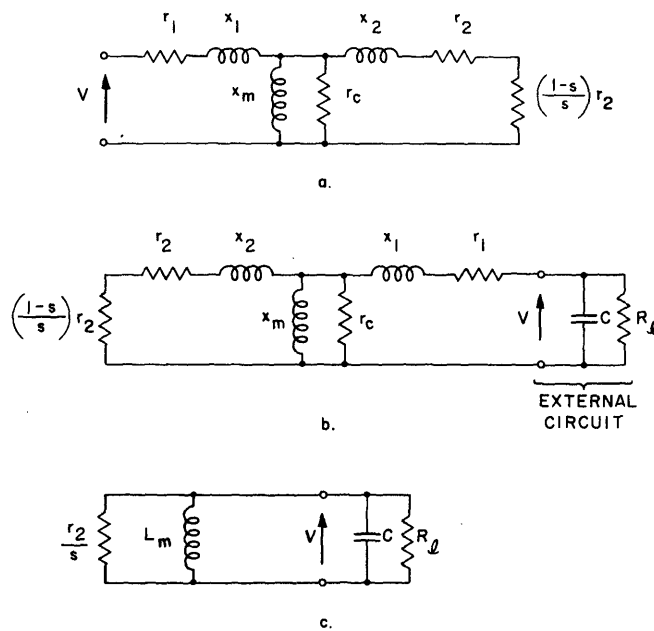


Fig. 37. Equivalent circuits for induction machine.

- a. Standard representation for motor.
- b. Modified form for induction alternator.
- c. Simplified form for induction alternator.

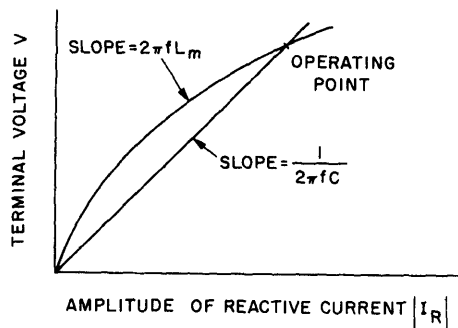


Fig. 38. Determination of machine operating point by intersection of curves of inductive and capacitive reactance.

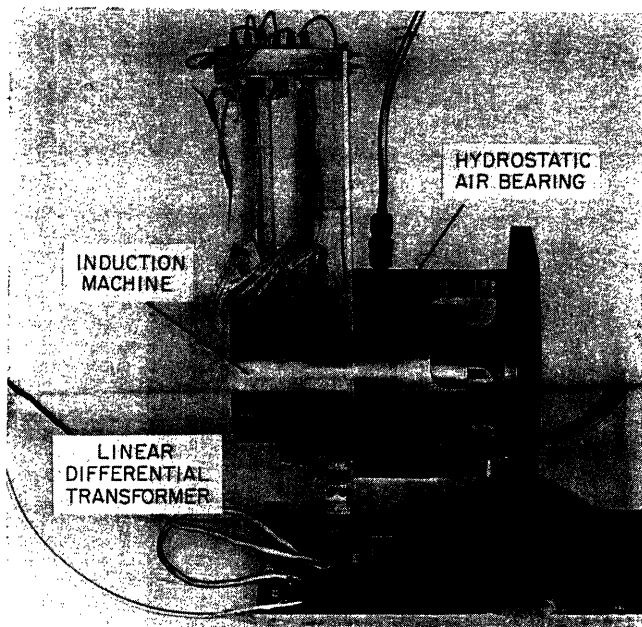


Fig. 39. Electrical dynamometer.

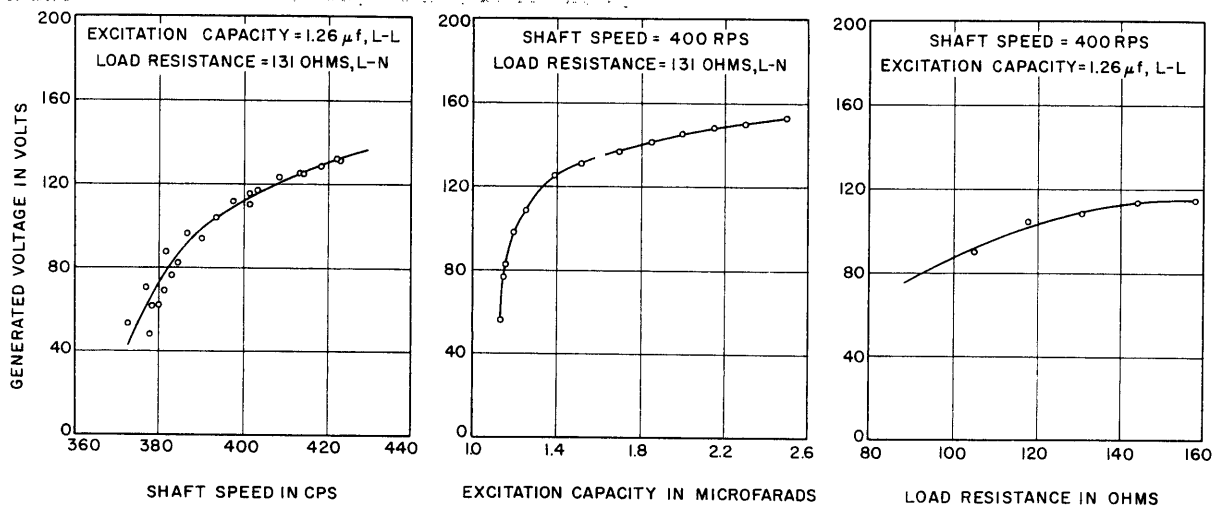
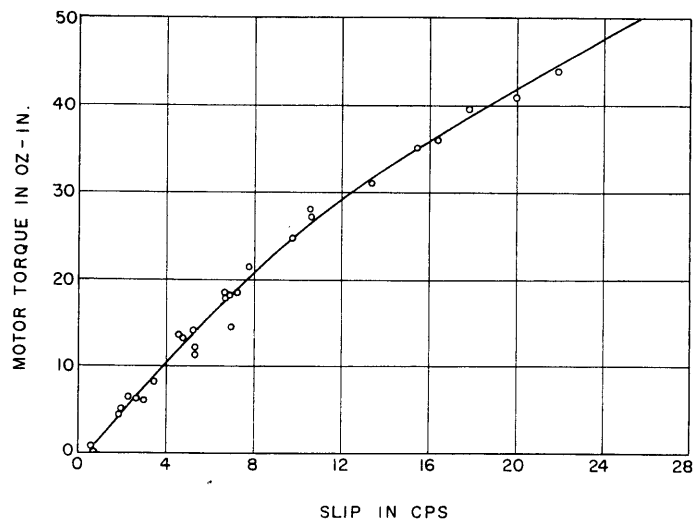


Fig. 40. Induction-alternator voltage as a function of shaft speed, excitation capacity, and load resistance.

Fig. 41. Torque-slip characteristic of induction machine.



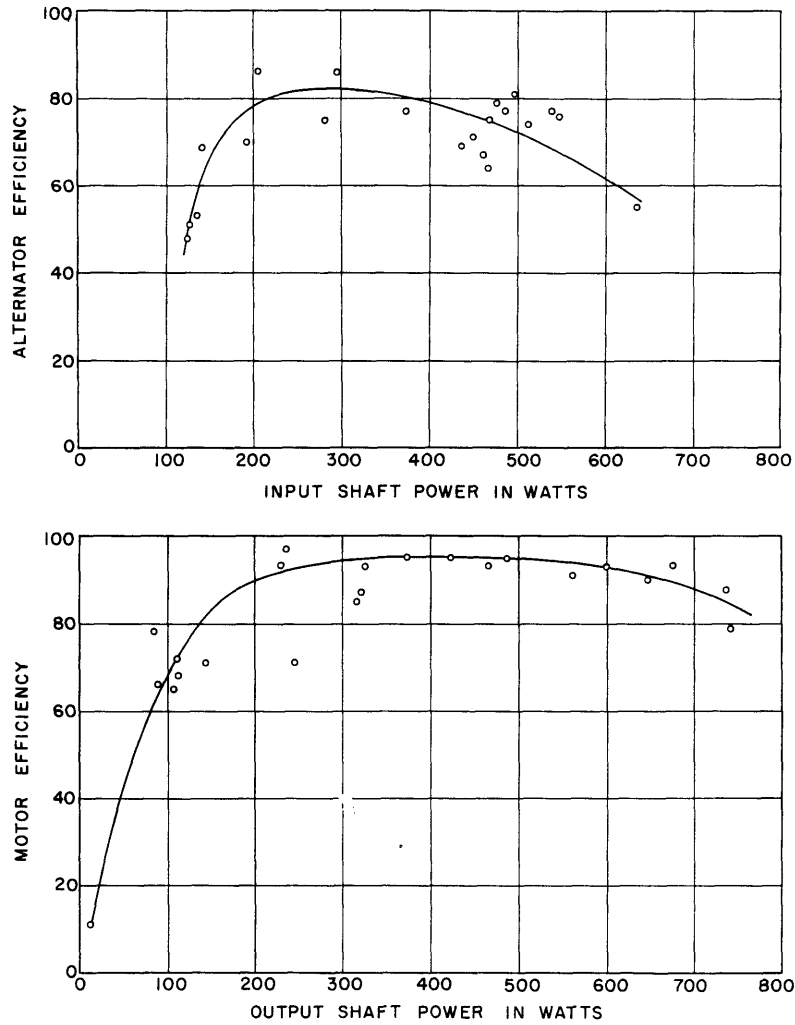


Fig. 42. Efficiency of induction machine both as an alternator and as a motor.

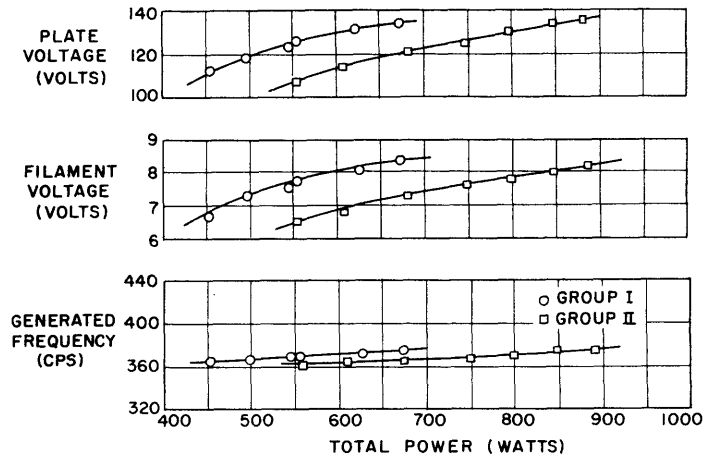


Fig. 43. Results of input-power changes.

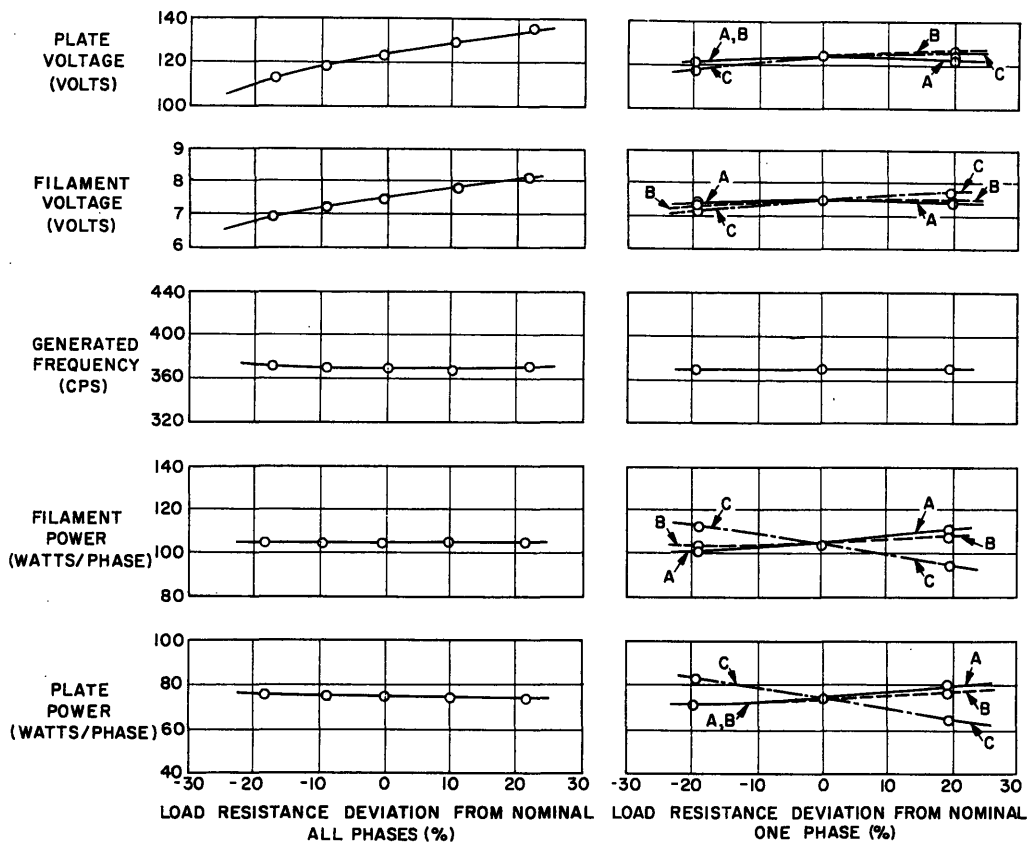


Fig. 44. Results of load-resistance changes--Group I.

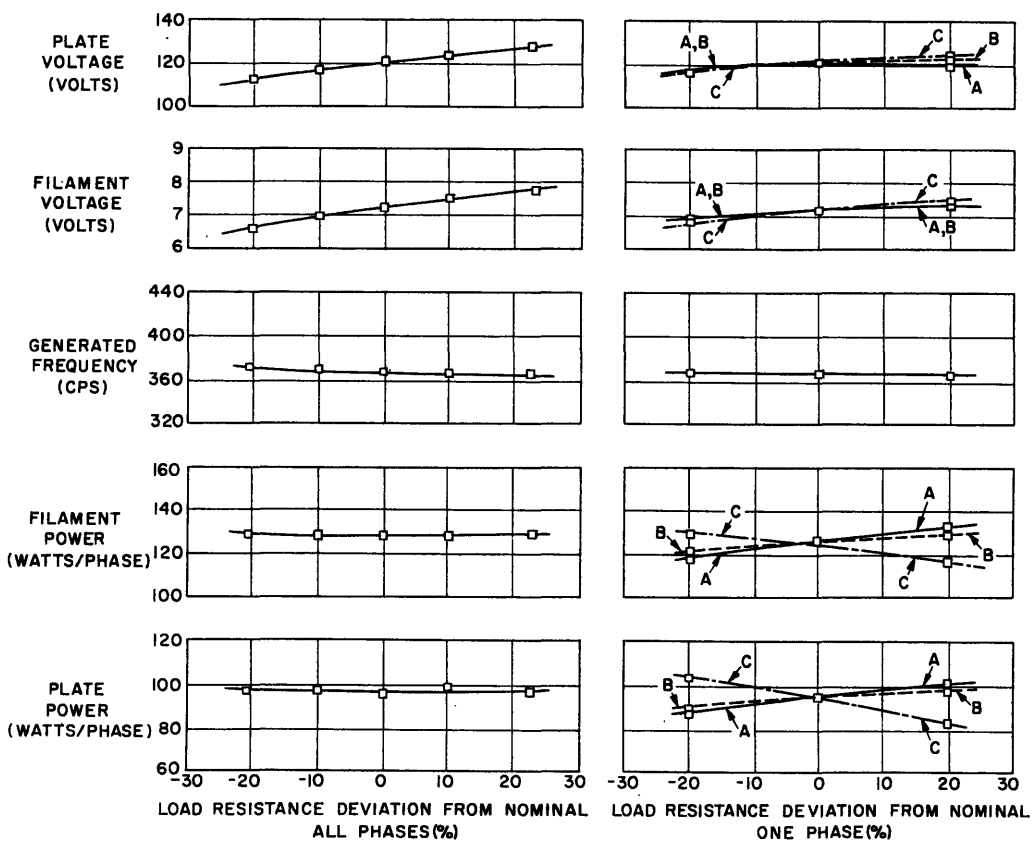


Fig. 45. Results of load-resistances changes--Group II.

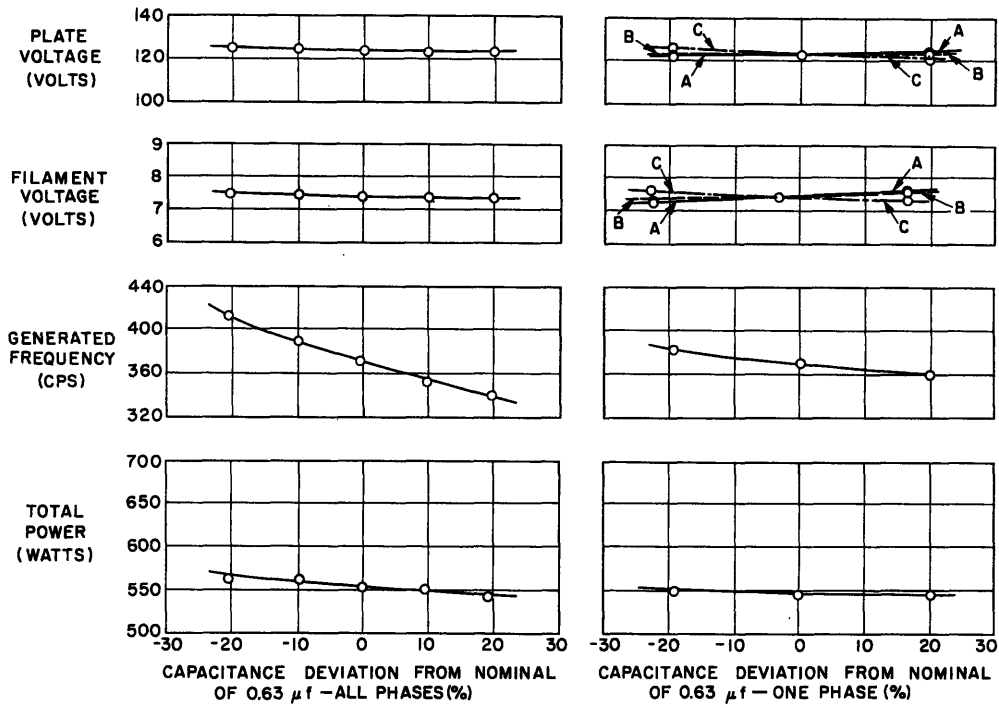


Fig. 46. Results of capacitance changes---Group II

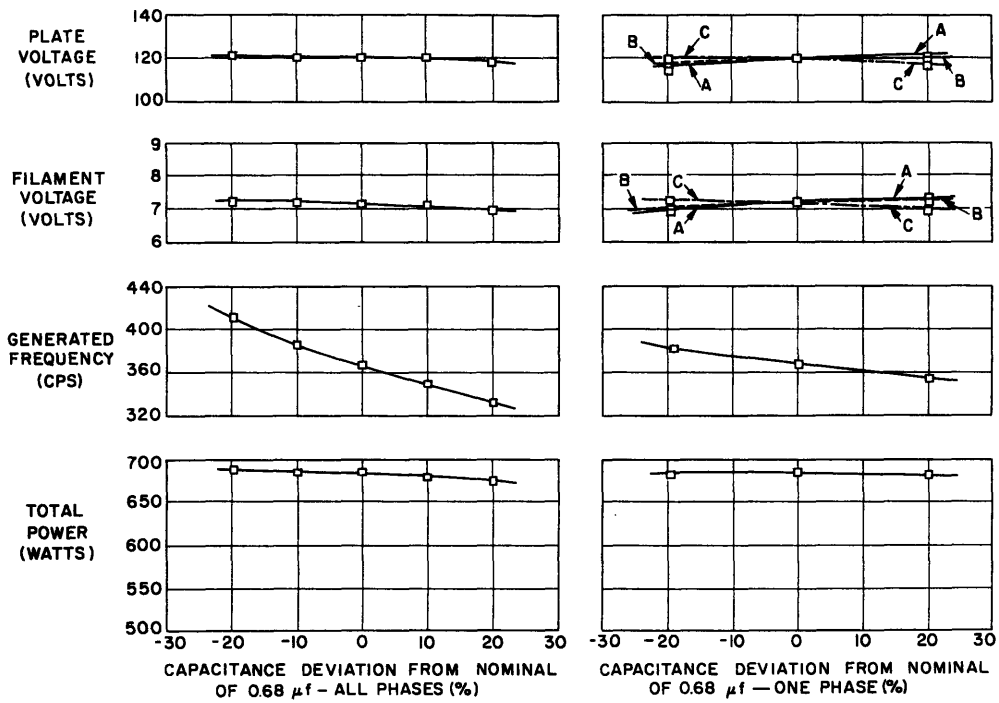


Fig. 47. Results of capacitance changes--Group II

6. REGULATION TECHNIQUES

Section 3.5 discusses the problem of regulation to achieve constant frequency or voltage output of a solid-fueled turbine alternator power supply. The conclusion reached was that the most satisfactory technique, consistent with simplicity, reliability and performance, will be a dissipative control system which will compensate for fuel burning-rate dependence on storage temperature, manufacturing tolerances, and load changes. The broad category of dissipative systems may be divided into input power regulators and load regulators depending on which side of the prime mover the dissipation occurs.

In input power regulators the gas power to the turbine is regulated either statically or dynamically in response to an output variable, whereas in load controllers, the excess energy of the gas is converted into mechanical shaft power from which torque is controllably dissipated, or, the power is converted into its final form, (perhaps electrical power) where in response to an error signal power is dissipated.

In the course of the EPU investigations at D. A. C. L., several specific regulation schemes were explored analytically and experimentally and several were brought to the state of refinement adequate for missile prototype hardware. The purpose of this section is to describe these systems and the components of which they were made, to evaluate their performance and to compare them as control techniques for solid fuel systems.

6.1. Input Power Regulators

For all stable burning pressures of solid fuels and turbine exhaust pressures the pressure ratio across the turbine nozzle is in excess of

critical. Thus controlling upstream turbine stagnation pressure will fix the mass flow rate through the turbine if one discounts change in the combustion-gas temperature which influences mass-flow rate in an inverse square root manner, see Eq. (1). In practice, the combustion gas temperature varies very little from grain-to-grain. Furthermore, during the course of a single operation the rate of heat-transfer does not change appreciably so that stagnation temperature drop due to heat transfer is not significant. Under these circumstances input power can be regulated by means of a pressure controller in which the actual combustion chamber pressure is compared with the pressure which will provide the mass-flow through the nozzle necessary to provide the desired output power. The resulting error actuates an exhaust valve diverting from the combustion chamber part of the products of combustion so as to reduce the pressure error to zero.

A system with a pressure regulator is a constant power system from the turbine on, assuming that speed changes and therefore turbine-efficiency changes are negligibly small. As indicated in Sec. 4.31 partial-admission efficiency changes very little over a broad range of exhaust pressures. The combustion chamber with pressure regulator accepts from the solid fuel a wide range of input power depending upon storage temperature and fuel manufacturing variations and delivers to the turbine a predetermined and constant power.

For many MIP applications this open-loop control technique is perfectly acceptable, provided that the characteristics of the equipment beyond the nozzle are known in advance and can be maintained sufficiently constant despite manufacturing and operational variations, and provided that the desired output is either a constant power or that the load remains

sufficiently constant to fix within reasonable limits the desired output variable be it voltage or frequency or hydraulic pressure.

For systems with electrical load, changes in resistance result in voltage changes proportional to the square root of the resistance change, since for a constant power system $P = V^2/R_{\ell}$. The design of a static pressure regulator and its performance is described in Sec. 6.11.

The "desired pressure" can be related to the regulated output variable thus achieving closed-loop operation. The design and evaluation of a system using output-speed as the reference variable is discussed in Sec. 6.12.

6.11. Static Pressure Control

The simplest kind of regulator is one which regulates pressure upstream of the turbine.^{5,7} The force resulting from combustion-chamber gas-pressure operating on a known area is compared to a known spring force with a fixed set-point thereby regulating the area of an aperture through which the dumped gases exhaust. The range of mass flow for the regulator is fixed on the upper end by the difference between load-required mass-flow and the mass flow which becomes available at the highest environmental temperature. It proves impractical to reduce the dumped flow to zero at the lowest environmental temperature since the valve performance for very small apertures is unpredictable.

Extremely simple in basic function, the regulator design is dictated by the high temperature (as high as 3000°F) of the exhausted gases, the erosive and clogging nature of the solid particles present in the gas, and the effects of vibration and acceleration loading on the regulation of the valve.

Early work was performed with a cone-shaped pintle and square-edged seat having a relatively small working area and a long soft spring to achieve small change in spring force for displacements up to 0.020 in. which was erroneously thought to be a minimum practical value. The reduction in stagnation pressure on the pintle corresponding to high-velocity flow was equivalent to a ten-fold increase in the effective spring constant. Furthermore, the spring constant and concomitant natural-frequency was much too low for the acceleration and vibration loading anticipated. Increasing the working area and peripheral length of the exhaust orifice reduced the maximum flow displacement to 0.003 in., permitting the use of a stiffer spring and a higher preload which both increased the natural frequency of the mass-spring system and decreased the effect of acceleration loading on the valve. Reducing the moving mass to a minimum further reduced vibration-and-acceleration-loading effects. The stagnation pressure decrease associated with flow was compensated for by applying the momentum force of the fluid to the valve plate by turning the fluid through 180° by the plate. Since the momentum forces are proportional to flow the effects cancel.

Although the pressure and spring forces in a valve such as this are relatively large (20 to 40 pounds), at the regulated pressure these forces are balanced and the differential operating forces moving the plate about the equilibrium position are of the order of 1 per cent of this force level. Thus frictional forces restricting free movement can be serious. Guiding of the spring, particularly if it is of low spring-constant and long, can be a serious source of friction. The Model I design, Fig. 48b eliminates this by means of a short, stiff spring. Lateral support of the plate and alignment of the plate with the seat requires a guide, and friction here, too, must be kept low. The use of graphite bearings and a well-finished

shaft (with a 5 microinch rms surface roughness) reduce friction to an acceptable level. The undamped mass-spring system of the regulator will tend to oscillate at low flows due to flow forces and coulomb friction. When excited as in vibration tests, it will oscillate with considerable amplitude at its natural frequency (approximately 190 cps). The frequency of the resulting pressure oscillation is too high to affect the performance of the high-inertia turbine-alternator system provided the mean value of the oscillating pressure is unchanged from the nonoscillating value. For large-amplitude oscillations and for small valve openings, the excursion of the plate is limited in one direction, resulting in a change in the effective mean-pressure. To minimize or eliminate these oscillations, viscous damping is obtained through the use of a high-viscosity silicone fluid (1000 centistokes) in the annular space around the shaft supporting the plate.

An obvious solution to the vibration and acceleration forces is to counterbalance the moving portions of the regulator. An early version of a regulator incorporated such a scheme, as shown in Fig. 48a. Although it can be demonstrated analytically that the spring mass for such a device can be balanced for constant accelerations in either direction, it does not appear possible to balance the spring mass for rapidly varying acceleration such as in vibration testing. Vibration tests during operation on air indicated that the improvement in regulation with the balance weight was negligible. Accordingly, the considerable complication of the balance mass and linkage was eliminated in the final version of the Model I regulator, Fig. 48b.

Experiments with a restriction upstream of the metering orifice indicated increased valve stability. In the Model I regulator this restriction

consists of the small clearance (0.012 inch at closed position) between the plate and the land at the inner diameter of the seat followed by the annular groove 0.025 inch deep immediately before the metering edge. The groove in the seat serves the further purpose of minimizing carbon buildup at the metering edge of the valve. The finely divided particles of carbon in the gas stream tend to pile up on the metering edges, thus changing the working area upon which the gas pressure operates, resulting in deterioration of regulation. The presence of the groove alters the particle buildup in such a way that it does not assume serious proportions but rather exhausts through the regulator.

The hot, particle-laden gases flowing across and eroding the regulator metering edges seriously affect regulation and cause high leakage. After experimentation with a variety of materials, molybdenum was found to combine the characteristics of high erosion resistance, machinability, and resistance to thermal shock.

Heat transfer from the gas through the regulator structure to the spring can seriously affect performance by partially annealing the spring, giving it a permanent set. To avoid such heating, the plate is insulated from the shaft and spring by a ceramic wafer, and the valve seat is insulated from the regulator main body, which houses the spring, by a thin stainless-steel ring which incorporates a baffle to deflect hot gases.

Figure 49 indicates the regulation characteristics of the Model I regulator when operated on air over the range which corresponds, with temperature and specific-heat correction, to the range of hot-gas flows necessary in a typical EPU. Regulation characteristics on hot gas were investigated by introducing a step change in flow during a hot-gas run by

opening an auxiliary nozzle. Recordings of such a test indicated a 1 per cent change in pressure for a 100 per cent change in flow rate, corroborating the air-regulation data. The ability of the regulator to eliminate the ignition pressure peak was described in Sec. 3.3.

An alternative design of the pressure regulator is shown in Fig. 48c. This Model II version utilizes Belleville springs rather than a helical spring and does not deflect the gas flow as much. Natural frequency is higher (515 cps) because of stiffer springs and smaller moving mass, reducing acceleration-loading effects. Damping (and thermal protection of the springs) is accomplished by filling the spring chamber with silicone fluid. Regulation is somewhat poorer owing to the higher spring constant and reduced flow-force compensation.

During the development of the pressure regulator an analysis was made to investigate how the parameters of the system affected the valve stability.⁷ The study included gas properties, the combustion chamber volume, the turbine nozzle flow, the regulating valve flow, stabilizing orifice flow, spring rate and set point, the viscous damping, and the effect of gas momentum forces. Applying Routh's criteria to the system characteristic equation indicated how variation of particular parameters would influence valve stability. By inserting the physical parameters of the system into the characteristic equation, the external damping coefficient was evaluated and compared with the damping coefficient based on fluid viscosity and bearing geometry. The agreement was within 20 per cent.

An example of typical performance for a system utilizing only a pressure regulator of this type is given in Fig. 50. The components

consist of a combustion chamber, a pressure-regulating valve, and a turbine directly coupled to an induction-alternator which motored the auxiliary power supply prior to ignition of the solid fuel, thereby reducing the transient of voltage and frequency when the power unit was actuated. A transient in shaft speed is inevitable since pre-initiation speed is determined by the external electrical power source and post-initiation speed is determined by the characteristics of the isolated EPU. In the case shown in Fig. 50, pre-initiation speed was higher than post-initiation speed so some of the kinetic energy of the rotating member had to be delivered into the load as an over-voltage before regulated voltage (determined by the pressure regulator setting and load resistance) could be accomplished.

6.12. Dynamic Pressure Control

The pressure regulator can be made into a closed loop rather than an open loop controller by summing into its displacement a variable which represents the desired output parameter. Figure 51 describes a system in which shaft speed is the controlled variable. A small centrifugal pump feeds back to a regulator valve, a pressure which is related to shaft speed. The regulator valve sums the hydraulic pressure representative of actual speed, a reference spring force characterizing desired speed, and the gas pressure of the solid fuel. The resulting output displaces a flapper valve which dumps combustion product flow in proportion to the speed error. This regulating system is particularly interesting since it is completely mechanical and therefore applicable to systems, such as a hydraulic power supply, where electrical power might not be available. The pump acts as a tachometer to measure speed,

and together with the regulator provides adequate power gain in the feedback loop without recourse to any external power source. The feedback pressure signal is proportional to speed squared. In the interests of generality the system studied included both d-c and a-c generators and the system performance was evaluated in terms of speed error, d-c voltage error and a-c voltage error.

This system was explored in detail, analytically, using conventional servoanalysis techniques and an analog computer, and experimentally.³⁰

The block diagram upon which the analyses were based is given in Fig. 52. The transfer function for each element was developed by deriving the basic equations relating the relevant variables and then considering small perturbations about the operating point. Certain of the system parameters were fixed by the fuel characteristics and other inflexible constraints, while others were determined by experimental studies of the hardware components. Using linearized versions of the equations, transient analyses were conducted using the log-modulus, contour, and root-locus techniques to determine the system gains for adequate stability thus establishing the values for the remaining parameters. The transient response was also studied on an analog computer in which it was possible to retain certain of the nonlinearities, particularly the effect of limiting the regulator valve stroke and the influence of friction in the regulator.

The analytical studies indicated that under the worst possible combination of loads, including effects of temperature on fuel characteristics and step load resistance changes of ± 10 per cent, maximum speed errors of ± 0.9 per cent and corresponding d-c voltage

errors of ± 1.2 per cent were to be expected. Due to the speed-voltage relationship of induction alternators the a-c voltage fluctuation for the same speed error is estimated to be about ± 10 per cent. Certain refinements, it was felt, would reduce these errors about in half.

Figure 53 shows the experimental centrifugal pump while Figs. 54 and 55 give its operating characteristics when pumping a silicone fluid with a viscosity of 20 centistokes at 25°C . The influence of ambient temperature on pressure, Fig. 56 introduces an erroneous error signal due to the changing density of the fluid. This effect was eliminated by providing heaters and a thermostat on the pump to keep it at the maximum environmental temperature. Also troublesome was the presence of dissolved gas in the fluid which accumulated on the suction side of the pump and reduced output pressure. This effect was eliminated by careful evacuation of all entrained gas from the fluid.

Figure 57 illustrates the experimental regulator showing the reference spring, double-acting hydraulic piston and the hot-gas dump valve. The major problem in the regulator was friction in the piston guides which could be reduced by various techniques.

The hot gas experimental work on this system was limited to studies of the regulator's effectiveness at ignition, and as a pressure regulator, and the response of combustion chamber pressure to pseudo-step changes in shaft speed. Figure 58 gives valve displacement, pressure, and speed for a typical run.

6.13. Turbine Efficiency Control

Rather than dissipating input power by dumping hot gas, techniques which affect the efficiency of the turbine could be employed to achieve a regulated system. One technique is to insert, in inverse relationship

to the desired output power, a spoiler in the nozzle which changes the effective angle and velocity of the flow leaving the nozzle, reducing turbine efficiency. The use of variable-angle nozzles to achieve the same result has also been proposed. A third technique would be to cant the nozzle so as to spill nozzle flow over the tip of the wheel controlling the spillage in proportion to the desired power dissipation. These techniques all raise serious questions of mechanical complexity, considering the high temperature of the fuel and the erosive and clogging nature of the solid particles in the gas. They were not investigated in the M. I. T. MIP program.

6.2. Load Regulators

The load regulator system achieves control by power dissipation downstream of the prime mover. All the fuel power is converted into mechanical shaft power, and therefore the output power of the turbine will vary with the variation of energy flow from the fuel. This imposes no additional weight or volume burden on the system since doubling or tripling the power of a partial-admission turbine does not alter its size. In fact for very low total power the turbine design and efficiency may be enhanced by operation at the higher power level. The effect of increased heat transfer to the turbine rotor must be considered as in Sec. 3.63.

One load control scheme is to subtract from the output torque of the turbine a variable controllable torque in response to an error signal. Torque control, by closing the control loop around the turbine, minimized the effects on performance of manufacturing variations in the small fluid passageways. The system and components of a torque controller are given in Sec. 6.21.

Power dissipation can also be achieved by varying the load across the output of the power supply so as to achieve desired regulation of an output variable. In all but very low power systems complete regulation by this means imposes upon the electrical machine or the hydraulic pump a capacity adequate to convert the maximum power ever available from the solid fuel. It is usually expensive in terms of system weight and volume to refine the form of the dissipated energy to the finally-desired type before throwing it away.

However, systems which use a device such as a static pressure regulator for gross input-power variations can compensate for residual power variations due to pressure-regulator operation tolerance, manufacturing tolerances in the turbine nozzle and the energy conversion devices, and small variations in the system load by means of a load power controller. The additional capacity imposed upon the electrical or hydraulic machine in such a case may be small compared with total system weight. An electrical load power regulator is described in Sec. 6.22.

6.21. Torque Control

As has been indicated in Secs. 4 and 5 both turbine efficiency and electrical generator output per unit weight are enhanced by high shaft speeds. At present the maximum limiting speed is usually dictated by electrical frequency specifications which Sec. 8 recommends be made much higher than the presently common 400 cps. At rotative speeds of 24,000 rpm (corresponding to a 2-pole generator delivering 400 cps) or higher, torque control by a mechanical braking device is unattractive considering the variability and unpredictability of the coefficient of friction,

the inherent dangers of mechanical contact at high relative velocities and wear of the mating surfaces. The absence of mechanical contact, consistency of performance, simplicity and high power gain of an eddy-current brake make it a desirable torque control device for MIP.

6.211. Eddy Current Brake

An eddy current brake consists of a disk of electrically conductive material that is rotated in a magnetic field maintained perpendicular to the face of the disk. Rotation causes a voltage difference to be induced in the disk between its inner and outer edge. The eddy-currents that flow in the disk as a result of this voltage difference produce a magnetic flux field which interacts with the flux field of the field poles so as to retard the motion of the disk. The torque characteristic of an eddy-current brake is approximately proportional to speed up to a maximum torque beyond which torque decreases. For most efficient utilization of materials the rated operating speed of the brake is set slightly below the speed corresponding to peak torques. Lof³¹ developed empirical equations for the design relationships of eddy-current brakes using disks of nonmagnetic material. Although Lof's constants were evaluated for brakes operating at lower rotational speeds than those encountered in the MIP program, experimental evaluation of several brakes during the program have shown his relationships to be valid for higher speed applications.

The equations which characterize the performance of the eddy-current brake are:

$$N_m = 9.4 \times 10^7 \frac{\rho}{r_o t} \left[\frac{l_e}{w_e} + 12.4g + 1.9 \right] \quad (6)$$

$$\frac{T_M}{\text{pole pair}} = 8.2 \times 10^{-10} \frac{r \phi_o^2}{A_e} \left[\frac{l_e}{w_e} + 12.4g + 1.9 \right] \quad (7)$$

where

N_m = speed at maximum torque, rpm,

ρ = resistivity of disk material, ohm-in.,

r_o = outside radius of the disk, in.,

t = disk thickness, inch,

l_e = air-gap cross-section equivalent length, in.

w_e = air-gap cross-section equivalent width, in.,

T_m = maximum torque, lb-in.,

r = radius of center line of field poles, in.,

ϕ_o = air-gap flux, lines,

A_e = effective area of field poles, in.² = $l_e w_e$

Mechanical considerations such as adequate disk strength and rigidity, adequate axial clearance between disk and field-pole faces, and space limitations, and the electromagnetic consideration of minimum air-gap length to minimize field coil and iron structure, together with Eq. (6) determine the disk geometry and material. Possible disk materials range in resistivity from 28.4 micro-ohm inch for nonmagnetic stainless steel to 0.6 micro-ohm inch for copper. The relationship, Eq. (7) defines the requirements of the field structure. To achieve minimum field-structure weight an optimization study is required which includes

as variables field-structure configuration, air-gap length, coil resistance, and iron and air-gap flux densities. This electromagnetic structure optimization problem is fortunately very much simpler than the case of rotating machinery alluded to in Sec. 5. Since the magnetic structure is a simple yoke with one air-gap, the coil is a conventional axisymmetric bobbin and heat-transfer problems are relatively simple. After (1) establishing the field-structure configuration to minimize iron-path-length and to provide approximately constant flux-density through the iron, (2) basing the air-gap length on mechanical considerations and disk material choice, and (3) impedance matching, for maximum power transmission, the field coil resistance and amplifier output characteristics, the optimum combination of iron and air-gap flux densities were determined by a digital computer study of a range of possible combinations.

For the particular case of a field-structure geometry shown in Fig. 60 the topography of the optimization study is shown in Fig. 61. Figure 67 shows the optimized eddy current brake disk and coil and a subminiaturized 7-tube voltage reference and amplifier used to drive the brake coil.

The torque-speed curve of this 4-inch diameter brake for fixed-field excitation is given in Fig. 63 and its torque and absorbed power at 24,000 rpm versus brake current given in Fig. 64. The power gain, brake-coil power to brake-shaft power, is about 100 and the brake disk is capable of dissipating up to 1000 watts steady state at 24,000 rpm.

6.212. Torque Control System.

An EPU system comprised of a turbine, induction motor-alternator, and transforming, rectification, and filtering equipment with eddy-current-brake torque control was studied analytically and experimentally.⁸ Figure 65 gives the block diagram representation of the system which was investigated

using an analog computer. The model does not include the combustion chamber since the initiation transient of the gas generator is over very rapidly (see Fig. 7 or 9, Sec. 3.3) and combustion chamber pressure is constant during a particular run.

As discussed in Sec. 4 turbine efficiency η_t is approximately proportional to velocity ratio and therefore shaft speed N . Turbine power is proportional to combustion chamber pressure P_c . Thus

$$T_t = \frac{K_t \eta_t P_c}{N} \quad (8)$$

Linearization of this equation is valid for small changes (identified by a hyphen) about nominal values (identified by the subscript o)

$$T'_t = \frac{T_{to}}{P_{co}} P'_c - \frac{T_{to}}{N_o} N' \quad (8a)$$

The load torque T_l imposed on the turbine by the generator is

$$T_l = K_l \frac{W_l}{N} \quad (9)$$

or as linearized

$$T'_l = \frac{T_{lo}}{W_{lo}} W'_l - \frac{T_{lo}}{N_o} N' \quad (9a)$$

From Sec. 6.211, the torque of the eddy current brake T_b is proportional to the square of the brake coil current I_b^2 . The dynamics between coil flux and coil current are negligible:

$$T_b = K_b I_b^2 \quad (10)$$

Linearization of this expression about a nominal value would not be valid since I_b varies from zero to a large value for small variations in speed and voltage, that is to say, the system gain is high. Fortunately, the analog computer elements permit the retention of Eq. (10) in its entirety. Assuming friction and windage torques to be negligible, summing the torques and equating the net torque to the resulting acceleration of the system inertia J , in Laplace transform notation, results in

$$T_t(s) - T_l(s) - T_b(s) = J_s N \quad (11)$$

or

$$T_t'(s) - T_l'(s) - T_b(s) = J_s N! \quad (11a)$$

As discussed in Sec. 5.3, the output voltage of a capacitively excited induction alternator E_g is proportional to a power of speed where the exponent is between 3 and 4.

$$E_g = K_g N^\sigma \quad 3 < \sigma < 4 \quad (12)$$

or

$$E_g' = \sigma K_g N_o^{\sigma-1} N! \quad (12a)$$

This equation is valid only for steady-state operation over a small speed range. Ignorance of and omission of the dynamic characteristics of the alternator introduced serious error into the analog study as will be shown. The dynamics of the transformer and rectifier can be neglected and their effects combined as a linear gain

$$E_r = K_r E_g \quad (13)$$

or

$$E'_r = K_r E'_g \quad (13a)$$

The power delivered to the unity-power-factor missile load, which is assumed constant, is

$$W_l = \frac{E_r^2}{R_l} \quad (14)$$

or

$$W'_l = \frac{2E_{ro}}{R_l} E'_r \quad (14a)$$

The delays in the amplifier are small compared with other significant system lags. However, the delay between applied voltage E_b and brake coil current I_b , caused by the brake coil inductance, is important.

Therefore

$$I_b = \frac{E_b}{R_b} \cdot \frac{1}{\tau_b s + 1} \quad (15)$$

where R_b is the resistance of the brake coil and τ_b is the time constant of the coil.

This system analog was investigated with both off-on control and proportional control of the brake. In the case of proportional control the relationship Eq. (15) was represented by the analog of

$$I_b = \frac{K_a E_r}{R_b} \cdot \frac{1}{\tau_b s + 1} \quad (16)$$

except that a saturating amplifier was assumed. In the model of the proportional controller Fig. 65 the limiter causes the steady-state brake current to be proportional to the error signal only over a certain limited range.

In the case of off-on control, the coil current is zero when the control is off and takes the form of Eq. (15) when control is on. Rather than represent the off-on controller by computer elements, the actual controller, consisting of a voltage-sensitive amplifier that operates a relay, was employed in the analog study, insuring faithful representation of complicated but important controller characteristics such as amplifier limits, relay-coil-inductance dynamics, and relay hysteresis.

The performance of the off-on controlled system on the analog computer, set up as in Fig. 65 with actual control hardware, was compared with the performance of an actual hot-gas system comprised of combustion chamber, turbine, alternator, controller, etc. Figure 67 compares the recorded performances of the analog model and of the actual system. Whereas the amplitude of the voltage variation for the analog was 13 volts with a frequency of oscillation of 4.67 cps the actual unit voltage amplitude fluctuation was 20 volts and the frequency of oscillation was 3.33 cps.

These results show that the response of the model was faster than that of the real system. A series of computer runs determined that the cause of this discrepancy is a lag between the speed and voltage of the induction alternator. The dynamics of induction machines have subsequently been studied further in order to formulate a more accurate mathematical model³². Under any circumstances, the large amplitude and low frequency of the voltage fluctuations are not acceptable in an

EPU system and so off-on control was abandoned in favor of proportional control.

The performance of a complete EPU with proportional control of an eddy current brake is given in Figs. 68 and 69 which record the significant system variables at the high and low temperature extremes of operation. Figure 70 illustrates how the brake power varies with variations in input power (as with soaking temperature) to maintain acceptable regulation of the output variable---in this case, 258 ± 5 per cent volts.

6.22. Electrical Power Control

Control of an output variable can be achieved by dissipating a portion of the total generated power in an element arranged in parallel with the load and controlled by an error signal related to the output variable. For instance in an electrical power system a frequency-sensitive shunt may be arranged so that power-frequency increases above a certain desired range decrease the shunt resistance. This increases the total load on a synchronous generator which, for constant input power, reduces shaft speed and consequently frequency. Schemes of this type have proven feasible only for relatively wide frequency tolerances, of the order of ± 10 per cent.

For systems with turbine-driven, asynchronous induction-alternators, variable inductances (saturable-core reactors) in parallel with the load and excitation capacitors prove suitable for controlling voltage, but frequency variations are not affected.²⁷ Attempts at controlling frequency by means of a dissipative load, such as a non-linear resistance (Thyrte), in parallel with the primary load, are also

ineffective due to the poor inherent voltage regulation of the induction machine, (typically 20 per cent, expressed as no-load voltage minus full-load voltage divided by full load voltage). Dynamic braking, by means of a parallel resonant circuit in series with a rectifier, all arranged in parallel with the load, was explored. Since the stator iron of the induction machine must be designed to saturate under normal operating conditions, the additional direct current drawn from the stator for dynamic braking has little effect.

For voltage control of an EPU for which the frequency tolerance was not severe, a thyatron-controlled dissipative load was developed to compensate for residual power variations due to pressure-regulator operating-tolerance and manufacturing tolerances in the turbine nozzle and missile load. The power dissipating resistors (three in this case for a three-phase system) are arranged in the plate circuits of the thyatron tubes. The conduction angle of the thyatrons is controlled by a d-c voltage which is proportional to the error difference between the load voltage and the constant voltage drop across a voltage reference tube. As the conduction angle is changed, the current and power conducted by the thyatron plate circuits into the power dissipating resistors varies proportionately, tending to reduce system over-voltage to the desired voltage level.

The performance of a voltage control system comprised of a pressure regulator for gross input-power variations and the thyatron load regulator for residual input-power and load variations is shown in Figs. 71 and 72 at two different temperature levels. Particularly notable is the contribution of the load regulator to transient performance at

initiation. Compare Fig. 50 for pressure-regulator control only with Fig. 71 or 72 for pressure plus load regulator. The over-voltage at initiation for the latter cases results in substantially increased power dissipation in the load regulator, rapidly decelerating the EPU rotating system to correspond to post-initiation frequency. Regulated output voltage is accomplished in less than 30 milliseconds. To avoid those frequency mismatches between pre-initiation parent system and post-initiation EPU system which would require extensive transient acceleration of the EPU rotary system, two conditions are satisfied. First, an "optimum" isolated EPU frequency is determined from consideration of the range of possible pre-initiation parent system frequencies and the acceleration and deceleration characteristics of the EPU. Secondly, the load regulator is biased to dissipate very little power up to the output voltage corresponding to the lower tolerance limit. This negligible power dissipation in the load regulator prior to the attainment of low tolerance voltage means that the difference between normal power from the hot gas (as regulated by the pressure regulator) and the low missile load power (low due to low alternator voltage) is almost all available to accelerate the unit to desired speed and frequency.

The thyatron tube, which only conducts during the positive voltage half-cycle, acts as a half-wave rectifier in delivering power to the power regulator resistors. This introduces some harmonic distortion into the EPU output voltage waveform. Where harmonic distortion specifications are rigid, complication of the regulator to the extent of full-wave rectification will minimize distortion, or a power device which delivers continuous power, such as a magnetic amplifier, could be used.

6.3. Comparison of Regulation Techniques

Based on the experience of the project, the following generalizations may be made on the several dissipative control schemes investigated.

The static pressure regulator for combustion-chamber pressure-control is a feasible and practical device for the control of very hot fluids under the environmental conditions imposed on missiles. Effective heat isolation of the reference element from the metering orifice is essential: the useful duration of operation depends on the effectiveness of this insulation. Regulation of pressure to ± 5 per cent, corresponding to the same range of turbine power, is probably the best regulation achievable. The adjustment of the set-point of the reference spring, which must be done by means of flow tests using a high-pressure gas, is somewhat awkward and indeterminate within a percent or two.

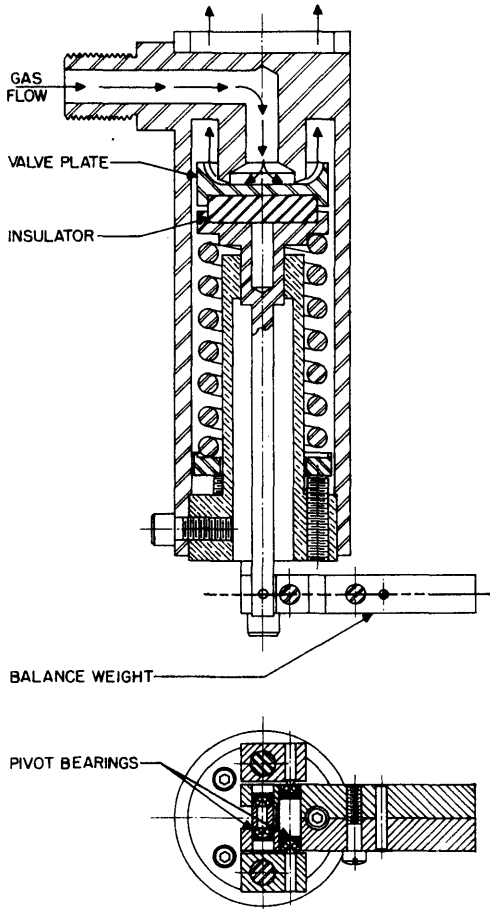
The pressure regulator seems best suited to systems where overall regulation requirements are not severe, particularly where open-loop control from the turbine on to the load is adequate. Static pressure control can also serve well when a subsidiary control scheme is not adequate to the very large input-power variations of solid fuels due to storage temperature changes.

Dynamic pressure regulation, where an output variable is used to position the exhaust valve, poses a number of problems, which, although not insurmountable, are substantial when one considers alternative schemes. Variations in fluid density, due to temperature and absorbed gases, affects the hydraulic tachometer. An electrical tachometer would require a power amplifier to operate the valve. The high temperature of the metering part of the valve complicates the design and isolation of the force transducer, be it hydraulic or electric. Friction in the valve must be kept to a minimum.

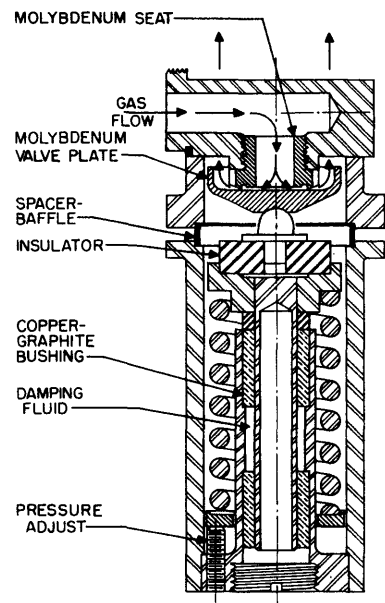
The calibration of the set-point of the reference spring remains a problem as with the static regulator.

Power regulators are a very desirable control scheme if the range of power to be dissipated compared with the total power is not so great as to place an undue burden on the energy conversion machinery and if the controlled-variable tolerance can be broadened sufficiently to permit regulation by static elements, such as a tuned-circuit with series resistor shunting the load. When, in order to meet more stringent specifications, they become more complicated, their application should be carefully reviewed.

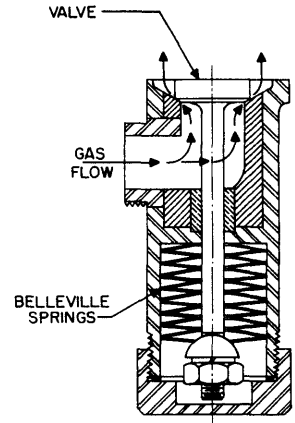
Of the control schemes considered during the M. I. T. program, and of all presently proposed schemes, the eddy-current brake torque control seems most suited to solid-fuel systems. No weight burden is imposed on the system due to the increased power of the turbine and the problem of metering high temperature gases is avoided. No excess power is required from the electrical machine and no undesirable harmonics are introduced into the voltage input waveform. The mechanical design of the brake system is simple, and close tolerances, friction-free supports, and difficult heat insulation problems are avoided. Due to the high power gain of the brake, the brake coil amplifier requirement is not severe, with the result that the over-all weight of the eddy-current brake system is the lowest of all comparable systems. Finally, in the case of induction alternators, for which the voltage output is approximately proportional to the cube of frequency, adequate control of the output voltage insures sufficient frequency control.



a. Breadboard regulator.



b. Model I regulator.



c. Model II regulator.

Fig. 48. Pressure regulator.

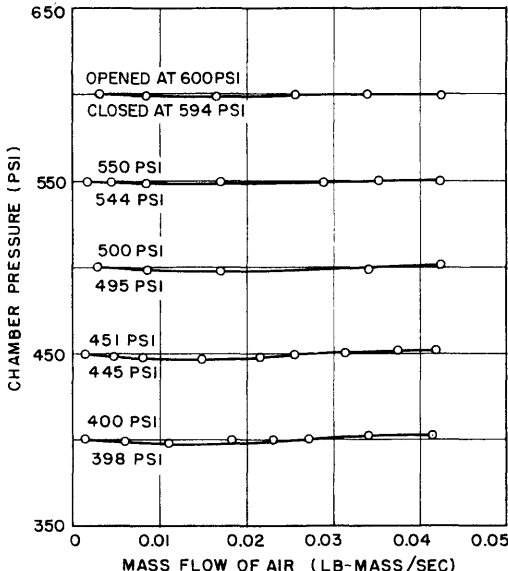


Fig. 49. Regulation characteristics of Model I regulator.

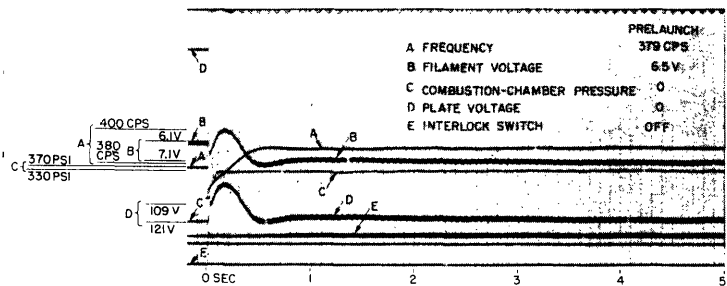
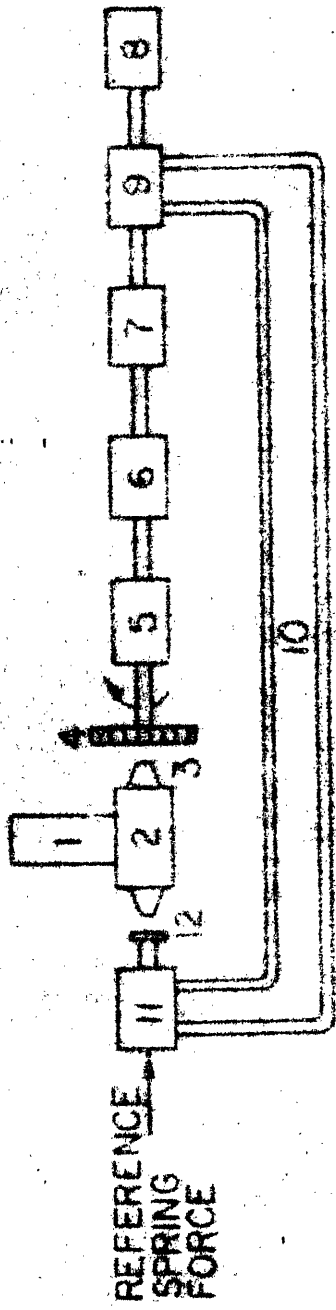


Fig. 50. Recording with pressure regulator.



Basic System

Regulator

- | | |
|------------------------|------------------------------|
| 1. Solid fuel. | 9 Centrifugal pump. |
| 2. Combustion chamber. | 10. Hydraulic Tubing. |
| 3. Turbine nozzle. | 11. Controller. |
| 4. Turbine. | 12. Flapper-Type dump valve. |
| 5. D-C Generator. | |
| 6. D-C Generator. | |
| 7. A-C Alternator. | |
| 8. Run-up motor. | |

Fig. 51. Schematic diagram of basic system and regulator.

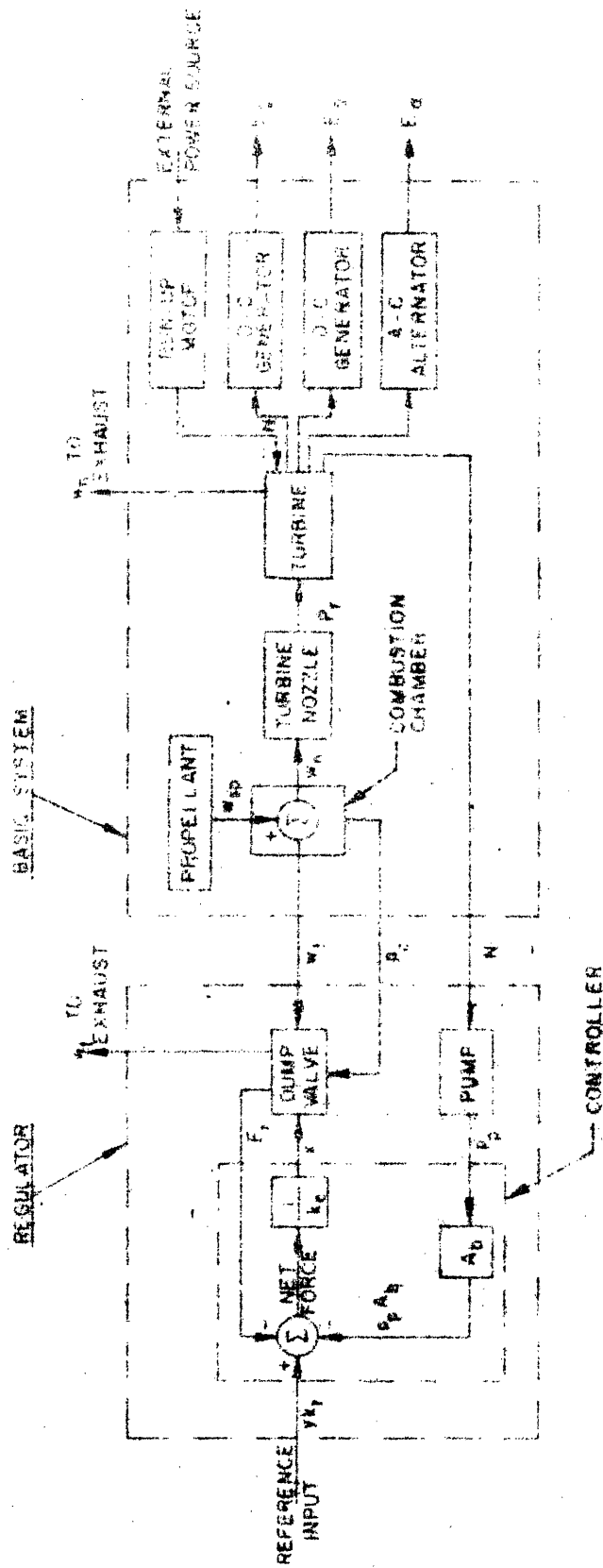


Fig. 52. Signal flow diagram of basic system and regulator.

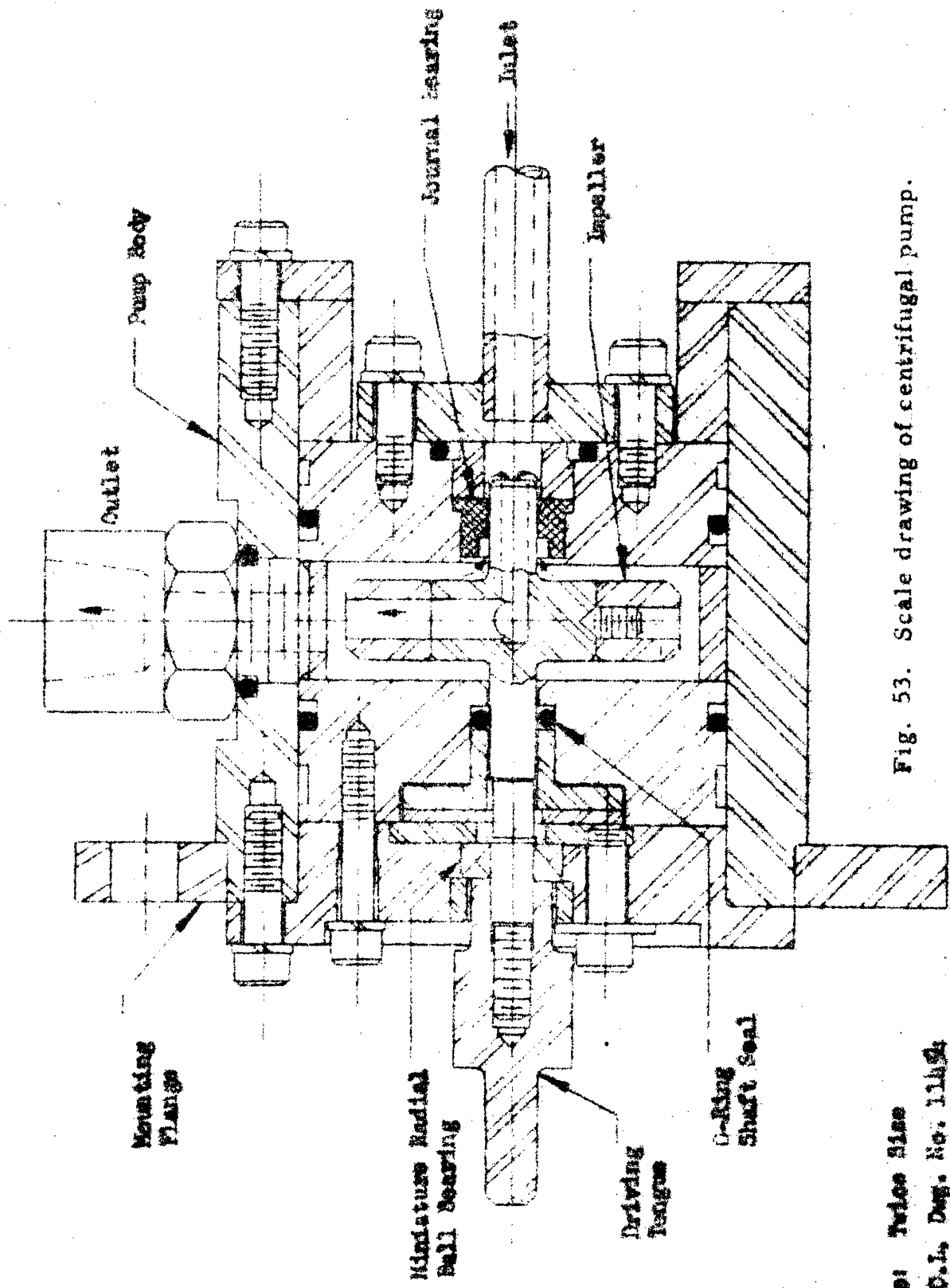
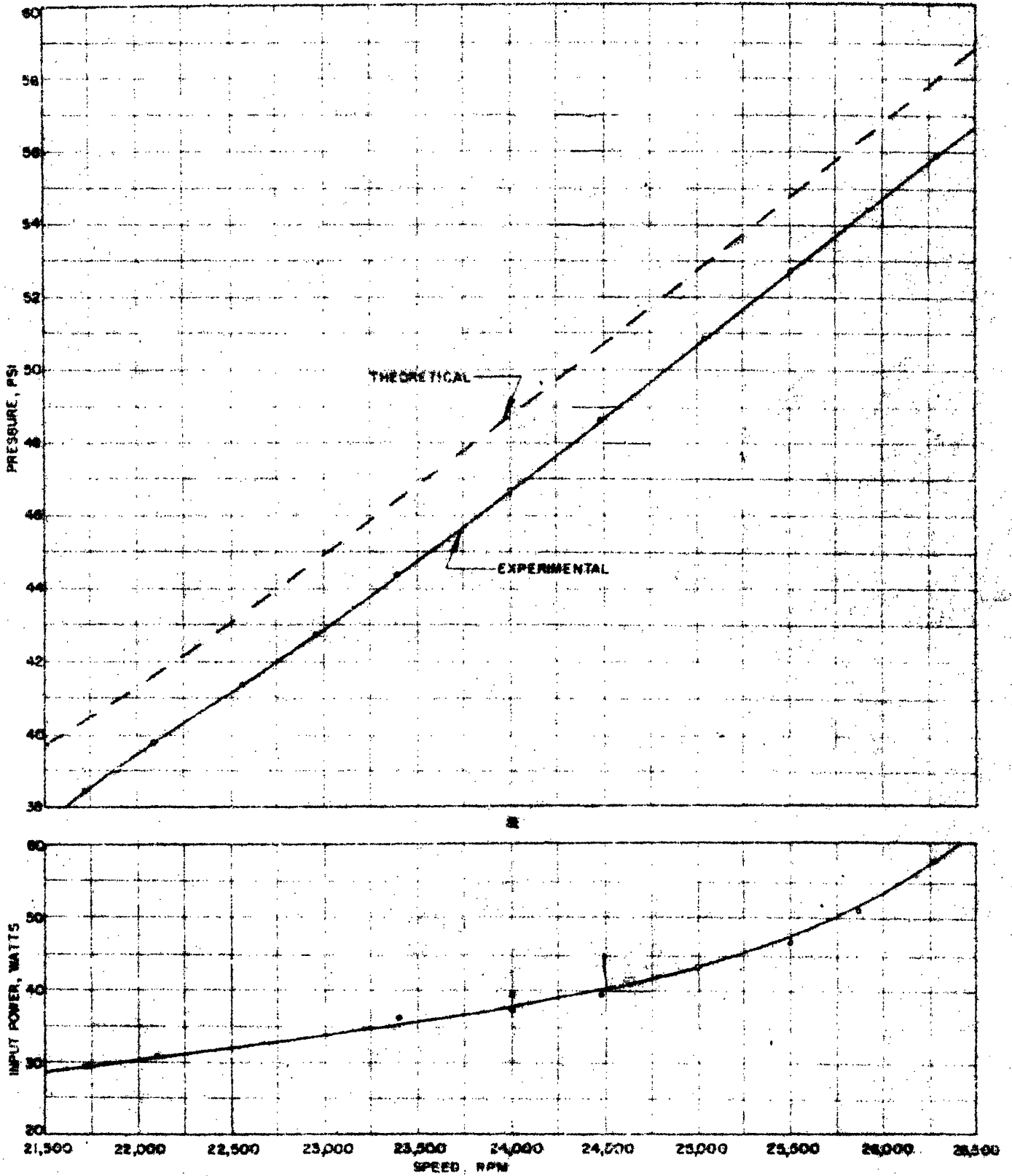


Fig. 53. Scale drawing of centrifugal pump.

Scale: Twice Size
 D.A.C.I., Des. No. 11494



Ambient temperature = 78° F

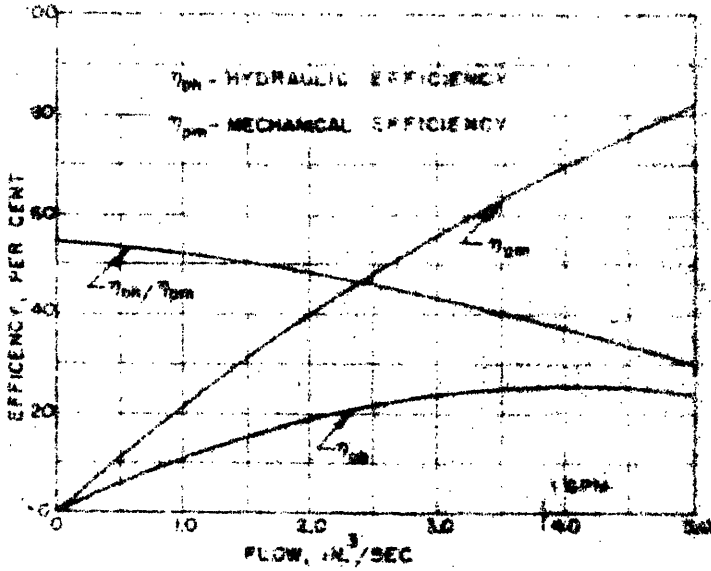
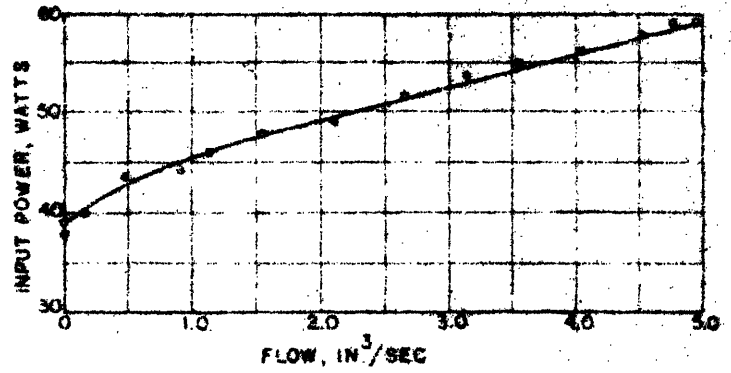
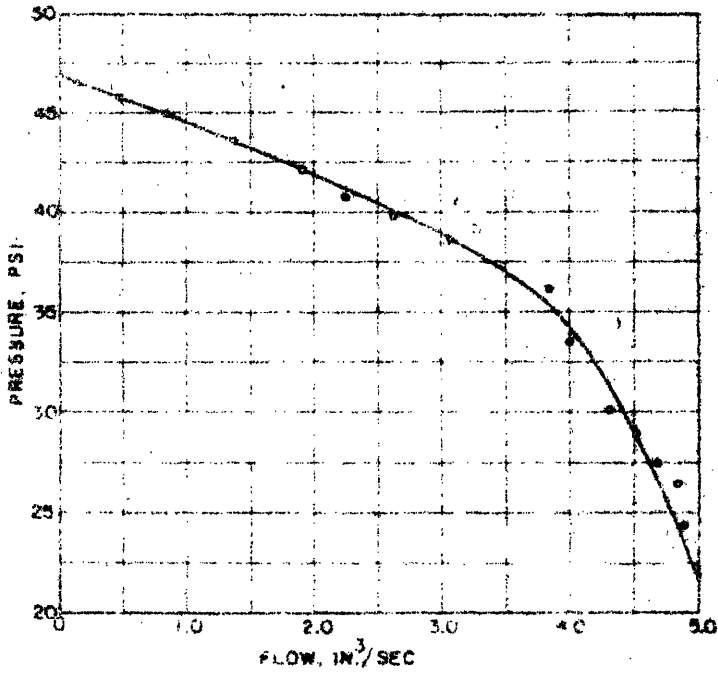
Pump temperature = 180° F

Flow = 0

a. Pressure vs. speed

b. Input power vs. speed

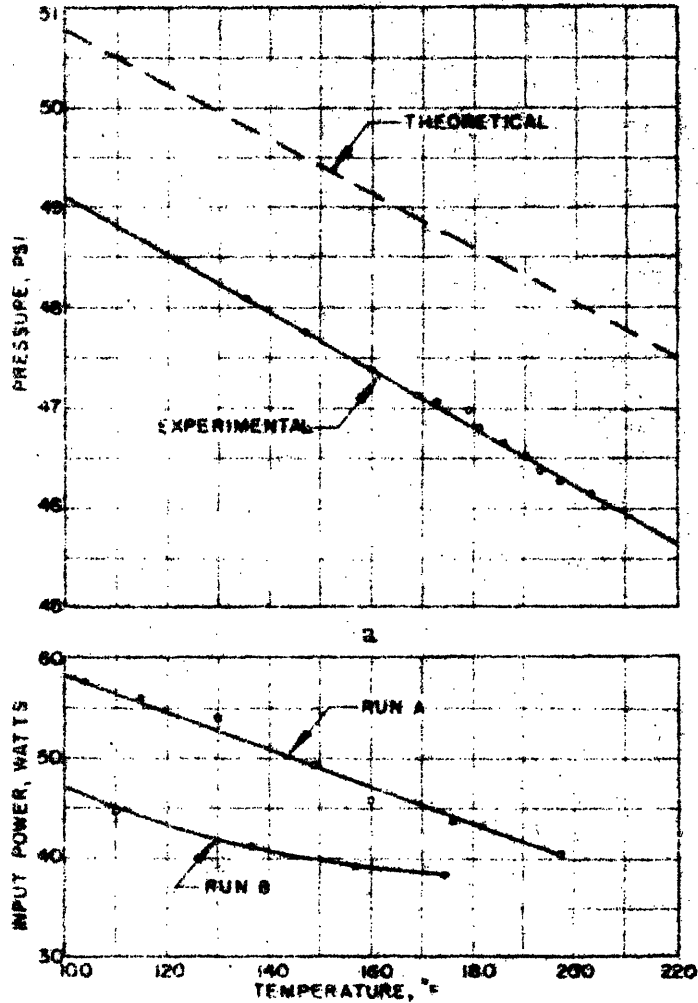
Fig. 54. Speed characteristics of centrifugal pump
 (Impeller diameter = 0.814 in.)



Ambient temperature = 78° F
 Pump temperature = 165° F
 Speed = 24,000 rpm

- a. Pressure vs. flow
- b. Input power vs. flow
- c. Hydraulic and mechanical efficiencies vs. flow

Fig. 55. Flow characteristics of centrifugal pump (Impeller diameter = 0.814 in.)



Speed = 24,000 rpm

Flow = 0

- a. Pressure vs. pump temperature
- b. Input power vs. pump temperature

Fig. 56. Temperature characteristics of centrifugal pump (impeller diameter = 0.814 in.)

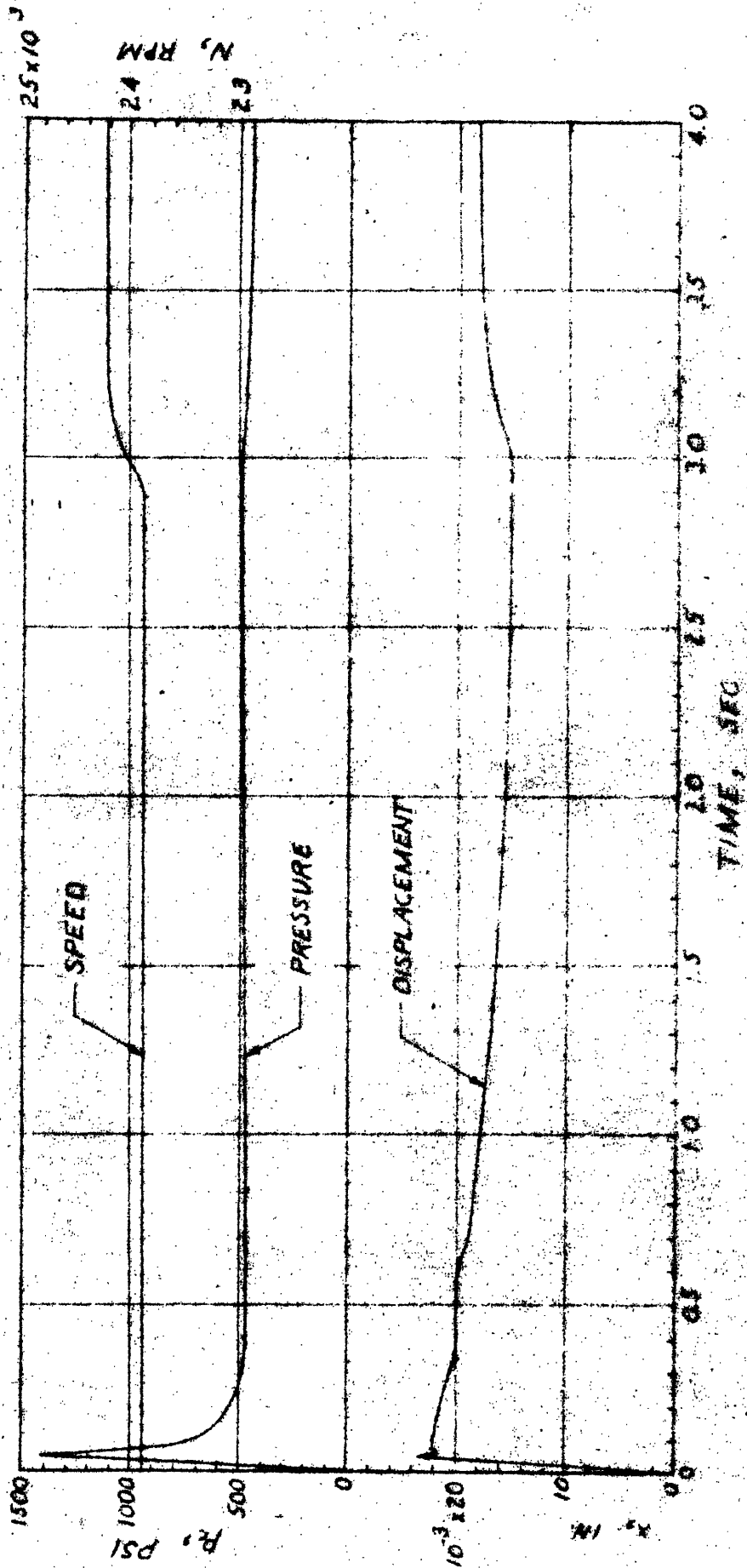


Fig. 58. Solid fuel ignition transient using entire regulator system:

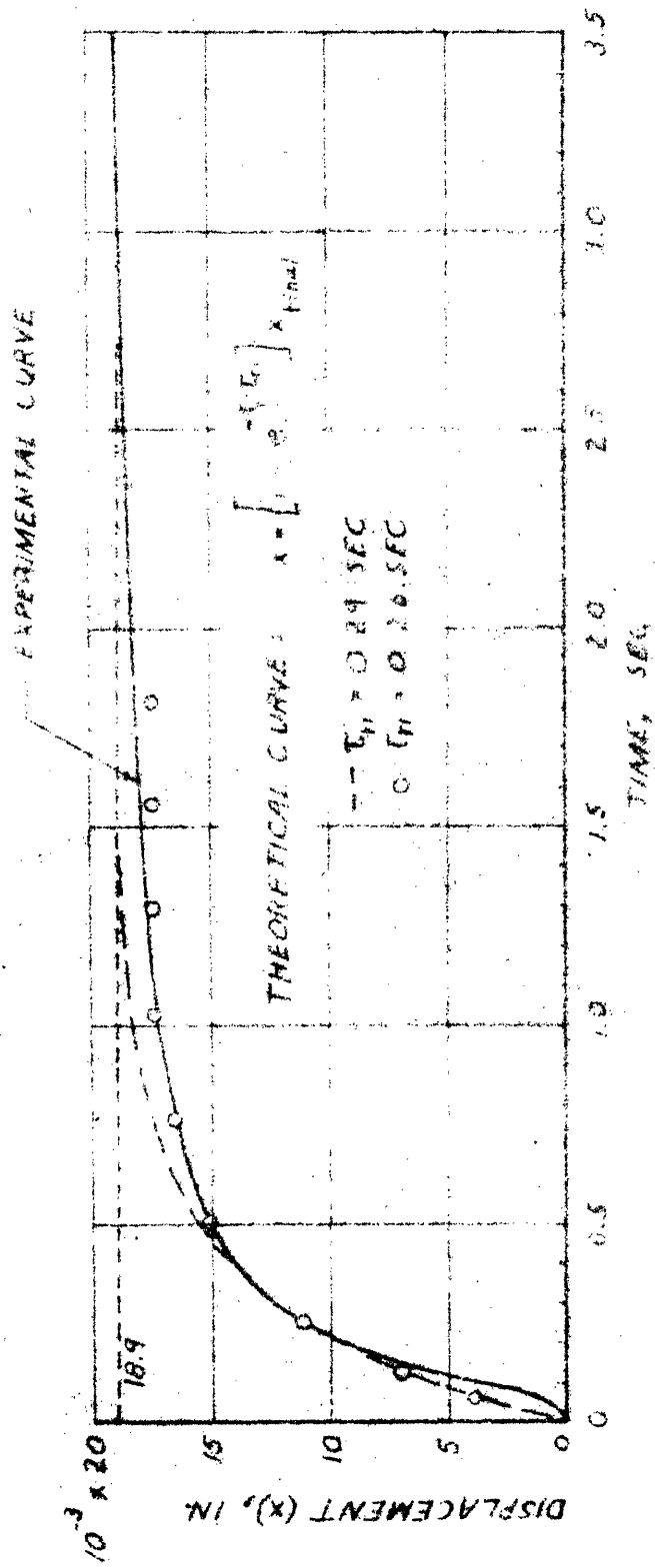


Fig. 59. Experimental transient response of controller shaft.

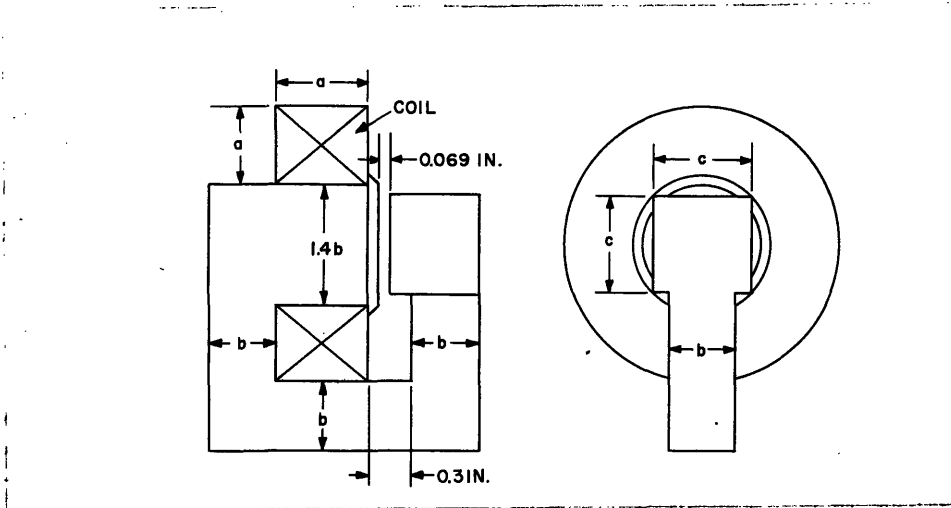


Fig. 60. Geometry of eddy-current-brake field structure.

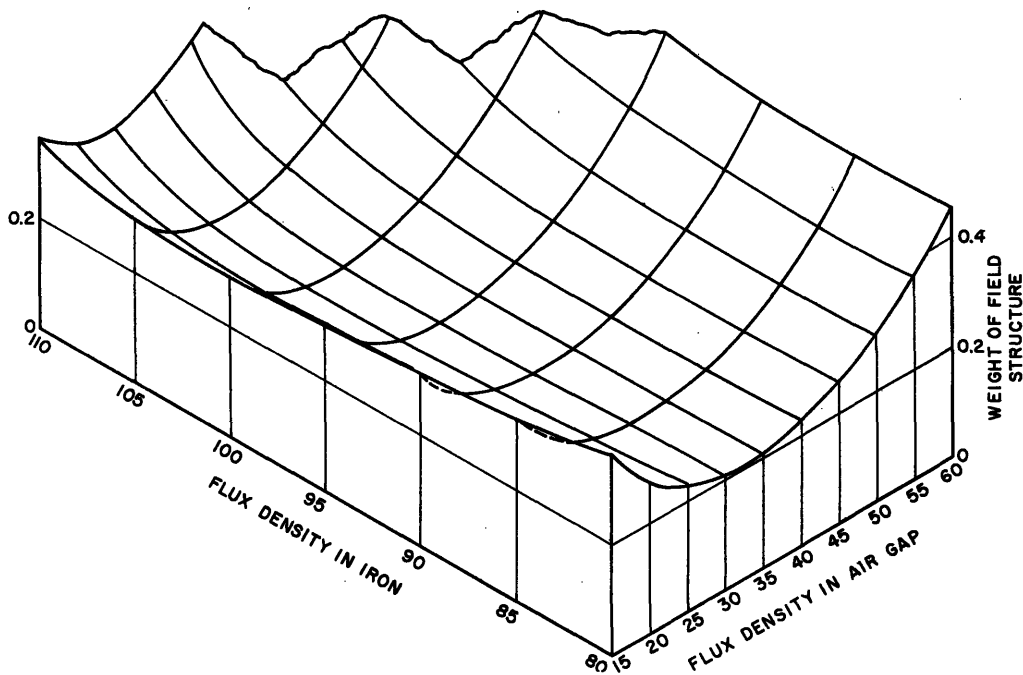


Fig. 61. Weight of field structure as a function of air-gap and iron flux density for a conventional wire coil.

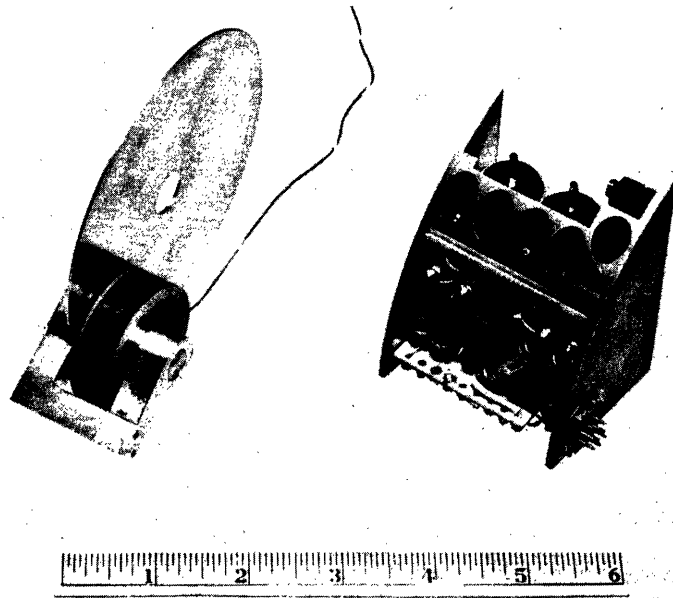


Fig. 62. Eddy-current brake and control amplifier.

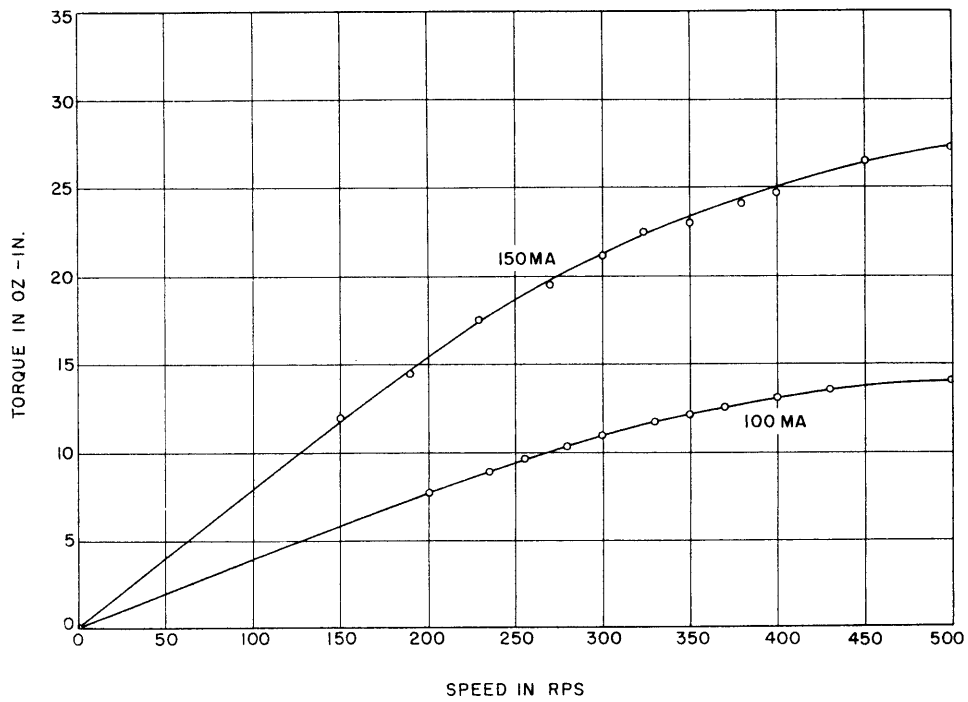


Fig. 63. Characteristic of eddy-current brake for fixed field current.

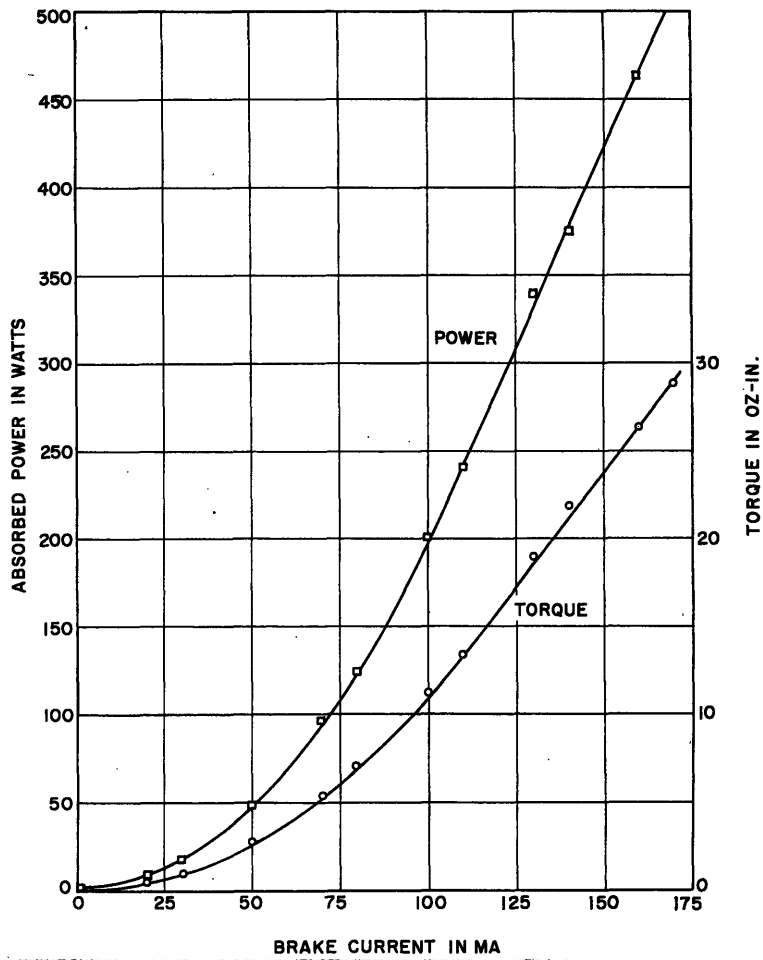


Fig. 64. Eddy-current-brake torque and absorbed power as a function of brake current for fixed shaft speed.

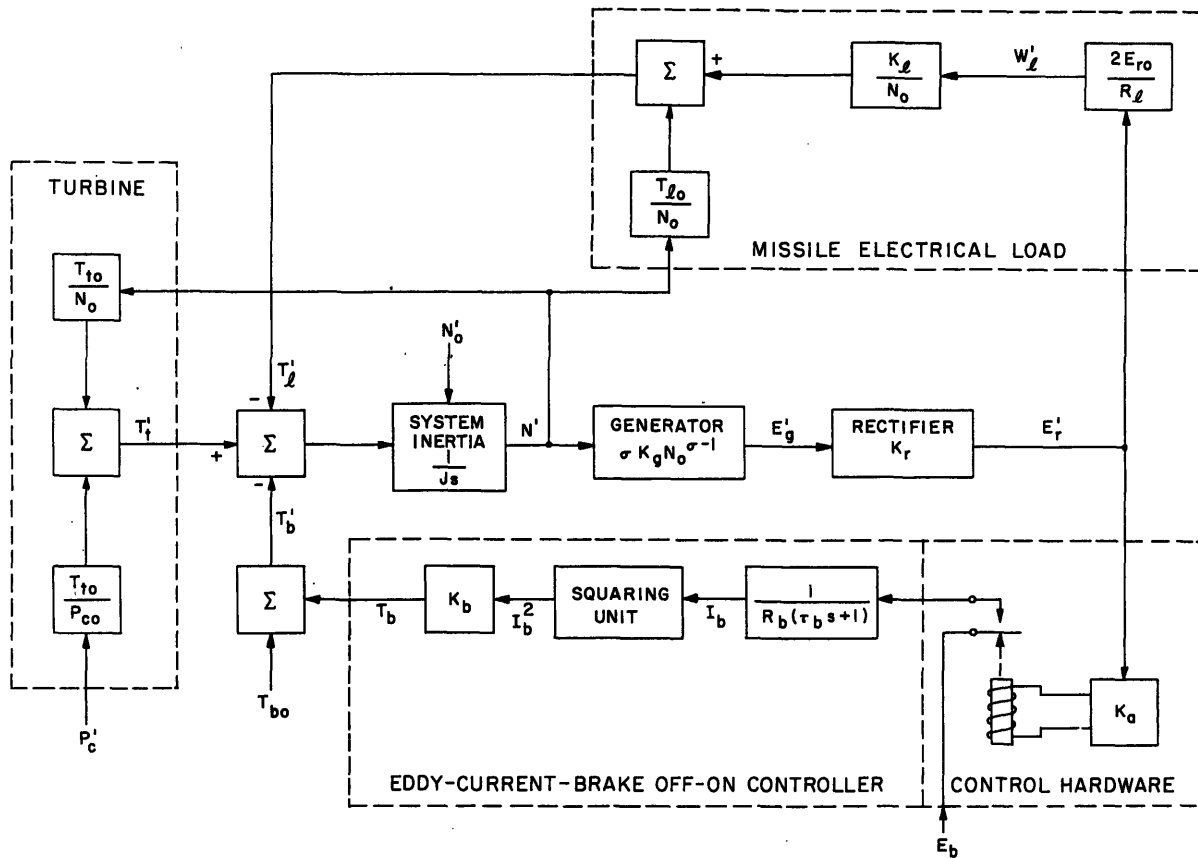


Fig. 65. Mathematical model of EPU system.

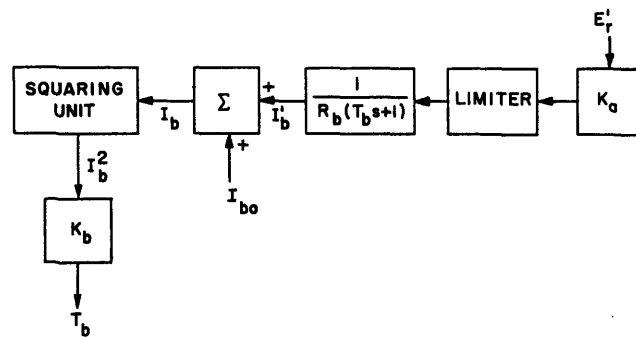


Fig. 66. Mathematical model of proportional controller.

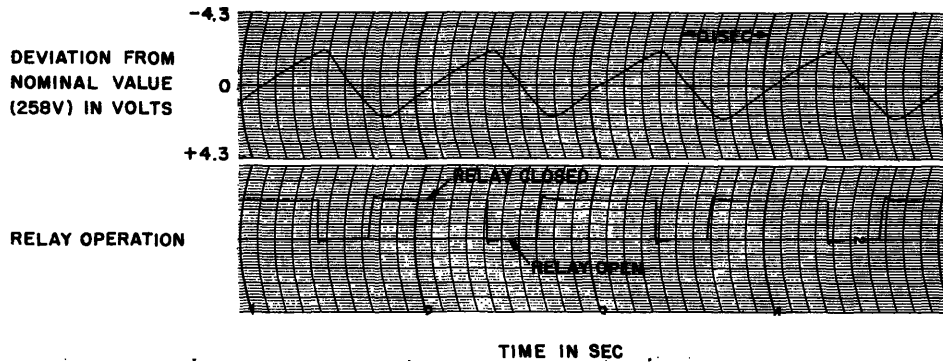


Fig. 67a. Computed performance of EPU system model with off-on control.

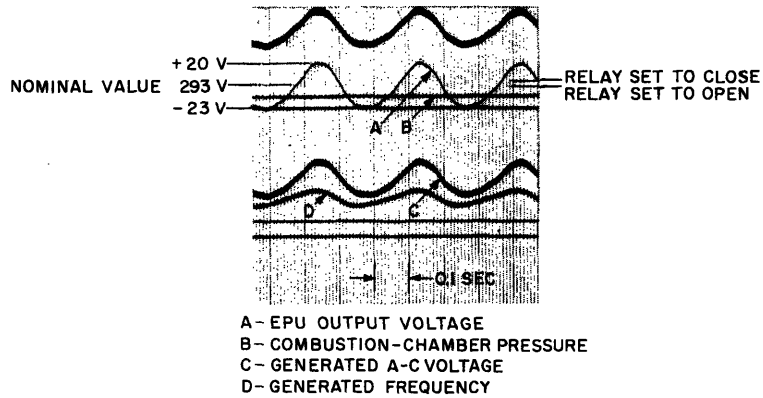


Fig. 67b. Recorded performance of simulation unit with off-on control.

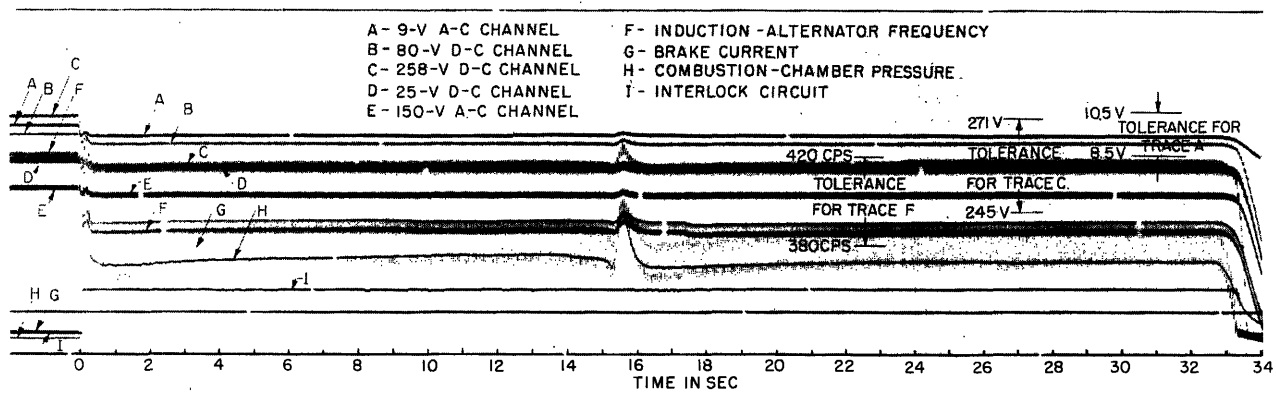


Fig. 68. Recording of EPU operation in self-powered mode at 165°F.

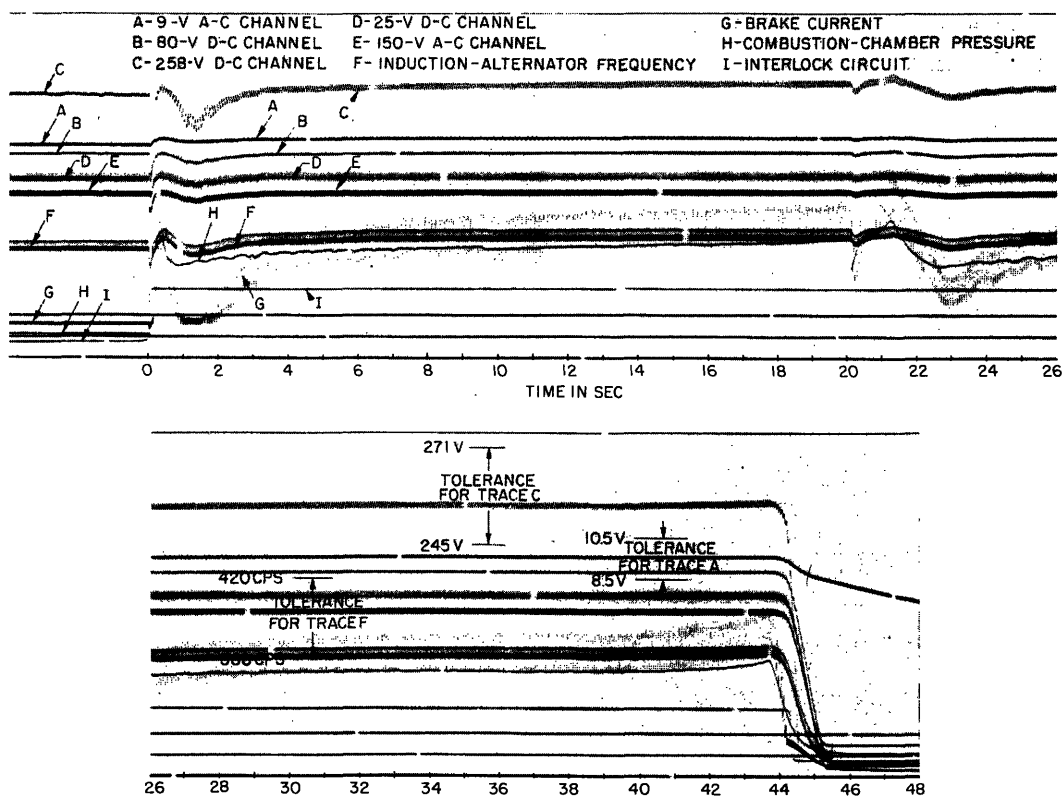


Fig. 69. Recording of EPU operation in self-powered mode at -65°F.

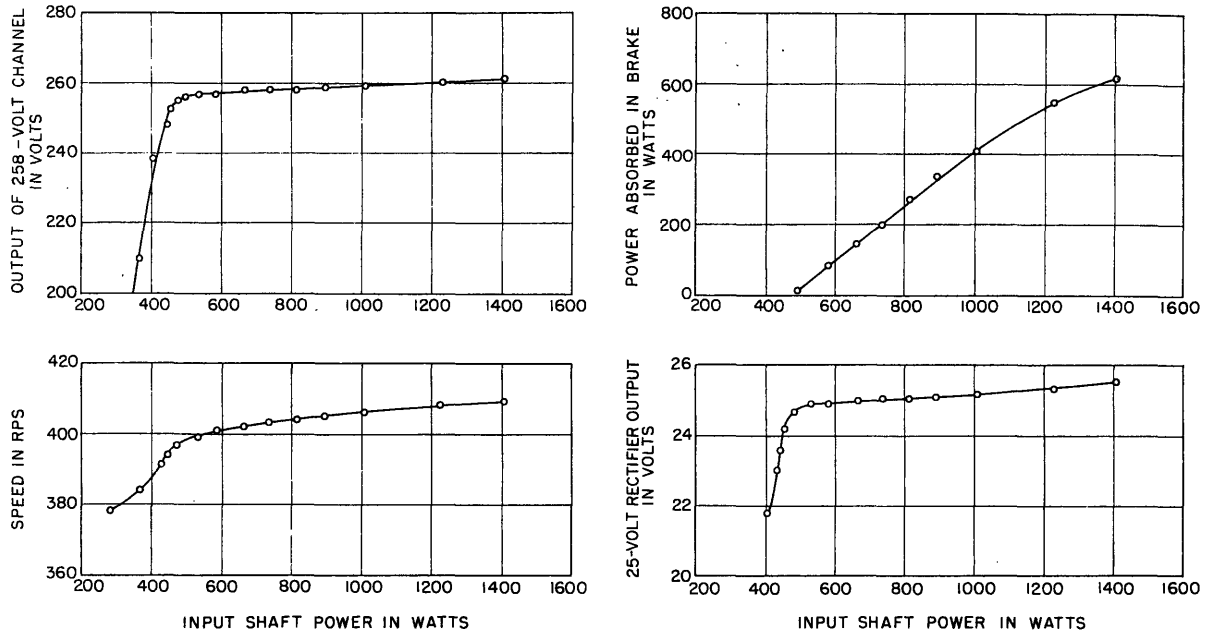


Fig. 70. Operating characteristics of EPU in self-powered mode.

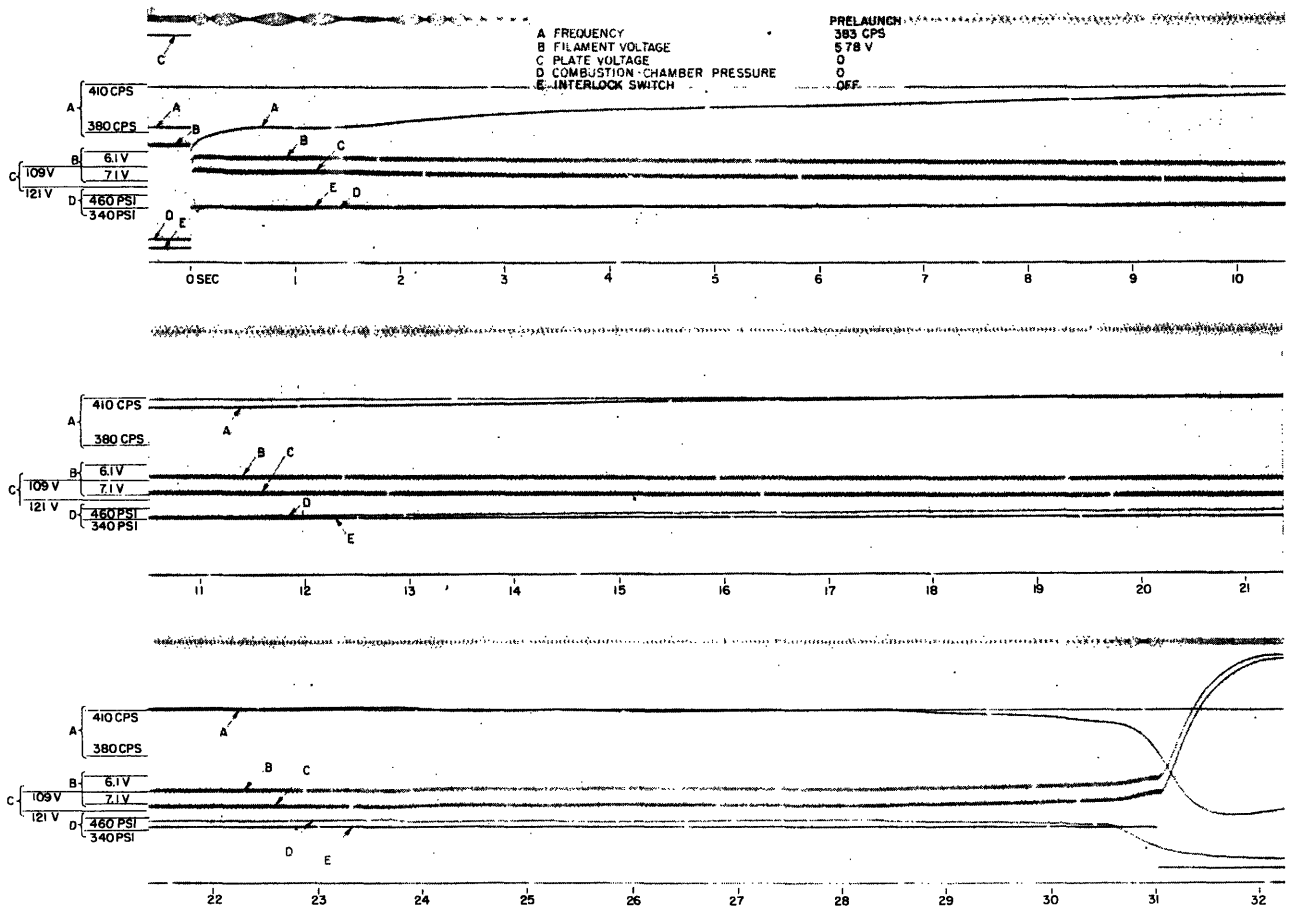


Fig. 71. Recording of EPU operation at high ambient temperature (+135°F).

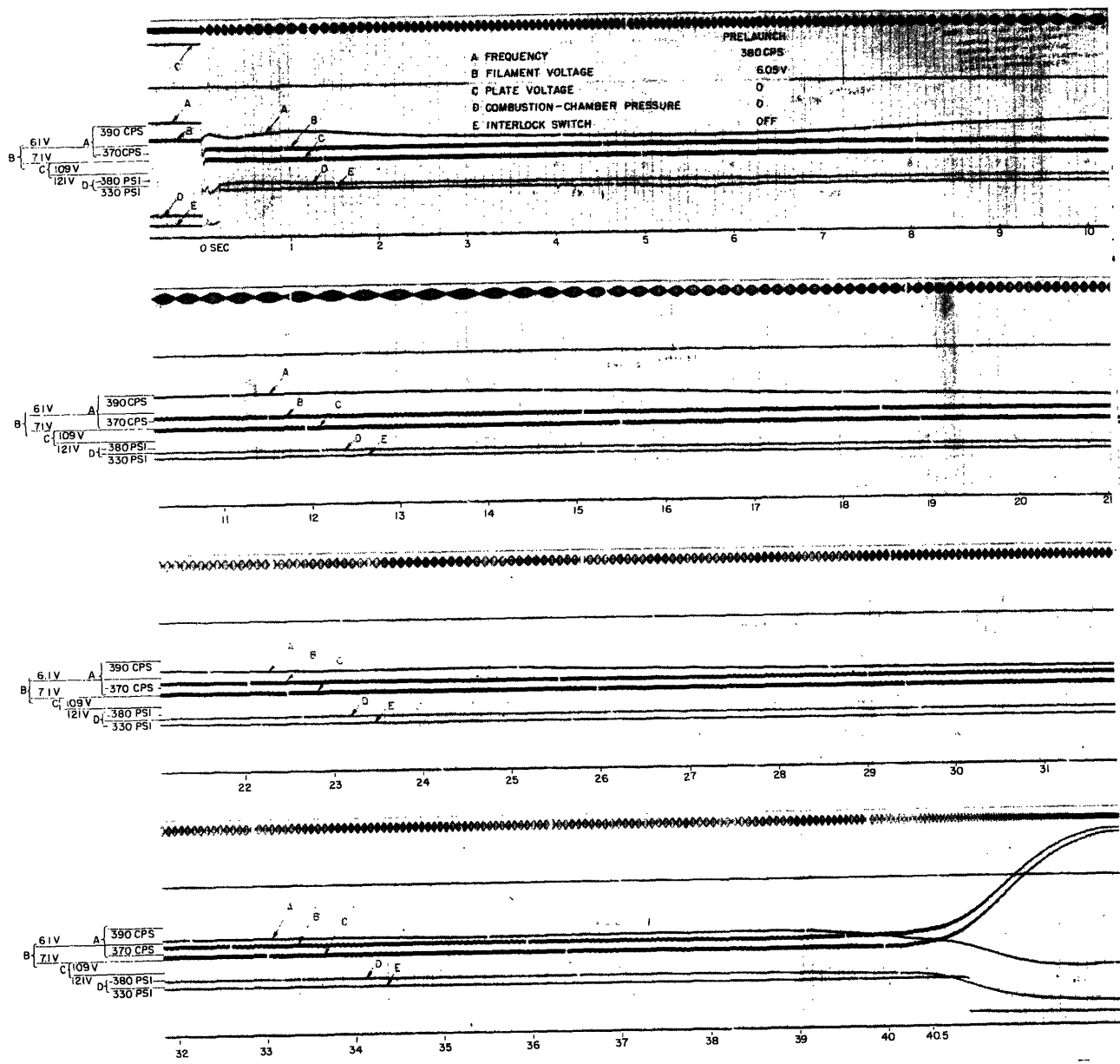


Fig. 72. Recording of EPU operation at minimum ambient temperature (-70°F).

7. PROTOTYPE DEVELOPMENT

As indicated in Sec. 1.1 the tangible goal of the M. I. T.-D. A. C. L. MIP program has been the development of several EPU's which have been carried through the prototype stage. The purpose of this section is to discuss briefly the design philosophy which guided the development of the several components and their integration into minimum-weight, practical units and to describe, within the restrictions of military security, the characteristics of the EPU's developed.

7.1. Design Philosophy

After the completion of the broad exploratory study of various prime-energy sources and resulting systems (Sec. 2.2) and consideration of the compatibility of such systems with the requirements and specifications of an air-to-air missile power system (Sec. 2.1), the generalized and basic investigations of solid fuels, small turbines, and electrical alternators, and the developmental effort directed toward specific missile specifications were carried on concurrently. This overlapping of research and development posed the problem of delaying commitment to a particular prototype EPU design as long as possible, in order to capitalize on the fruits of the basic investigations, aspects of which were absolutely essential to rational design. In addition, although the development of the prototypes was urgent, it was not considered reasonable to proceed without exploring certain vital design questions by direct experiments with solid-fuel systems.

7.11. Breadboard Hardware.

The compromise in this dilemma was to design what came to be known as "breadboard hardware". The separate entities of an EPU system, combustion chamber, regulating valves, turbine, electrical machine, regulating system, etc., were designed for function only.

No consideration was given to the ultimate need for minimum weight, rather the designs were made rugged to insure long experimental use. Each element was designed to permit easy alternation of its important geometrical parameters over a broad range estimated to cover all contingencies as results were derived from the basic investigations. In order to facilitate a variety of system studies, provisions were made for the easy and accurate alignment and assembly of different combinations of elements with adequate provision everywhere for experimental instrumentation.

A typical assemblage of breadboard hardware is shown in Fig. 73. Combinations such as this permitted evaluation of the performance of individual components, using, for example, an electrical machine whose efficiency had been calibrated on one of the high-speed dynamometers developed in the course of the M. I. T. program. The efficacy of various control systems could likewise be determined. This hardware has served faithfully a number of these investigations up to the present time and gives every indication of continued useful service.

While this approach of separating component parts to facilitate investigation and revision of each separately seems completely obvious, the author's experience with industrial organization is quite the opposite. Invariably, prototype systems are designed from the very beginning, often in complete ignorance of the performance of the components, usually culminating in ~~disappointing~~ results.

7.12. Basic Unit

Space and weight considerations require that the components of an EPU, that is fuel, turbine and alternator, be mounted contiguous to each

other with a minimum of supporting structure, quite unlike the arrangement of the breadboard hardware. The reduction of the effective heat capacity of the structure and increased heat transfer from and to the several components raises serious questions as to the extent to which the prototype package can be reduced in size. Important considerations here are the electrical machine heating due to losses when motoring for periods exceeding several hours prior to launch, the temperature rise at various points of the unit during solid-fuel operation (the exhaust port of the hot gas regulator becomes an incandescent orange, in excess of 2000°F), and the maximum soak-back temperature of the unit after a hot gas run. Also in question were certain of the manufacturing techniques to be employed on the prototypes, particularly the furnace-brazing of the complex combustion chamber assembly.

In order to resolve these questions, that their answers might influence the prototype design, and since, at the time, the final specifications for the EPU were uncertain, a "basic unit" was designed and fabricated as shown in Fig. 74. The design was kept as simple and flexible as was consistent with the problems to be resolved. Up to the completion of the first EPU prototype and its final testing, this basic unit bore the brunt of system testing and proved an invaluable experimental tool. Temperature sensitive paints and thermocouples were used to determine temperatures at various vital locations. The influence of vibration testing on parts in the design were determined. The radial flow turbine design, which had not been incorporated in the breadboard hardware, was confirmed. The close-coupled arrangement of the assembly permitted the study of hot-gas operation after storage of the unit at the upper and lower operational temperature extremes.

The extent of integration of the elements of the prototype EPU's is indicated by Figs. 75 and 76 which show respectively, the arrangement of a typical energy source and prime mover with auxiliaries and a typical rotating assembly.

7.13. Test Facilities

Throughout the program great emphasis was placed upon the development of test facilities to insure adequate and accurate coverage of performance and to validly simulate the systems external to the items under development.

The turbine test facility and air-absorption dynamometer are described in Sec. 4. The electric dynamometer is mentioned in Sec. 5. Dynamic recording of EPU performance is accomplished by a 14-channel optical oscillographic recorder with temperature, pressure, and speed transducers, and appropriate amplification and demodulation equipment, much of it developed by and for the MIP project. Solid fuel testing is accomplished in a steel test chamber.

For the test of electrical components and system much special purpose test equipment was developed including air-turbine drives for steady state tests, load resistor banks, a permanent-magnet pulse magnetizer, and an eddy current brake test unit. Since the EPU and missile load comprise a dynamic system, accurate simulation of the dynamical properties of the missile system was accomplished by the design and fabrication of appropriate electronic circuitry. In order to insure the satisfactory performance and reliability of certain of the commercial components, notably tubes and capacitors, whose service, as applied in the EPU's, was not guaranteed by the component manufacturers, some environmental life testing was conducted.

All test facilities and equipment used in various phases of the MIP program are described in detail in the appropriate report or thesis listed in the Bibliography.

7.2. Prototype EPU's

Military security precludes any detailed discussion of the EPU's developed in the M. I. T. MIP program. In general, it may be said that prototype power supplies were developed for two different air-to-air missiles. In the design of these prototypes every effort was made to insure the compatibility of the units with the specifications outlined in Sec. 2.1. These were in no sense experimental, laboratory, or developmental units. Full consideration was given to the problems of large-scale manufacture. In fact the respective missile prime contractors subsequently manufactured quantities of both units directly from the manufacturing drawings provided by M. I. T.

In both cases severe space and weight restrictions were imposed since the units were replacements for experimental power supplies. The first EPU⁵ was over-all slightly smaller and lighter than the battery supply it replaced. Whereas the battery only provided low voltage d-c, the EPU provided several high and low a-c voltages eliminating other components previously necessary. The prototype of this EPU was developed, tested and delivered in one calendar year.

The second EPU,⁸ benefiting somewhat from the experience of the first unit and, more importantly, from some compromise between missile system requirements and EPU capability, furnished directly, in final rectified and filtered form, all the missile internal requirements. This second EPU is 44 per cent lighter than the power supply it replaces and it occupies 38 per cent less volume. Furthermore it eliminates from the parent-airplane a heavy and complex installation.

Both units have been exhaustively system tested with the missiles of which they are a part and both have been found completely satisfactory. Both units have been subjected to a wide variety of environmental testing in accord with the conditions generalized in Sec. 2.12 and both have performed satisfactorily.

Finally, both units have been successfully flight tested.

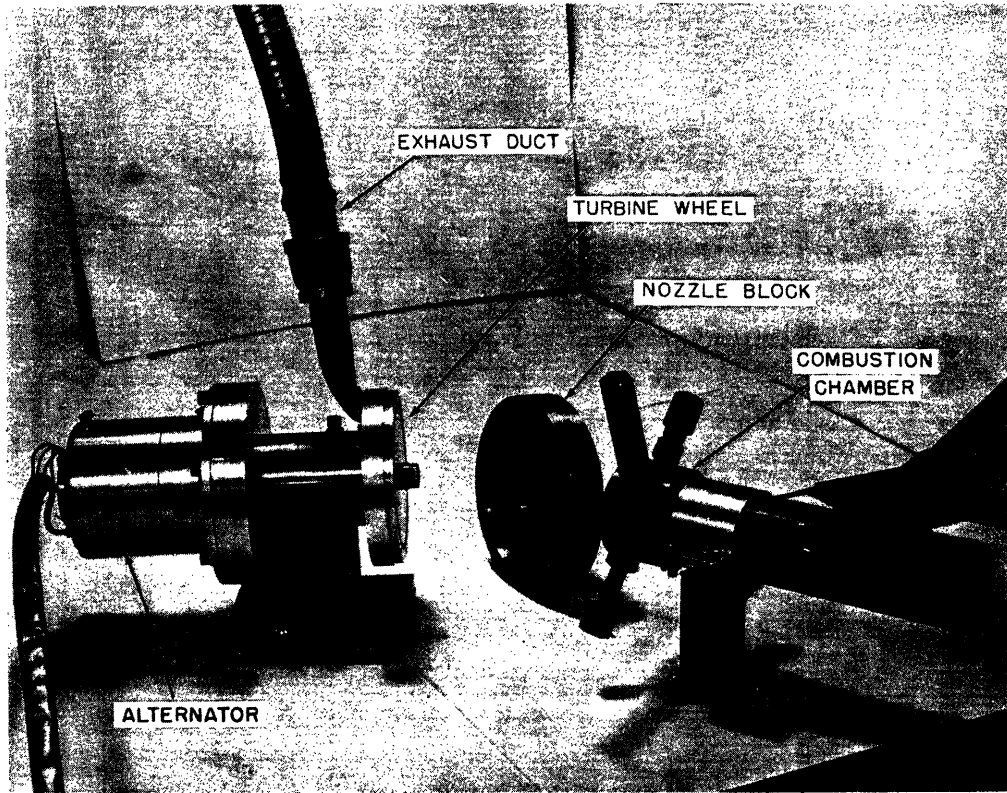


Fig. 73. Test setup of "breadboard" hardware.

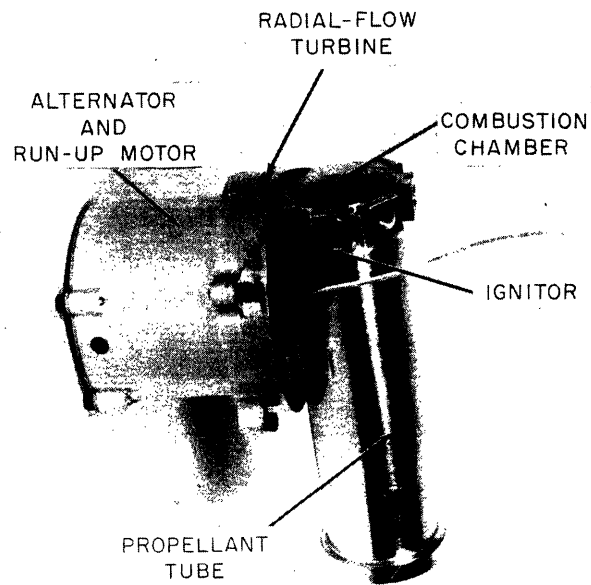


Fig. 74. Basic unit.

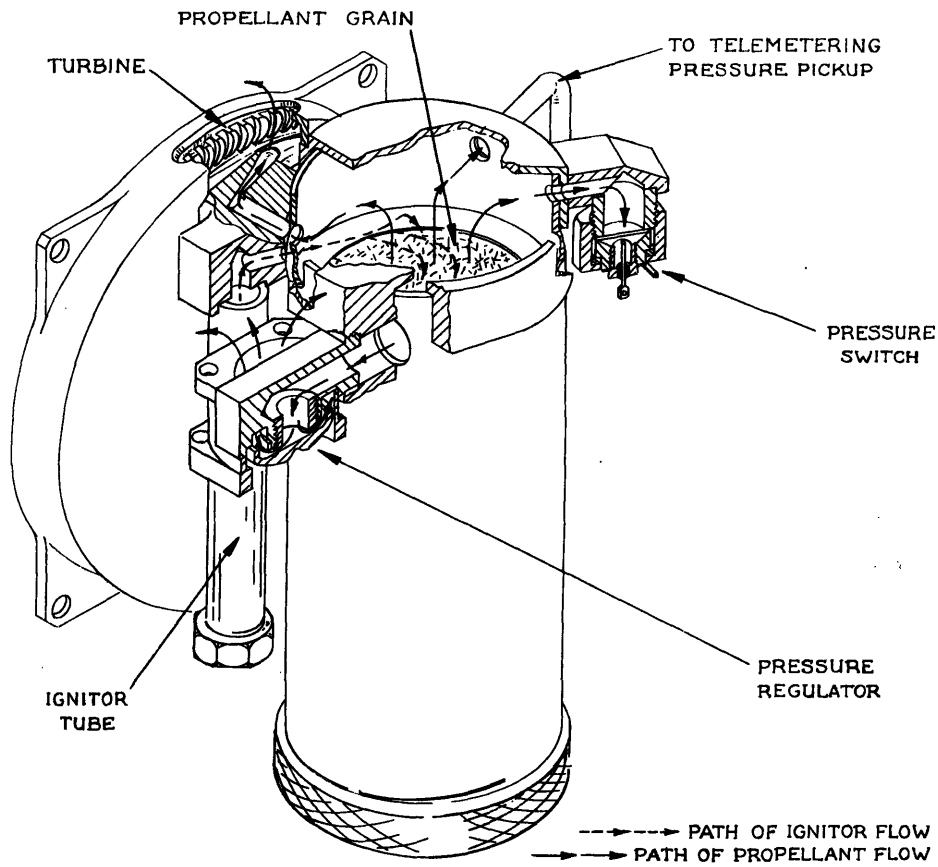


Fig. 75. Energy source and prime mover.

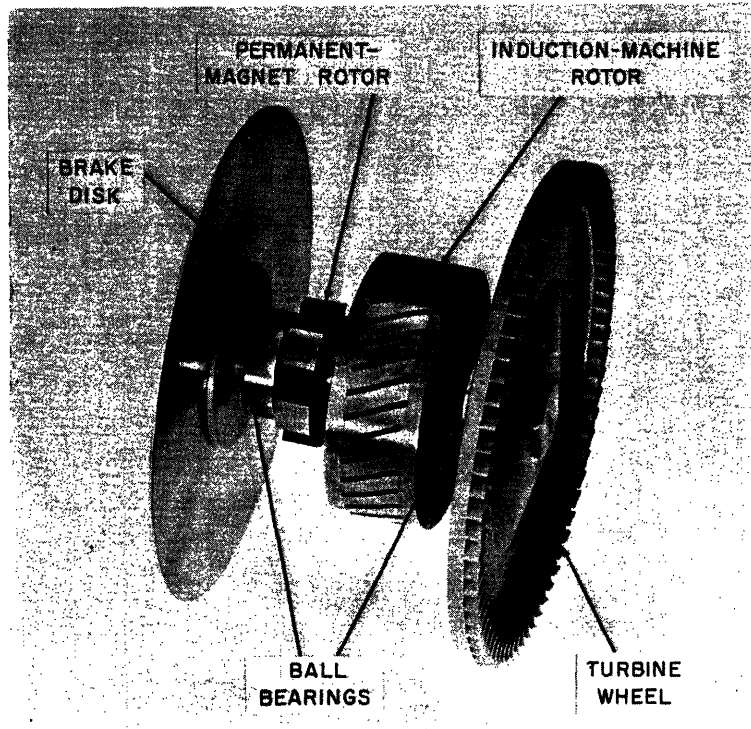


Fig. 76. Assembly of EPU rotating parts.

8. MISSILE ELECTRICAL SYSTEM STUDY

While the specific hardware developments of the M. I. T. - D. A. C. L. MIP program have been directed toward the design, fabrication, and test of EPU's for existing missile systems with established system voltage and frequency requirements, the basic work on prime movers, alternators, shaft support, rectification and filtering, and control has indicated that substantial advantages should result from revised power standards for missile electrical systems. The electrical system is defined as consisting of all equipment involved in the generation, conversion, regulation, distribution, and utilization of electric power.

By studying the influence of primary voltage and frequency on utilization equipment sec. 8.1, on a-c transmission and distribution Sec. 8.2, on power generation and conversion equipment Sec. 8.3, and on the prime energy source and prime mover Sec. 8.4, an optimum frequency and voltage standard can be determined which will result in minimum electrical system weight consistent with maximum reliability and performance.³³

As has been previously noted with respect to EPU optimization, electrical system optimization may not always be achieved with minimum-weight components. However, owing to the unpredictable distribution of components in a missile system and the magnitude of a true optimization task, a study of the weight-frequency and the weight-voltage relationships of the separate components that make up the electrical system is mandatory.

This section of this paper is not limited to low-power short-duration systems as is most of the rest of the paper, but considers all missile systems ranging in operating time from fractions of a minute to hours and in power levels from 100 watts to 30 kw. The study is based on the analytical and experimental program at M. I. T., published reports and

technical papers, and a two-year liaison program during which the staff of the M. I. T. -D. A. C. L. MIP program discussed past experience, current practice, and future predictions on missile electrical systems with military agencies, missile system companies, and missile component manufacturing companies.

8.1. Power Utilization Equipment

The obvious advantages of 400 cps over lower frequencies for aircraft, and capacitive coupling, high leakage reactance and phase shift difficulties at very high frequencies defines the frequency range of interest to be 400 - 5000 cps.

High frequency power would not adversely affect electron tube circuits in guidance, autopilot or fuze circuits. In most cases, high frequency a-c can be used directly as filament-heating power. Transistor circuits which use only direct voltages would not be affected. For magnetic amplifiers operating characteristics such as the time constant τ , power gain K_p , and figure of merit $M = K_p/\tau$ improve with increased frequency, or for a given gain or figure of merit, weight can be decreased as in Fig. 77. The relative weight reduction possible with signal transformers for increasing frequency is given in Fig. 78. Gyro design is largely dictated by the shaft support problem which presently limits speeds to about 50,000 rpm. In miniaturized versions, mechanical limitations restrict the number of slots for the gyro motor winding. Currently realizable designs would permit maximum power frequencies of 4.2 kc for 2-phase gyros and 2.5 kc for 3-phase gyros. Improvements in bearings and mechanical refinements would raise the maxima to 5 and 3.3 kc respectively. Pickoffs, synchros, and resolvers are in no way limited by frequencies up to 5 kc. Motors and actuators are most efficient

weightwise when designed for d-c power. At 400 cps the weight increase is approximately one-third more than d-c motors for the same stall torque. Increases in frequency above 400 cps could result in further weight increases; however, electrical motors and actuators are not widely used in missiles because hydraulic, pneumatic and hot gas³⁴ force and torque devices have a much higher power-to-weight ratio.

Since very few components of the missile load operate directly from the primary ac power, utilization devices do not strongly influence the primary-voltage standards. Appropriate considerations are the additional insulation necessary at high voltage levels, the limit of minimum practical conductor area which can result in winding volume increases if too high a voltage is chosen, and the standard use of 6.3 volt electron-tube-heater power.

8.2. Power Transmission

The length and extent of power transmission varies widely among missile systems. Frequency choices that may result in objectionable beat frequencies with other adjacent systems, i. e., 400 cps parent aircraft power for air-to-air missiles, should be avoided. Transmission line impedance as a function of frequency is shown in Fig. 79 for several wire sizes and spacings.

Provided extremes are avoided the influence of the primary voltage choice on transmission is not significant. Very low voltages require prohibitively large conductors and connectors while voltages higher than 150 volts can lead to corona and voltage breakdown in high-altitude non-pressurized missiles.

8.3. Power Generation and Conversion

Since the selection of an optimum frequency depends in large measure on the relationship between frequency and weight of the electrical generation and conversion equipment, this relationship was studied analytically, maintaining all other independent system parameters, such as power rating, output, voltage, operating life, ambient temperature and quality of design constant. Rather than base the weight dependency of frequency on specific designs, which would be a laborious task and dependent upon empirical methods which often can only be verified experimentally, the influence of frequency was determined by model theory. An experimentally proved model designed for operation at a particular frequency was scaled analytically, maintaining gemoetric similarity, in order to evaluate generalized units at all other frequencies of interest. Figures 80 and 82 show curves of the relative weight of the electromagnetic portions of alternators and transformers as functions of frequency for constant volt-ampere output. Unity relative weight is assumed for a 400 cps unit. Since the most important consequence of high frequencies in electromagnetic devices is the increase in core loss that results in an increase in internal temperature, thinner core material, decreased core flux-density, or both must be resorted to. For example, the ratio of the maximum flux density in a temperature-limited 4000-cps transformer to that of a 400-cps unit with the same operating requirements is 0.16 when 2-mil Hypersil is used for the cores.

For the wound rotor synchronous alternator, Curve 1 in Fig. 80 the maximum internal temperature and the number of poles are maintained constant, and 5-mil Tran-Cor T is assumed for the core material. At low

frequencies, weight reduction is limited by field winding temperature. As frequency increases iron losses increase until at 1500 cps the stator iron has reached the maximum allowable internal temperature; beyond 1500 cps stator winding and stator iron temperatures are held constant at the maximum allowable. Field temperature decreases over this high frequency portion, decreasing to 0.308 of the maximum temperature allowable at 5000 cps.

For the permanent-magnet alternator Curve 2 in Fig. 80, stator winding and iron temperature and the number of poles are maintained constant. Because negligible heating occurs in the rotor, due to its high permeability and lack of winding, Curve 2 has essentially the same slope as the higher frequency portion of Curve 1.

Since induction alternators, Curve 3, in Fig. 80, must operate with the cores saturated, (see Fig. 38, Sec. 5.3), the flux-density, stator winding temperature and number of poles are held constant. Due to iron heating from operating saturated at high frequencies more effective cooling methods than presently used may be essential to practical designs. Accordingly the portion of Curve 3 above 3000 cps is shown as a dashed line.

The curves of Fig. 80, although calculated for the three specific types of alternators are sufficiently basic to be indicative of the weight-frequency dependence for all other alternator types.

Since higher frequencies can be obtained either by higher speeds of rotation or by increasing the number of magnetic poles on the alternator the effect of the number of poles on alternator weight is presented in Fig. 81. Curve 1 is based on design calculations for a 4-1/2 kw induction alternator operating at 24,000 rpm; Curve 2 is

drawn through points calculated for a 10 kva 12,000 rpm synchronous alternator and Curve 3 is for a 6,000 rpm synchronous alternator. These curves show that, for 12 poles or less, alternator weight is almost independent of the number of poles. For the mathematical model of the alternators the induced volt-ampere product depends only on the ratio of frequency to the number of poles and is independent of pole-number alone. The differences between the model and the curves in Fig. 81 are due mainly to (1) decreased end-turn volume for poles greater than two, (2) practical limitations on minimum mechanical dimensions and strength of materials, and (3) the impossibility of maintaining both geometric similitude and the same degree of saturation in the stator teeth and yoke when the number of poles is changed.

The relative weight of power transformers as a function of frequency is shown in Fig. 82 computed for constant volt-ampere output and constant temperature rise. Unity relative weight is for a 400 cps unit with 5-mil Hypersil core. Curve 2 represents transformers with 2-mil Hypersil cores.

Since the weight of alternators and transformers is a function of the volt-ampere rating rather than a function of voltage alone, the choice of primary voltage has only secondary effects on size and weight such as requiring additional conductor or coil insulation.

Rectifier units will not be affected by the use of a high frequency. The weight of L-C filters for a given ripple attenuation is approximately inversely proportional to input frequency because component weight is

approximately proportional to inductance and capacitance.

8.4. Prime Energy Source and Prime Mover

The most significant factor affecting the weight optimization of the prime energy source and prime mover of an electrical power system is the efficiency of the turbine. For most applications turbine efficiency is approximately proportional to its rotor tip-speed. Thus fuel weight for a given total energy requirement is inversely proportional to turbine efficiency. Although the fuel system equipment weight is not simply related to fuel weight (see Sec. 2.222) it too can be approximated as being proportional to fuel weight and therefore inversely related to turbine efficiency and turbine-blade-speed. Design considerations limit turbine diameter to a rather narrow range with the result that turbine shaft speed for maximum efficiency is high, in the range 36,000 to 80,000 rpm.

The use of such turbine shaft speeds with 400 cps generators requires the inclusion of gear boxes. The cost and weight (as much as 50 pounds for long-duration high-power systems) and reliability factor of these gear boxes could be reduced or eliminated if a high primary-power frequency, permitting direct drive of the alternator was standardized. The compatibility of turbine speed and generator speed over the range from 400 - 5000 cps is illustrated in Table VII which shows the results of applying the model theory discussed in Sec. 8.3 to two 12-kva 400-cps alternators, a wound rotor salient-pole alternator and a permanent-magnet alternator. The maximum permissible rotor-tip speeds of 600 ft/sec. for a wound-rotor alternator and 700 ft/sec. for a permanent-magnet alternator are in accordance with current manufacturing practice.

Table VII

RELATIONSHIP BETWEEN FREQUENCY, SPEED, AND NUMBER
OF POLES

Wound Rotor Alternator

Frequency (cps)	No. of poles	Shaft Speed (rpm)	Rotor Diameter (in.)	Tip Speed (ft/sec)	Weight Factor (Fig. 5)
400 - 1670	4	12,000 - 59,100	3.94 - 2.74	247 - 600	1.00
1670 - 2660	6	33,400 - 53,200	2.74 - 2.58	400 - 600	0.98
2660 - 3710	8	39,900 - 55,650	2.58 - 2.48	450 - 600	0.99
3710 - 4800	10	44,520 - 57,600	2.48 - 2.39	480 - 600	1.03
4800 - 5920	12	48,000 - 59,200	2.39 - 2.32	500 - 600	1.11

Permanent-Magnet Alternator

400 - 635	2	24,000 - 38,100	4.74 - 4.22	468 - 700	1.00
635 - 1400	4	19,050 - 42,000	4.22 - 3.82	350 - 700	0.94
1400 - 2230	6	28,000 - 44,600	3.82 - 3.60	467 - 700	0.94
2230 - 3100	8	33,450 - 46,500	3.60 - 3.46	525 - 700	0.94
3100 - 4000	10	37,200 - 48,000	3.46 - 3.34	560 - 700	0.98
4000 - 4930	12	40,000 - 49,300	3.34 - 3.26	583 - 700	1.06

The power voltage choice has no effect on the primary power source.

8.5. Design Example

The potential reduction in weight of a turbo-alternator power supply that can be achieved through the use of a high power frequency is illustrated by Fig. 83. This figure contrasts the weight of the 400-cps EPU designed during the M. I. T. -D. A. C. L. MIP program for an air-to-air missile with the estimated weight of a hypothetical 3200-cps EPU with the same output characteristics. The EPU selected for comparison purposes has a tactical operating time of less than one minute and a maximum output power of approximately 1 kilowatt. The four major functional parts of this EPU are (1) the prime mover, which includes fuel, gas generator, and turbine, (2) the electrical generating equipment, which includes a 400-cps three-phase induction machine that functions both a prelaunch motor and a postlaunch alternator, (3) the electrical conversion equipment, including a 400-cps transformer and a rectifier-filter unit that delivers several d-c voltages, and (4) regulating equipment, which consists of an eddy-current brake and a five-tube amplifier. The unit operates with a shaft speed of 24,000 rpm.

The weight of the hypothetical 3200-cps EPU has been obtained by scaling the existing 400-cps unit in accordance with the following assumptions:

1. an increase in the shaft speed to 96,000 rpm results in increased turbine efficiency and permits the use of a smaller turbine and gas generator,
2. induction-alternator and transformer weight vary as shown in Figs. 80 and 82,
3. filter-component weight is inversely proportional to frequency,

4. total diode weight is constant,
5. the decreased torque level permits a reduction in the weight of the eddy current brake, and
6. the amplifier weight is constant.

In each case, an appropriate fraction of the weight of the supporting EPU structure is assigned to each of the four major segments.

As shown in Fig. 83, the weight reduction that can be realized by using a frequency of 3200 cps is approximately 70 per cent.

8.6. Conclusions

The effects of voltage and frequency on electrical power generation, conversion, transmission, and utilization in missile systems may be summarized as follows:

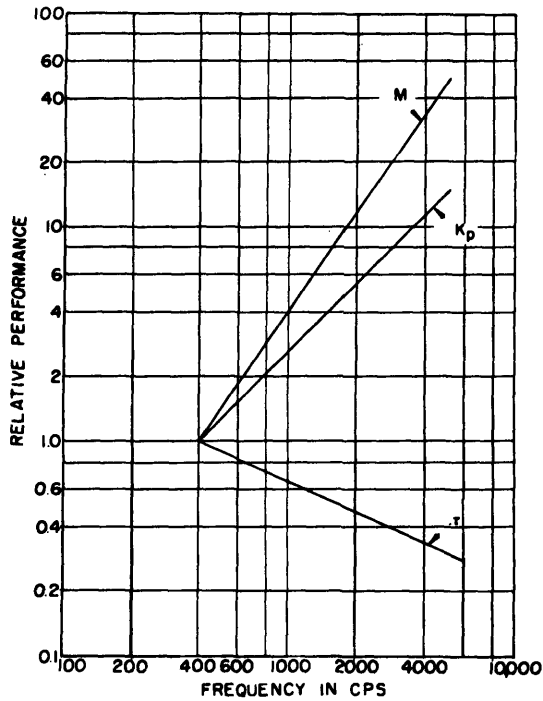
1. Missile utilization equipment and the weight of the electrical-power system generally are not affected by the primary-voltage level, provided extreme values of voltage are avoided.
2. The primary missile frequency affects the various missile components in the following manner:
 - a. The weight of passive L-C filters and of most electromagnetic components, such as signal transformers, magnetic amplifiers, alternators, and power transformers decreases with increasing frequency up to 3000 cps. The possibility of weight reductions between 3000 and 5000 cps is uncertain for low-power components owing to practical limitations on minimum mechanical dimensions and strength of materials.

- b. Synchros, resolvers, and gyros are relatively unaffected by frequency. Size reductions generally are not possible.
- c. The impedance of a-c transmission lines does not increase significantly with frequency for cables with No. 14 AWG or smaller conductor size when conductors are nearly adjacent.
- d. The potential weight reduction of 70 per cent for a hypothetical 3200 cps turbo-alternator supply compared with an equivalent existing 400-cps supply for an air-to-air missile illustrates the superiority of a high power frequency.

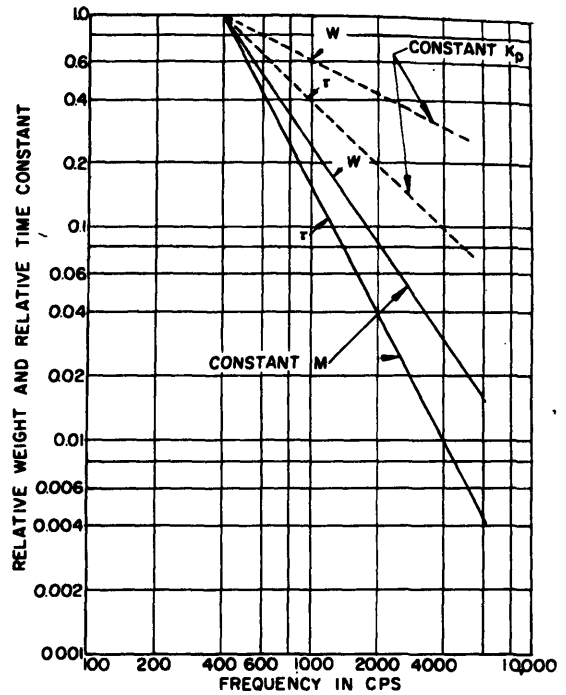
Therefore, the following conclusions can be drawn:

1. The optimum missile primary voltage lies between 75 and 150 volts.
2. The optimum missile primary frequency lies between 2400 and 4000 cps.

The selection of specific values for the optima from these ranges is somewhat arbitrary owing to the unpredictable distribution of utilization components and their power levels. However, full realization and implementation of the weight reductions in the electrical power system that can be achieved through the use of a power frequency higher than 400 cps, as well as the need to encourage the production of standard power-supply and a-c utilization components, makes essential the adoption of specific voltage and frequency standards.



a. Curves of relative M , K_p , and τ for constant W .



b. Curves of relative W and τ for constant M and K_p .

Fig. 77. Relative characteristics of magnetic amplifiers (figure of merit M , power gain K_p , time constant τ , and weight W) vs. supply frequency.

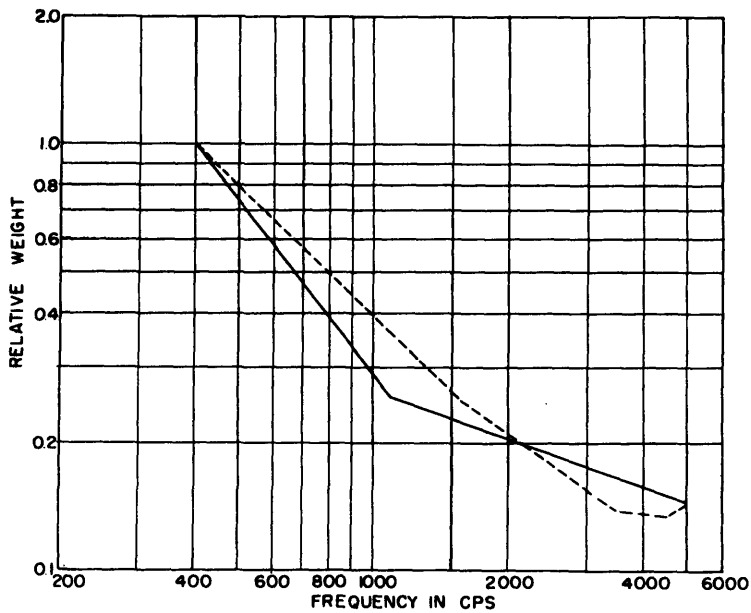


Fig. 78. Relative weight of signal transformers as a function of frequency. Solid curve is for input impedance greater than or equal to a given value; dashed curve is for phase shift less than or equal to a given value.

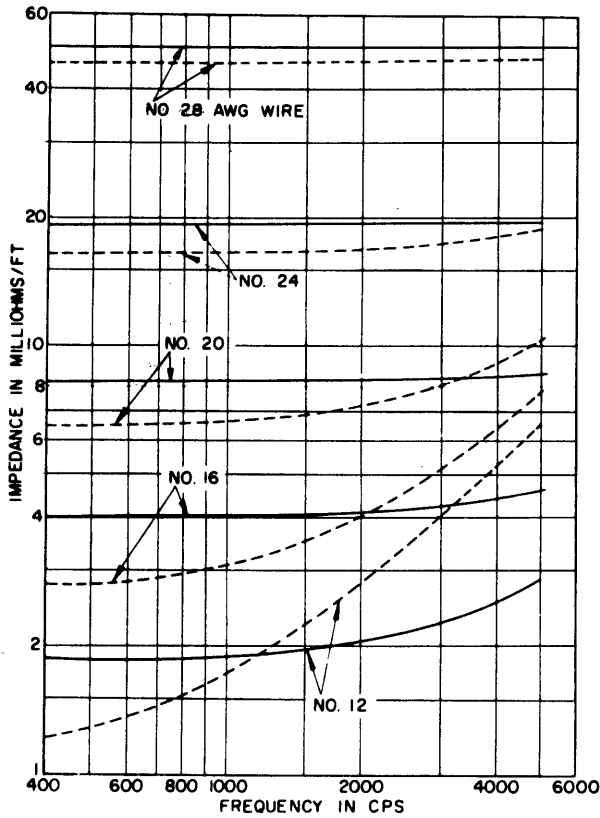


Fig. 79. Transmission-line impedance per conductor vs. frequency for different wire sizes. Solid curves are for zero space between conductors, and dashed curves for 1-in. spacing between centers of conductors.

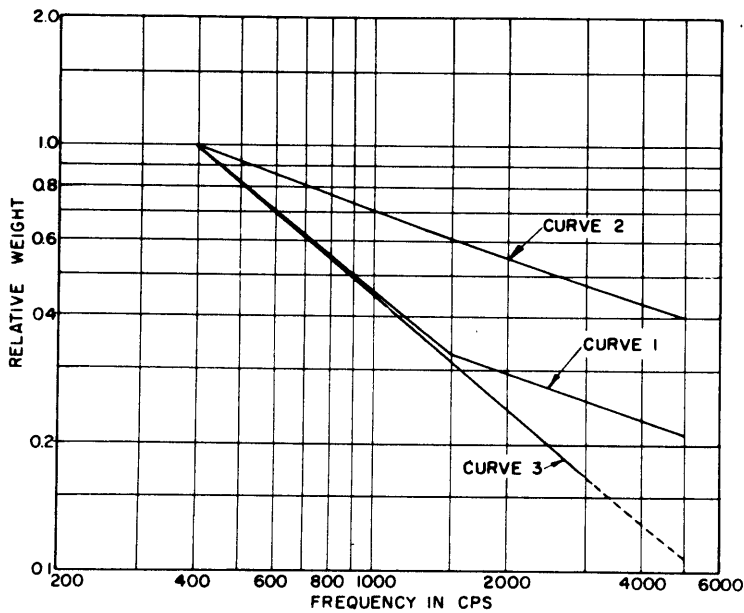


Fig. 80. Relative weight of alternators as a function of frequency.
 Curve 1 - wound-rotor synchronous alternator.
 Curve 2 - permanent-magnet alternator.
 Curve 3 - induction alternator.

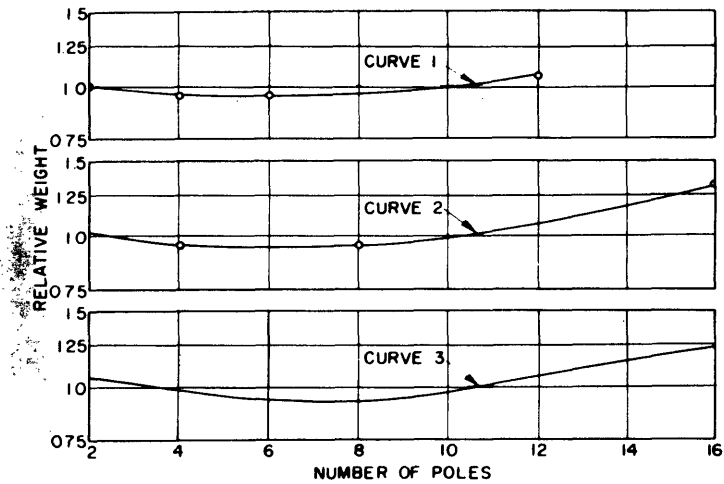


Fig. 81. Relative weight of alternators as a function of number of poles.

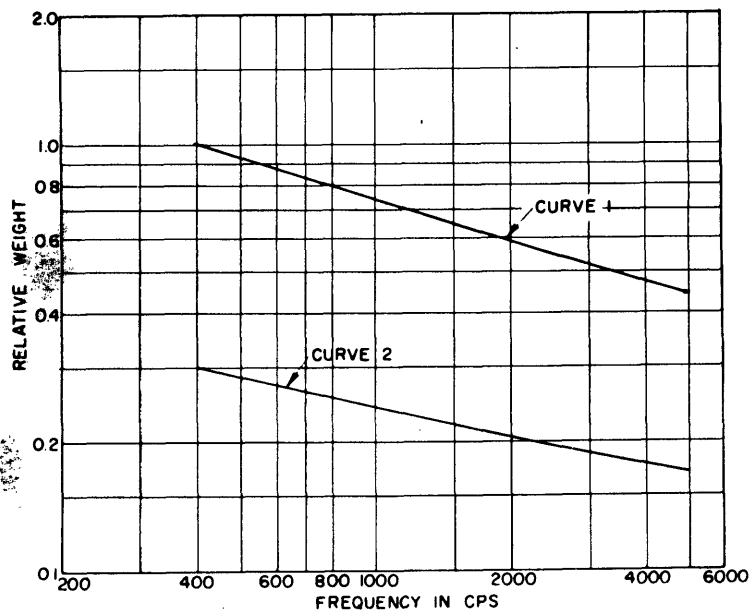


Fig. 82. Relative weight of power transformers as a function of frequency.

Curve 1 - 5-mil Hypersil core material.
 Curve 2 - 2-mil Hypersil core material.

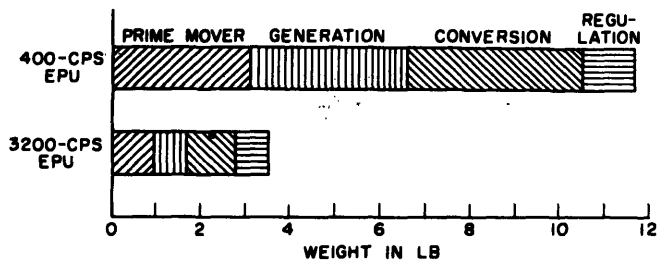


Fig. 83. Weight comparison of a 400-cps 450-watt and a 3200-cps 450-watt power supply.

9. CONCLUSIONS AND FUTURE WORK

The Missile Internal Power (MIP) project has studied the problem of developing integrated power supplies of minimum weight capable of providing regulated electrical power in an isolated environment subject to severe climatic and force conditions. An initial study of alternative energy sources and components revealed the most promising system. Basic investigations of the properties and characteristics of solid fuels and of design criteria for partial admission turbines and electrical machinery were conducted, as was the study of several competitive regulation schemes. Based on the results of the basic investigations, and adhering faithfully to the requirements imposed by the environment and the specifications of the missile system, two electrical power units (EPU's) were developed and tested at the Dynamic Analysis and Control Laboratory (D. A. C. L.). Both units were subsequently exhaustively and successfully tested in the respective missiles and both units have proven successful in missile flight. Extending the foregoing program, a study of optimum electrical voltage and frequency standards for missile systems has been made and recommendations which could materially reduce system weight have been advanced.

9.1. Educational Contributions

As of June 1957 the MIP project has provided the subject, support, and supervision of the following completed theses:

2 Sc. D. theses in Mechanical Engineering

1 Mech. Engr. thesis in Mechanical Engineering

2 Naval Engr. theses in Naval Architecture and Marine Engineering

6 S. M. theses in Mechanical Engineering
6 S. M. theses in Electrical Engineering
1 S. M. in Aeronautical Engineering
16 S. B. theses in Mechanical Engineering
2 S. B. theses in Electrical Engineering

The staff of the project, recent graduates, research assistants and students, none of whom had any prior industrial experience, have amply demonstrated their capacity to assume responsibility in a major engineering endeavor. Furthermore, they participated in the experience of carrying the design of prototype hardware to a degree of refinement and accomplishment well ahead of contemporary industrial practice.

9.2. National Significance.

The program has developed prototype hardware which is being applied to weapons intended for national defense. The results of the several basic investigations, particularly that directed toward the design of partial admission turbines, have become standard criteria nationally and have been widely applied by industrial and military organizations. The recommended electrical power standards can do much to accelerate the recognition of the possibility of, and development of components and systems, for improved missiles.

The project liaison with missile system and missile component companies and military agencies has promoted greater awareness of the significance of MIP and has culminated in symposia to which the project has contributed papers and organizational support. Current efforts include Advisory Board activity in the Department of Defense.

9.3. Future Work

Included in each of the relevant sections are recommendations for future work. They may be very briefly summarized as:

1. Conscious development and detailed study of solid and liquid fuels and fuel systems for relatively low mass flow, regulated systems of various time duration, subject to the severe conditions and requirements of missile flight.
2. Improvement of prime movers applied to low power systems utilizing high energy fuels.
3. Development of design techniques, and determination of relevant physical parameters, to facilitate rational design of electrical machinery, especially high-rated, transiently-operated devices.

The proposed electrical system standard and the growing awareness of the potential advantages of MIP system development integral and concurrent with the missile system design, makes feasible the design, fabrication and test of missile power units more nearly optimum than those described in this paper. Radical and unique designs can be conceived which will take advantage of the higher frequency, but which represent real design challenges and which will require novel approaches such as gas bearing shaft support, an area which has received attention at D. A. C. L. ³⁵⁻⁴⁰

Finally, the original system decisions are continually subject to reinspection and broadening as new prime energy sources and conversion techniques are proposed and appear fruitful of detailed investigations.

APPENDIX A. ENERGY SOURCE CALCULATIONS

1. Solid Fuels and Hydrogen Peroxide.

From the derivation of fuel mass flow rate in Sec. 3.2

$$G = \frac{P}{g^2 I_{sp}^2 \eta_t \eta_e}$$

where the symbols are defined in the nomenclature at the end of Sec. 4. Symbols used only in this appendix are defined herein. Omitting the conversion efficiencies and noting that

$$W_f = Gt$$

with appropriate conversion factors in terms of kilowatts KW of required power the fuel weight W_f (in lb-mass) is

$$W_f = \frac{45.9 \text{ KW} \cdot t}{I_{sp}^2}$$

and

$$V_f = \frac{W_f}{\rho_f}$$

The geometry of the fuel grain is determined by its combustion characteristics, thus from Sec. 3.2

$$L_f = t \cdot r$$

$$D_f = \frac{7.64}{I_{sp}} \sqrt{\frac{\text{KW}}{r}}$$

2. Flywheel

Assume:

1. Assume simple disk of radius r , thickness b , density ρ , and initial speed ω .
2. Utilize all the kinetic energy.
3. Losses are zero: windage eliminated by evacuation, bearing losses ignored, etc.
4. Maximum tip speed V of 1500 ft/sec.

$$J = \frac{\pi \rho b r^4}{2}$$

$$KW \cdot t = \frac{J \omega^2}{2} = \frac{\pi \rho b \pi^2 r^4}{4}$$

$$V = \omega r$$

$$W_{fw} = \pi \rho g b r^2$$

Combining:

$$W_{fw} = \frac{4g KW \cdot t}{V^2}$$

3. Battery

Highest short-duration power characteristics as of February 1952 were:

- 1.0 watt hours/in.³ for 45 sec. duration discharge.
- 15 watt hours/lb for 45 sec. duration discharge.

4. Compressed Air

Assume:

$$P_1 = 5000 \text{ psia}$$

$$P_2 = 1000 \text{ psia or } 0 \text{ psia}$$

For adiabatic reversible expansion of a perfect gas:

$$\frac{KW \cdot t}{Wg} = \frac{P_1}{\rho_1^{(k-1)}} \left[1 - \left(\frac{P_2}{P_1} \right)^{\frac{k-1}{k}} \right]$$

5. Spring (Ref: Handbook of Mechanical Spring Design)

Assume:

1. Material strength σ equals 1.73×10^5 psi.
2. Maximum diameter D equals 7 in.
3. Spring thickness h = 0.15 in.
4. Minimum diameter A equals approximately 15 h.

$$\tau = \frac{\sigma b h^2}{6} = 650 \text{ in. lb/in. of width}$$

$$n = \frac{\sqrt{2(A^2 + D^2)} - (A + D)}{2.55h} = 2.9 \text{ turns}$$
$$= 18.2 \text{ radians}$$

$$KW \cdot t = \frac{3n\tau b}{4}$$

$$b = 160 \text{ in. wide,}$$

which is, of course, unreasonable, but clearly demonstrates the weight and bulk of a spring.

APPENDIX B. WEIGHT COMPARISON OF SOLID-FUEL AND LIQUID-FUEL GAS-GENERATION SYSTEMS

In this Appendix gas generation systems are analyzed to provide a basis for the comparison of solid-fueled versus liquid-fueled systems for providing missile internal power. Geometric similarity is maintained in model liquid-fuel and solid-fuel systems that are analyzed for power levels from 1 to 100 isentropic-gas horsepower and for operating durations between 30 seconds and 10 minutes. Symbols are defined in the nomenclature at the end of Sec. 4, or if used only in this Appendix, they are defined herein.

Solid-Fuel Gas-Generation System. The geometry of the fuel grain, the fuel container, and the combustion chamber is based on MIP project experience and is shown in Fig. B. 1. The fuel grain is an end-burning configuration of the circular cross-section that is inhibited on its peripheral surface, see Sec. 3.2. The weight of the steel solid-fuel container and combustion chamber is given by:

$$W_c = \rho_s \left[\frac{12\pi D_1^2 h}{4} + (12h + L_f + H)\pi h(D_1 + h) + 36h\pi(D_1 + 6h) \right] \quad (B.1)$$

The inside diameter D_1 and length of the container are related to the fuel characteristics, and the wall thickness h is governed by strength considerations.

The tangential stress in the combustion-chamber wall of thickness h is:

$$\text{Stress} = \frac{P_{oo} D_1}{2h}$$

Because portions of the chamber walls may reach incandescent heat during operation, a reasonable maximum working stress for alloy steels is 20,000 psi. A maximum chamber pressure of 500 psi, which is compatible with the burning characteristic of most solid fuels, determines the relationship

$$h = \frac{D_1}{80} .$$

From rigidity and fabrication considerations, the minimum practical wall thickness is assumed to be 1/32 inch. Therefore,

$$h = \frac{D_1}{80}, \quad D_1 > 2\frac{1}{2} \text{ inches} \tag{B.2}$$

$$h = \frac{1}{32}, \quad D_1 < 2\frac{1}{2} \text{ inches}$$

The isentropic gas power from the solid fuel is

$$P_s = \frac{G(g I_{sp})^2}{2} \tag{B.3}$$

The rate of gas generation

$$G = \frac{\pi D_f^2 \rho_f r_f}{4} \tag{B.4}$$

where D_f is the diameter of the uninhibited fuel grain. Combination of Eqs. (B.3) and (B.4) yields isentropic gas power as a function of fuel geometry and characteristics:

$$P_s = \frac{\pi}{8} D_f^2 \rho_f r_f (g I_{sp})^2 .$$

A density of 0.055 lb/in.³, a specific impulse of 175 seconds, and a minimum burning rate, corresponding to a fuel equilibrium temperature of -65^o, of 0.12 in/sec, are assumed. Fuel diameter for a specific horsepower requirement is

$$D_f = 0.394 \sqrt{P_s} \text{ inches.} \quad (\text{B.5})$$

The following inhibitor thicknesses that relate fuel diameter D_f to over-all charge diameter D_1 are characteristic of solid fuels:

$$D_1 = D_f + \frac{1}{4}, \quad D_f > 1 \frac{1}{4} \text{ inches}$$

and

$$D_1 = D_f + \frac{1}{8}, \quad D_f < 1 \frac{1}{4} \text{ inches.}$$

(B.6)

If the inhibitor and fuel grain have the same density, which is reasonable assumption, then the weight of the fuel grain is

$$W_f = \frac{\rho_f \pi D_1^2 L_f}{4}$$

The maximum burning rate is assumed 30 per cent greater than the minimum burning rate, that is, 0.16 in/sec. Therefore,

$$W_f = 0.00674 D_1^2 t \quad (\text{B.7})$$

For any particular isentropic power requirement P_s in horsepower and operating duration t in seconds, the weight of the fuel grain W_f in pounds can be calculated by using Eqs. (B.5), (B.6), and (B.7). Furthermore, the weight of the combustion chamber W_c in pounds also can be calculated by using Eqs. (B.1), (B.2), (B.5), and (B.6), and the value for the density

of steel (0.28 lb/in.³) if a value of the initial free height above the fuel H is provided. Based on MIP experience, satisfactory ignition characteristics can be obtained by using a value of H equal to 1/2 D₁.

The weights of the combustion chamber and the fuel grain are combined to give the total gas-generation-system weights presented in Fig. 2 of Sec. 2.222.

Liquid-Fuel Gas-Generation System.

The basic components and significant geometric parameters of the model liquid-fuel gas-generation system are shown in Fig. B.2. Because the shape of the fuel container is independent of the fuel characteristics, computation of the liquid fuel weight is somewhat simpler than computation of solid fuel weight for the same power requirement. The basic relationship for available gas power is given by Eq. (B.3) in the preceding discussion, that is,

$$P_s = \frac{G(g I_{sp})^2}{2} \quad (B.3)$$

The weight W_f of liquid fuel required for a specific operating duration t is

$$W_f = G t.$$

Normal propyl nitrate, the fuel assumed for this system, has many desirable characteristics for auxiliary power systems. The specific impulse of propyl nitrate is 175 seconds, permitting direct comparison on an energy basis with the solid-fuel. Combination of Eqs. (B.3) and (B.8) yields an expression for fuel weight in terms of gas horsepower and operating duration t in seconds:

$$W_f = 0.00112 P_s t \text{ pounds.} \quad (B.8)$$

The weight of the fuel tank is related to the fuel weight, the combustion-chamber pressure P_{oo} , and the geometrical and material properties of the tank. The fuel-tank configuration is most simply assumed to be a circular cylinder with diameter D_t equal to one-half the length L_t . The fuel tank need not be subjected to temperatures above the ambient temperature. Therefore, the stress conditions for the operating pressure of 550 psi indicate that a 1/16-in. thick aluminum tank is satisfactory for the range of power levels and operating periods considered. The weight of the fuel tank (W_{ft}) is, then,

$$W_{ft} = \rho_a \pi h_t D_t \left[\frac{2D_t}{4} + L_t \right] \quad (B.9)$$

Simplification and insertion numerical values gives

$$W_{ft} = 0.049 D_t^2 \text{ pounds.} \quad (B.10)$$

The volume or diameter of the tank is related to the fuel weight as follows,

$$\text{Volume} = \frac{W_f}{\rho_f} = \frac{\pi D_t^3}{2} \quad (B.11)$$

If Eqs. (B.10) and (B.11) are combined and the value for the density of propyl nitrate (0.036 lb/in.³) is inserted, a relationship between fuel weight and fuel tank weight is obtained:

$$W_{ft} = 0.333 (W_f)^{\frac{2}{3}} \text{ pounds.} \quad (B.12)$$

The size and weight of the fuel pressurization system is related to the fuel weight, to the pressures in the compressed inert gas tank and in the fuel tank, and to the mechanical properties of the high-

pressure gas storage tank. A differential pressure of 50 psi is necessary to inject fuel into the combustion chamber, which operates at 500 psi. Therefore, the pressure-reducing valve maintains a fuel-tank pressure of 550 psi. The initial pressure in the nitrogen tank is 3000 psi, and the gas is assumed to expand reversibly and adiabatically to the fuel-tank pressure of 550 psi. With these assumptions, the size and weight of the nitrogen tank can be related to fuel weight:

$$\frac{\text{Initial nitrogen pressure}}{\text{Fuel-tank pressure}} - 1 = \frac{\text{Fuel-tank volume}}{\text{Nitrogen-tank volume}},$$

or

$$\frac{3000}{550} - 1 = \frac{W_f}{\rho_f V_n}.$$

Evaluation yields

$$V_n = 5.1 W_f. \quad (\text{B.13})$$

Spherical, high-pressure, Fiberglas containers have a weight and volume relationship of

$$W_n = 0.02 V_n. \quad (\text{B.14})$$

Therefore, the weight of the nitrogen tank W_n can be expressed in terms of fuel weight by combining Eqs. (B.13) and B.14):

$$W_n = 0.10 W_f. \quad (\text{B.15})$$

The weight of the nitrogen gas can be neglected because it is small compared with the weight of the nitrogen tank.

For systems in which the fuel weight exceeds 20 pounds a pump for pressurizing the fuel is lighter than gas pressurization although pump mechanical complications may offset its weight advantage. An empirical relation for the weight of a pump W_p , based on typical high-speed gear pumps, is

$$W_p = 1.5 + 0.03 P_s \text{ pounds.} \quad (\text{B.16})$$

The combustion chamber of a liquid-fuel system is a very small portion of the total weight, and the design of these chambers for particular power requirements cannot be expressed readily in analytical terms. An empirical relation for combustion-chamber weight W_c based on typical designs is

$$W_c = 0.5 + 0.015 P_s \text{ pounds.} \quad (\text{B.17})$$

The pressure-reducing valve and other piping, valves, and fittings are assumed to comprise 20 per cent of the combined weight of the fuel, fuel tank, nitrogen tank, and combustion chamber. Therefore, the total weight of the liquid-fuel gas-generation system can be computed by combining the separate parts of the system represented by Eqs. (B.8), (B.12), (B.17), and (B.15) or (B.16). The total system weight based on nitrogen pressurization is given in Fig. 3 of Sec. 2.222.

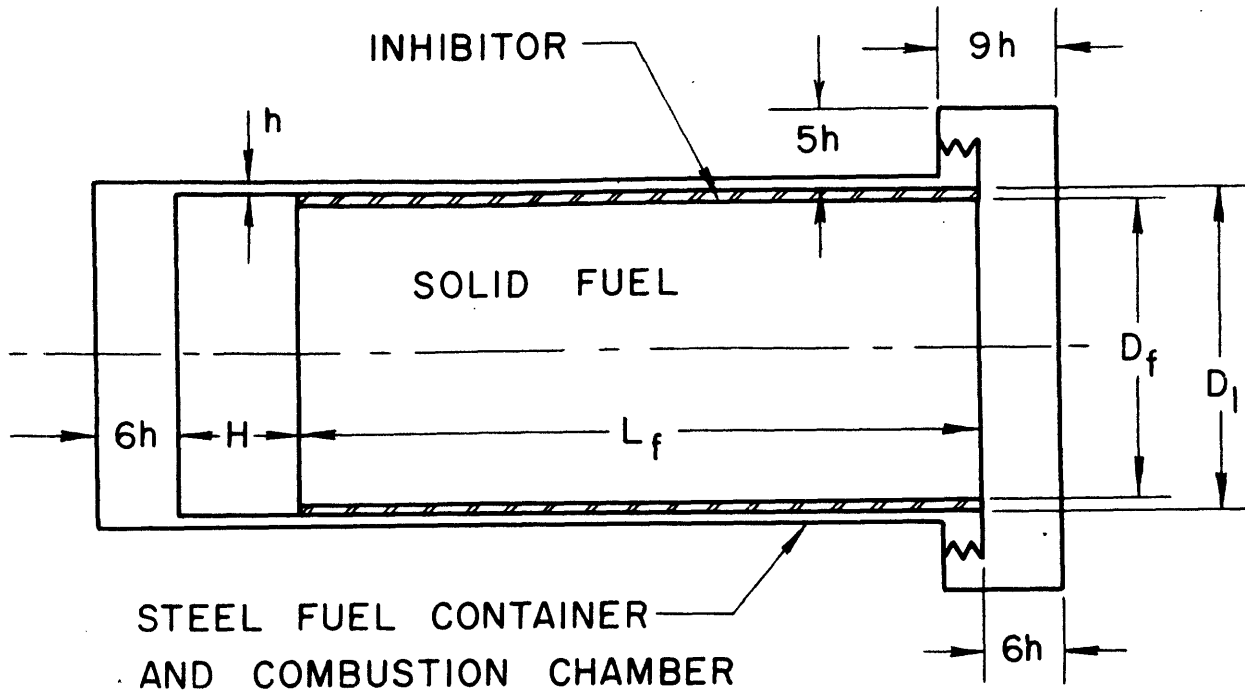


Fig. B.1. Geometry of solid fuel gas generation system.

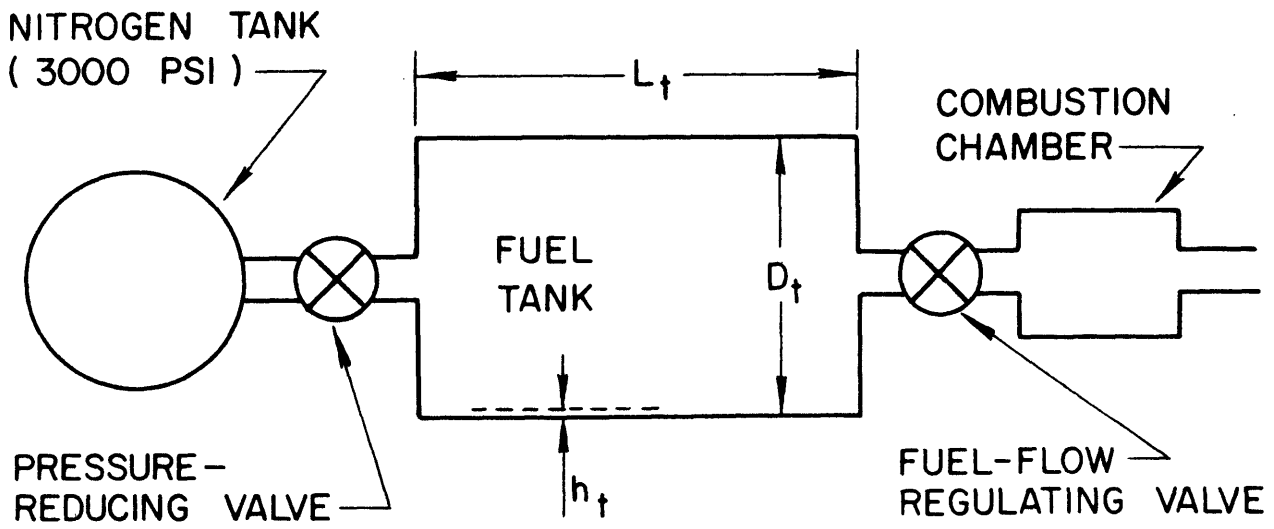


Fig. B.2. Geometry of liquid fuel gas generation system.

APPENDIX C. BIBLIOGRAPHY

- 1^Δ R. W. Mann, "Research Directed Toward Improved Auxiliary Power Units," paper presented at the Ordnance Advisory Committee 1956 Fall Meeting, National Security Industrial Association, Sacramento, Calif., November 12-18, 1956.
- 2^Δ R. W. Mann, "Fuels and Prime Movers for Rotating Auxiliary Power Units," paper presented at the Symposium on Auxiliary Power for Guided Missiles, Office of the Assistant Secretary of Defense Research and Development, Washington, D.C., February 5-7, 1957.
- 3^Δ R. F. Hamaker, Influence of Tactical Handling Problems on Designs for Navy Air-to-Air Missiles. Thesis, (S. M.), Dept. of Mech. Engr., Mass. Inst. of Tech., Cambridge, Mass., 1953. (Classified)
- 4 W. H. McAdams, Heat Transmission. New York, N. Y.: McGraw-Hill Book Co., Inc., 1933.
- 5^Δ R. W. Mann, Electrical Power Unit for the Sparrow I Missile, Dynamic Analysis and Control Laboratory Report No. 90. Cambridge, Mass.: Mass. Inst. of Tech., January 31, 1955. (Classified)
- 6^Δ J. F. Bonarrigo, and H. J. Durivage, Performance of High Speed Low-Power Solid Fuel Turbine. Thesis (S. B.), Dept. of Mech. Engr., Mass. Inst. of Tech., Cambridge, Mass., 1957.
- 7^Δ R. B. Downey, A Solid Propellant Gas Generating System for a Small Turbine Driven Power Supply. Thesis (S. M.), Dept. of Mech. Engr., Mass. Inst. of Tech., Cambridge, Mass., 1955. (Classified)

^Δ Publications so indicated were originated by individuals associated with the MIP project as part of the over-all investigation of the optimization of missile power systems.

- 8^Δ S. K. Grinnell, Rotary Electrical Power Unit for the Sparrow III Missile, Dynamic Analysis and Control Laboratory Report No. 104. Cambridge, Mass.: Mass. Inst. of Tech., August 20, 1956. (Classified)
- 9^Δ J. M. Uzdavinis, Comparison of Solid Propellants for EPU Application, Dynamic Analysis and Control Laboratory Research Memorandum No. R. M. 7216-1. Cambridge, Mass.: Mass. Inst. of Tech., January 17, 1955. (Classified)
- 10 O. E. Balje, "Drag Turbine Performance," (Paper No. 56-AV-6), presented at the ASME Aviation Conference, Los Angeles, Calif., March 14-16, 1956.
- 11 W. A. Wilson, M. A. Santalo, and J. A. Oelrick, "A Theory of The Fluid-Dynamic Mechanism of Regenerative Pumps," Trans. ASME, Vol. 77, No. 8, pp. 1303 -1316, 1955.
- 12^Δ G. Ohlsson, Partial Admission, Low Aspect Ratios and Supersonic Speeds in Small Turbines. Thesis (Sc.D), Dept. of Mech. Engr., Mass. Inst. of Tech., Cambridge, Mass., 1956.
- 13^Δ A. H. Stenning, Design of Turbines for High-Energy-Fuel Low-Power-Output Applications, Dynamic Analysis and Control Laboratory Report No. 79. Cambridge, Mass.: Mass. Inst. of Tech., September 30, 1953.
- 14 R. I. Sinclair, Preliminary Investigation into the Performance of Miniature Impulse Turbines, English Electric Ltd. Guided Weapons Division Report No. LC.t.036, Luton, Bedfordshire, England, November 16, 1956.
- 15^Δ H. H. Dearing and R. V. Hayes, Design and Test of a Small Single Stage Turbine. Thesis (S.M.), Dept. of Aero. Engr., Mass. Inst. of Tech., Cambridge, Mass., 1952.
- 16 H. Schlichting, Boundary Layer Theory. New York, N. Y.: McGraw-Hill Book Co., Inc., 1955.

- 17^Δ M. G. Forest, An Experimental Study of Disk Friction and Windage Losses in Small, High Speed Turbo-Machinery. Thesis (S.B.), Dept. of Mech. Engr., Mass. Inst. of Tech., Cambridge, Mass., 1956.
- 18 "The Development of Turbine Engines in France---III," Aircraft Engineering, Vol. 21, October, 1949, pp. 328 - 330.
- 19 H. Davis, H. Kottas, and A. M. G. Moody, "The Influence of Reynolds Numbers on the Performance of Turbomachinery," Trans. ASME, Vol. 73, No. 5, pp. 499 - 509, 1951.
- 20^Δ P. W. Pillsbury, Leakage Loss in the Axial Clearance of a Partial Admission Turbine. Thesis (S.M.), Dept. of Mech. Engr., Mass. Inst. of Tech., Cambridge, Mass., 1957.
- 21^Δ L. Colucciello, Brush Wear at High Altitudes. Thesis (Naval Engr.) Dept. of Naval Arch. and Marine Engr., Mass. Inst. of Tech., Cambridge, Mass., 1954.
- 22^Δ F. C. Anderson and W. L. Aitkenhead, Permanent Magnet Alternator Control by Means of Magnetic Saturation. Thesis (Naval Engr.), Dept. of Naval Arch. and Marine Engr., Mass. Inst. of Tech., Cambridge, Mass., 1953.
- 23^Δ J. T. Duane, The Design of a High-Speed Inductor Alternator. Thesis (S.M.), Dept. of Elec. Engr., Mass. Inst. of Tech., Cambridge, Mass., 1954.
- 24^Δ F. E. Steinberg, An Inductor-Type Alternator. Thesis (S.M.), Dept. of Elec. Engr., Mass. Inst. of Tech., Cambridge, Mass., 1953.
- 25^Δ W. H. Gable, Design of a High-Speed Induction Generator. Thesis (S.M.), Dept. of Elec. Engr., Mass. Inst. of Tech., Cambridge, Mass., 1953.
- 26^Δ M. S. Pathak, Investigation of the Optimum Excitation in Induction Machines as Viewed from Power Transfer Considerations. Thesis (S.M.), Dept. of Elec. Engr., Mass. Inst. of Tech., Cambridge, Mass., 1955.

- 27^Δ W. T. Peake, Automatic Control of an Induction Generator. Thesis (S. M.), Dept. of Elec. Engr., Mass. Inst. of Tech., Cambridge, Mass., 1953.
- 28 R. M. Saunders and D. C. White, Study of Aircraft Alternating-Current Generating and Voltage-Regulating Systems, WADC Technical Report 55-311. Cambridge, Mass.: Servomechanisms Laboratory, Mass. Inst. of Tech., Chaps. 5 and 6., August, 1955.
- 29^Δ K. M. Becker, Design Construction and Testing of a Thermal Conductivity Apparatus for Small Samples. Thesis (S. M.), Dept. of Mech. Engr., Mass. Inst. of Tech., Cambridge, Mass., 1956.
- 30^Δ W. Fincke, A Speed Control for Small Solid Propellant Turbogenerators. Thesis (S. M.), Dept. of Mech. Engr., Mass. Inst. of Tech., Cambridge, Mass., 1955.
- 31 J. L. Lof, Investigation of the Properties of Eddy-Current Brakes, Thesis (S. M.), Dept. of Elec. Engr., Mass. Inst. of Tech., Cambridge, Mass., 1941.
- 32^Δ M. Lorber, Analysis of a Three Phase Induction Generator. Thesis, (S.B.), Dept. of Elec. Engr., Mass. Inst. of Tech., Cambridge, Mass., 1956.
- 33^Δ S. K. Grinnell, R. W. Mann and R. E. Turkington, Determination of an Optimum Primary Power Frequency and Voltage for Missiles, Dynamic Analysis and Control Laboratory Report No. 107 Cambridge, Mass.: Mass. Inst. of Tech., forthcoming, 1957. (Classified).
- 34 G. Reethof, Development of Solid Propellant Powered Control Surface Actuator for Guided Missiles. Thesis (ScD.), Dept. of Mech. Engr., Mass. Inst. of Tech., Cambridge, Mass., 1955. (Classified).
- 35 S. K. Grinnell, A Study of Pressurized Air Bearing Design Steady Loading - No Rotation. Thesis (S. M.), Dept. of Mech. Engr., Mass. Inst. of Tech., Cambridge, Mass., 1954.

- 36 H. H. Richardson, A Dynamic Analysis of Externally Pressurized Air Bearing. Thesis (S. M.), Dept. of Mech. Engr., Mass. Inst. of Tech., Cambridge, Mass., 1955.
- 37^Δ B. Blaschitz, Development of Design Information for Externally Pressurized Air Bearings. Thesis (S. B.), Dept. of Mech. Engr., Mass. Inst. of Tech., Cambridge, Mass., 1956.
- 38^Δ C. D. Hazard, III., The Design of a Fixture for Testing the Dynamics of Pressurized Air Bearings - Rotational Speeds up to One Hundred Thousand R. P. M. Thesis (S. B.), Dept. of Mech. Engr., Mass. Inst. of Tech., Cambridge, Mass., 1956.
- 39^Δ R. B. Currie and J. P. Zurfleih, The Design of Equipment for Non-Rotating Testing of Pool-Type Pressurized Gas Bearings, Thesis (S. B.), Dept. of Mech. Engr., Mass. Inst. of Tech., Cambridge, Mass., 1957.
- 40^Δ P. R. Duevel, Investigation of Capacitive and Inductive Methods of Measuring Small Displacements. Thesis (S. B.), Dept. of Mech. Engr., Mass. Inst. of Tech., Cambridge, Mass., 1957.
- 41^Δ B. Agusta, Study of Reset-Type Magnetic Amplifiers with High-Frequency Supply. Thesis (S. M.), Dept. of Elec. Engr., Mass. Inst. of Tech., Cambridge, Mass., 1954.
- 42^Δ V. V. Hukee, The Characteristics of a Three-Phase Mechanical Inverter. Thesis (S. B.), Dept. of Elec. Engr., Mass. Inst. of Tech., Cambridge, Mass., 1956.
- 43^Δ J. W. Hurley, Design of a Speed Sensitive Switch of an Off-On Speed Regulator. Thesis (S. B.), Dept. of Mech. Engr., Mass. Inst. of Tech., Cambridge, Mass., 1955.
- 44^Δ M. E. Hazel, Jr., Design of a Simple, Easily Installed Speed Pick-up for High Speed Shafts. Thesis (S. B.), Dept. of Mech. Engr., Mass. Inst. of Tech., Cambridge, Mass., 1956.

- 45^Δ G. Gartner, Disk Friction Losses in Small Centrifugal Pumps. Thesis (S.B.), Dept. of Mech. Engr., Mass. Inst. of Tech., Cambridge, Mass., 1956.
- 46^Δ J. C. Walter, Power Transmissions for Low Torque, High Speed and Short Life Devices. Thesis (S.B.), Dept. of Mech. Engr., Mass. Inst. of Tech., Cambridge, Mass., 1956.
- 47^Δ J. L. Materas, System Analysis of an Auxiliary Power Supply. Thesis (S.B.), Dept. of Mech. Engr., Mass. Inst. of Tech., Cambridge, Mass., 1956.
- 48^Δ E. Christensen, Cinematic Investigation of a Ball Bearing. Thesis (S.M.), Dept. of Mech. Engr., Mass. Inst. of Tech., Cambridge, Mass., 1956.
- 49^Δ D. A. Appling, A Comparative Weight Study of Monofuel Supply Systems for Low Power Applications. Thesis (S.B.), Dept. of Mech. Engr., Mass. Inst. of Tech., Cambridge, Mass., 1957.
- 50^Δ R. J. Jantzen, Heat Transfer in Silicon Diodes. Thesis (S.B.), Dept. of Mech. Engr., Mass. Inst. of Tech., Cambridge, Mass., 1957.
- 51^Δ B. B. Abrahams, A Centrifugal Pump With a Rotating Housing. Thesis (S.M.), Dept. of Mech. Engr., Mass. Inst. of Tech., Cambridge, Mass., 1957.
- 52^Δ G. E. Ervin, Determination of Power Output of Small Solid or Liquid-Fuel Gas Generators. Thesis (S.B.), Dept. of Mech. Engr., Mass. Inst. of Tech., Cambridge, Mass., 1957.
- 53^Δ D. E. Hasselmann, Design of a Centrifugally Operated Hot Gas Valve for a Speed Control. Thesis (S.B.), Dept. of Mech. Engr., Mass. Inst. of Tech., Cambridge, Mass., 1957.
- 54^Δ H. R. Smart, Design of a High-Speed Timing-Belt Test Fixture. Thesis (S.B.), Dept. of Mech. Engr., Mass. Inst. of Tech., Cambridge, Mass., 1957.

BIOGRAPHICAL NOTE

Robert Wellesley Mann was born on October 6, 1924 in Brooklyn, New York. He attended the Public School System of the City of New York and graduated from the Terminal Mechanical Course of the Brooklyn Technical High School in January 1942. Upon graduation he worked as draftsman for the Bell Telephone Laboratories, Inc., in New York City until he entered military service in March 1943. He served in The U. S. Army Signal Corps as an enlisted man with the specialty of teletype and cryptographic installation and repair until January 1946 including 14 months overseas service in the Western Pacific Theatre of Operations.

In March 1946 he returned to the Bell Telephone Laboratories as a draftsman until February 1947 when he entered M. I. T. He received his S. B. in Mechanical Engineering in June 1950 and S. M. in Mechanical Engineering in June 1951.

He joined the Division of Industrial Cooperation staff at M. I. T. as a research engineer in the Dynamic Analysis and Control Laboratory (D. A. C. L.) in July 1951. In December 1952 he became supervisor of the Design Division of D. A. C. L. In September 1953 he received an academic appointment as Assistant Professor in the Mechanical Engineering Department at M. I. T. and continued as Design Division supervisor at D. A. C. L. until February 1956 when he became a consultant to the director of D. A. C. L.

Since 1953 his academic assignments have included undergraduate machine design courses in the Mechanical Engineering Department and a graduate seminar in production in cooperation with the School of Industrial Management of M. I. T. Faculty committee responsibilities include election as chairman of the Activities Development Board and election to the Committee on Academic Performance. He is an elected Director of the M. I. T. Faculty Club.

He has consulted for a number of industrial companies including General Electric, Ingersol-Rand, Raytheon, National Pneumatics, Arthur D. Little, etc.

He was president of student government at M. I. T. and of his senior class and is president of his alumni class, and is a member of Tau Beta Pi, Pi Tau Sigma, and Sigma Xi.

He is married to the former Margaret I. Florencourt of Arlington, Massachusetts; they have two children: Robert W. Jr., 3-1/2 years and Catherine L., 2 years; and reside in Lexington, Massachusetts



Room 14-0551
77 Massachusetts Avenue
Cambridge, MA 02139
Ph: 617.253.5668 Fax: 617.253.1690
Email: docs@mit.edu
<http://libraries.mit.edu/docs>

DISCLAIMER OF QUALITY

Due to the condition of the original material, there are unavoidable flaws in this reproduction. We have made every effort possible to provide you with the best copy available. If you are dissatisfied with this product and find it unusable, please contact Document Services as soon as possible.

Thank you.

Some pages in the original document contain pictures, graphics, or text that is illegible.